



UNIVERSITÀ DEGLI STUDI DI MILANO  
FACOLTÀ DI FARMACIA

**Dottorato in chimica del farmaco (XXVI ciclo)**

**PLASMEPSIN V INHIBITION AS A NEW  
POTENTIAL ANTIMALARIAL STRATEGY**

Coordinatore: Chiar.mo Prof Ermanno VALOTI  
Tutor: Prof. Sergio ROMEO

Dr. Luca GAMBINI  
Matr. N°: R09063



# INDEX

	<b>Page</b>
<b>1 Introduction</b>	<b>3</b>
1.1 Malaria	3
1.2 Parasite Life Cycle	5
1.3 Pathogenesis	7
1.4 Red Blood Cells Membrane Remodeling	7
1.5 Antimalarial Therapies	10
1.6 Resistance	14
1.7 Natural Products Privileged Scaffolds in Drug Discovery	16
<b>2 Aim of the Research</b>	<b>18</b>
2.1 Plasmepsins	18
<b>3 Discussion</b>	<b>22</b>
3.1 Aspartic Proteases Inhibition	22
3.2 Compounds Stereochemistry	26
3.3 SAR Studies on Peptidomimetics	26
3.3.1 P3' Position	27
3.3.2 P2' Position	27
3.4 Antiplasmodial Activity of Compounds 1-9	29
3.5 Azaspiroundecane Scaffold	30
3.6 Scaffold Library	32
3.7 Activity of Compounds 10-19	34
3.8 Design and Activity of Compounds 30-32	35
<b>4 Synthesis</b>	<b>37</b>
4.1 Solid-Phase Peptide Synthesis	37
4.1.1 SPPS Features and Requirements	39
4.2 Organic Reactions	40

4.2.1	Aza-Michael Addition	40
4.2.2	Bismuth Role as a Catalyst	41
4.2.3	Ring-closing Metathesis	41
4.3	Reaction Schemes	43
4.3.1	Synthesis of Peptidomimetics 1-4	45
4.3.2	Synthesis of Peptidomimetics 5-6	47
4.3.3	Synthesis of Peptidomimetics 7-8	49
4.3.4	Synthesis of Peptidomimetic 9	50
4.3.5	Synthesis of Intermediates 10 and 11	53
4.3.6	Synthesis of Scaffolds A and B	54
4.3.7	Synthesis of Compounds 10-19	55
4.3.8	Synthesis of Compounds 20-29	58
4.3.9	Synthesis of Compounds 30-32	61
<b>5</b>	<b>Conclusions</b>	<b>63</b>
5.1	Closing Remarks	71
<b>6</b>	<b>Experimental Section</b>	<b>72</b>
6.1	Abbreviations	72
6.2	Reagents and Instrumentations	73
6.3	SPPs Genarl procedures	74
6.3.1	Resin-specific Solid-Phase Procedures	74
6.3.2	Common Solid-Phase Procedures	79
6.4	General Synthetic Procedures	80
6.5	Specific Synthetic Procedures	84
<b>7</b>	<b>Bibliography</b>	<b>125</b>

# 1. Introduction

## 1.1 Malaria

Malaria is a parasitic disease caused by *Plasmodium* protozoa and, with tuberculosis and HIV, is the third cause of death in the world. Five *Plasmodium* species are known to be infectious to humans: *P. falciparum*, *P. vivax*, *P. ovale*, *P. malariae* and *P. knowlesi*. These parasites are responsible for different manifestations of this pathology, with *P. falciparum* being the most deadly. In 2011, it has been estimated that 3.3 billion people were at risk of contracting malaria, especially in the sub-Saharan regions. According to the World Health Organization's data, 91% of the deaths due to malaria involved the regions of Africa (particularly sub-Saharan Africa), where the most affected people are children under 5 years and pregnant women (**Figure 1.1**).<sup>1</sup>

While Africa is at great risk, western Asia, the Middle East and Latin America are also regions with a great risk of malaria transmission, and even first world countries, where malaria has been eradicated, are at risk of reintroduction due to migratory fluxes.

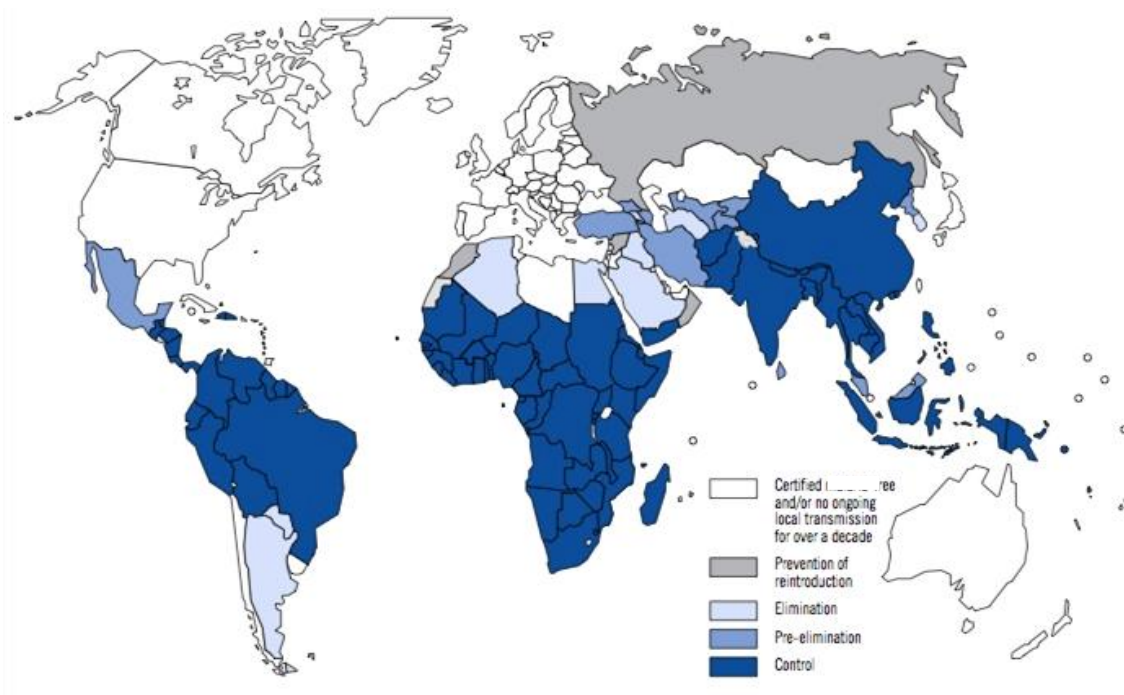


Figure 1.1

Geographical factors like temperature, humidity and rain are responsible for the distribution of the disease, limiting the ideal mosquito breeding ground in the tropical and subtropical regions. This localization had led many to consider malaria a “poverty disease”, because these areas are often associated with poor economical, social and health conditions typical of third world countries. What is often overlooked is that the disease is also one of the causes of impoverishment in these countries: in high-risk of transmission areas, malaria causes an average loss of economic annual growth of 1.3%. This fact can be observed comparing the GDP of countries where malaria is endemic and those where it has been eradicated. The infection has a direct impact on human resources because it hinders social development and decreases school attendance,<sup>2</sup> and direct costs of malaria include public and private spending for prevention and treatment of the disease. In some countries, malaria is the cause of 40% of public health expenditure, 39-50% of hospital admissions and 60% of day care consults.

Every year between 10,000 and 12,000 cases of imported malaria are reported.<sup>2</sup> In the European Union, the majority of imported malaria cases can be found in France, the United Kingdom, Germany and Italy.

For over 50 years alkaloids of *Cinchona* and their derivatives have been used to control malaria. Chloroquine, a synthetic derivative of natural alkaloid quinine, has been one of the most effective anti-malarial drugs ever produced, but *P. falciparum* strain resistant to this class of drugs, first observed in South East Asia and South America, are now common also in Africa and Asia. This has led to a global resurgence of malaria, and the global effort to identify another therapeutic agent effective against malaria. This research led to the identification of artemisinin, a terpene extracted from *Artemisia Annua*.

Artemisinin, a very effective antimalarial and expensive compound, quickly became a first line drug. Unfortunately, in some regions, resistance to this class of antimalaric has already been observed.<sup>3</sup>

Therefore, there is a huge need to develop new antimalarial agents that, compared to traditional drugs, will be active against these resistant strains with improved pharmacokinetic properties, fewer side effects and lower costs.

## 1.2 Parasite life cycle

Malaria is transmitted from person to person almost exclusively by a female mosquito of the genus *Anopheles*, though cases of accidental transmission due to blood transfusions or use of contaminated syringes have been reported.

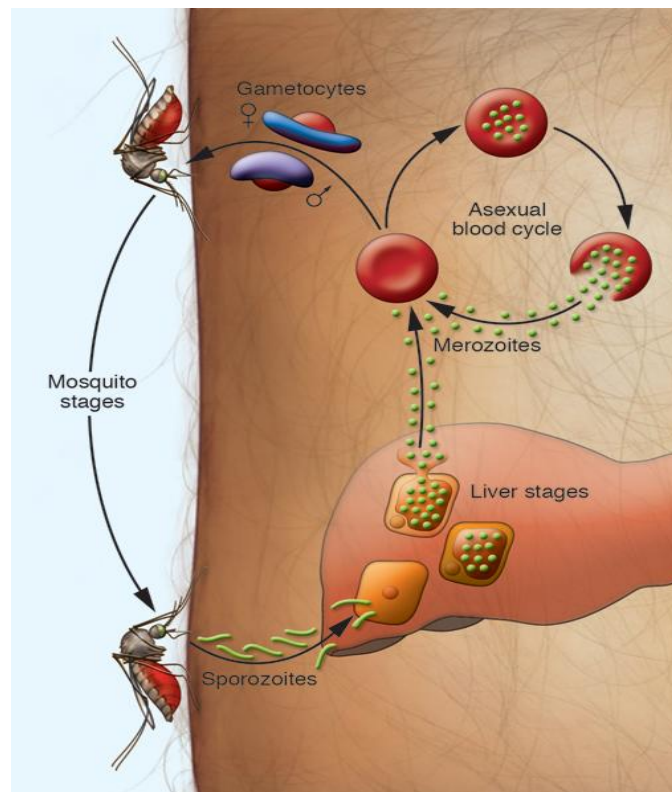


Figure 1.2

Infected mosquitoes are able to transmit malaria with every bite during its life cycle, inoculating the infectious forms of the parasite, called sporozoites. Sporozoites remain in circulation for less than half an hour, after which they move into the parenchymal cells of the liver, starting the hepatic phase. During this phase, the sporozoites undergo a first cycle of asexual multiplication with the production of plurinuclear schizonts which then divide into intracellular mononuclear merozoites. Infected hepatocytes then break and release merozoites into the blood stream, where they adhere to the red blood cell (RBC) membrane and infect the erythrocytes, starting the second asexual phase called "red-cell cycle". Merozoites turn in trophozoites which are recognizable under the microscope due to typical ring shape.

Trophozoites initially grow feeding on hemoglobin, maturing to the stage of schizont with the ability to generate new merozoites. After a series of nuclear divisions, schizonts break free from the infected RBC and release numerous merozoites (from 6 to 36 per schizont), able to start a new invasion (**Figure 1.2**).

Malaria symptoms are characterized by fever (due to the breakdown of red blood cells and the subsequent invasion of new erythrocytes), shivers, splenomegaly and anemia.

Depending on the *Plasmodium* species infecting the host, the infection cycle repeats at regular intervals: in cases of *P. falciparum* (malignant tertian malaria), *P. ovale* and *P. vivax* (benign tertian malaria) fever appears every 48 hours, while in the case of *P. malariae* (quartan malaria) every 72 hours. RBC destruction causes anemia, while in several vital organs microvasculature clots consisting of erythrocytes fragment leads to a blockage of blood vessels, causing decreased oxygenation of organs such as liver, kidneys or brain (cerebral malaria), which may lead to death.<sup>4</sup>

*P. vivax* and *P. oval* hepatic parasites may persist in the liver as hypnozoites to generate, even after months or years, new infections of red blood cells known as "malarial relapse".

In order to complete the replication cycle, some trophozoites may transform into male and female gametocytes. After a mosquito bites an infected person, ingesting the sexual forms, they mature in its stomach (sporogonic cycle), producing numerous oocyst. The oocyst become sporozoites and accumulate in the salivary glands of the vector. Subsequent bites are capable of transmitting malaria to a new subject.



### 1.3 Pathogenesis

The parasites presence inside the erythrocytes causes significant changes in the RBC membrane in order to replicate and avoid detection. Protuberances called *knobs*, consisting in specific proteins of the parasite (HRP-"*histidin rich protein*"), appear on the RBC membrane and adhesion of parasitized erythrocytes on vascular endothelium lead to the formation of *rosettes* (aggregates composed by a parasitized red blood cell surrounded by RBC not parasitized and 4-hydroxynonenal [4-HNE]).<sup>5</sup> The phenomenon of adhesion and occlusion of capillaries together with the high production of inflammatory factors, such as NO and TNF, is responsible of tissue damage, hypoxia and metabolic acidosis that characterize cerebral malaria and cause its symptoms.<sup>6</sup>

Anemia, that can be observed in cases of severe malaria (SMA), is a complication caused by *P.falciparum* due to the loss of parasitized or not parasitized erythrocytes, coupled with a reduced erythropoiesis.<sup>7</sup> That can be characterized by a reduction of the number of circulating reticulocytes, a normal or increased production of erythropoietin (EPO) and the altered morphology of erythroid precursors.<sup>8,9</sup>

### 1.4 Red Blood Cells Membrane Remodeling

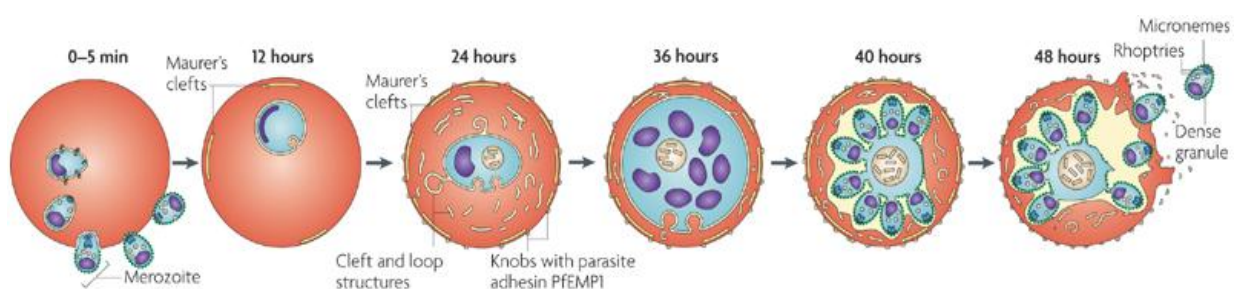


Figure 1.4<sup>10</sup>

The Plasmodium parasite is one of the few pathogens able to invade and overtake mature erythrocytes. In order to infect these cells, the parasite creates a localized disorganization of the RBC membrane architecture, introducing various features, like adhesive and permeability properties, necessary for its survival (**Figure 1.4**).<sup>11-13</sup>

A group of parasite proteins, a complex called exportome, is responsible for the modifications imposed on the erythrocytes membrane, and a complex mechanism regulates the trafficking of these proteins over the plasma membrane and the parasitophorous vacuole (PV) in which the parasite resides and selectively direct them at specific sites of the host cell.<sup>14-17</sup>

The exported proteins modify the architecture of the erythrocyte membrane, affect its elasticity and facilitate the transport of adhesins on the surface of red blood cell. To regulate proteins transport within the red blood cell, the parasite develops new membranous structures in the cytoplasm of the host cell, known as the tubulovesicular network and Mauer's clefts.<sup>18-20</sup>

The human erythrocyte is a highly specialized cell, tasked of carrying oxygen to the tissues. While the terminal stages of maturation lead to a loss of the nucleus and the ability to synthesize protein, its membrane allows him to make a journey of over 500 km inside the blood vessels, suffering extreme deformations without incurring in any lethal fragmentation.<sup>21</sup> This remarkable elasticity and resistance is conferred by the presence of a hexagonal membrane skeleton consisting in spectrin heterodimers, which associate to form tetramers.<sup>22</sup> The deformability of the red cell membrane is partially due to the structural flexibility of the linker that connect the helical tetramers of spectrin and in part to the ability of tetramers to associate and dissociate to accommodate the distortions imposed by the circulation in the blood vessels,<sup>23-26</sup> and genetic defects of the proteins that compose the membrane skeleton results in hemolytic anemia.<sup>27-29</sup>

The lack of a phagocytosis mechanism is one of the first problems that the parasite has to face to initiate the infection. In the initial stages the surface proteins of the merozoite, EBA175 and EBA140, bind to sialoglycoproteins and glycoporine A and C present on the membrane of the red blood cell, or otherwise use proteins capable of promoting invasion strategies independent from the presence of sialic acid.<sup>10</sup>

After a bond between the two cells is established, the activation of an actine-miosine motor<sup>30</sup> allows the penetration into the host cell. Simultaneously, lipids and proteins, including proteases, are secreted on the red blood cells membrane by some organelles known as rhoptri, micronemes and mononemes.<sup>31</sup> The proteolytic activity

of these enzymes destroys the normal architecture of the cell membrane and its connections with the skeleton that supports it, releasing the membrane proteins.<sup>32-34</sup>

In this phase of the invasion, the merozoite induces invagination of the membrane free of surface proteins,<sup>35</sup> initiating the PV formation and completing the cell invasion.<sup>36</sup>

During the final stages of the invasion, proteins secreted from rhoptries and dense granules are secreted into the PV and are transported, together with other proteins characteristic of the early stages, in the cytoplasm of the host cell, in order to initiate the cascades of events required for the remodeling of cell.<sup>37,38</sup> The erythrocytes containing mature forms of new merozoites are sequestered in various organs and removed from the bloodstream. The changes made by the plasmodium to the membrane give the RBC the ability to adhere to the endothelium via the formation of knobs (**Figure 1.5**), mainly consisting of *knob-associated His-rich protein* (KAHRP). These knobs act as platforms that expose a membrane protein responsible for adhering to endothelial cells and other vascular elements, called *P. falciparum* erythrocyte membrane protein 1 (PfEMP1).<sup>10</sup>

Through this adhesion process the parasite is able to prevent phagocytosis by the spleen, and is associated with lethal complications such as cerebral and placental malaria.<sup>39,40</sup> During the development of the parasite new structures extend from the PV membrane (PVM) in the cytoplasm of the host cell, forming the tubulovesicular network (TVN),<sup>40,41</sup> and Maurer's clefts appear along the plasmatic membrane of the red blood cells, probably originated by TVN.<sup>10</sup>

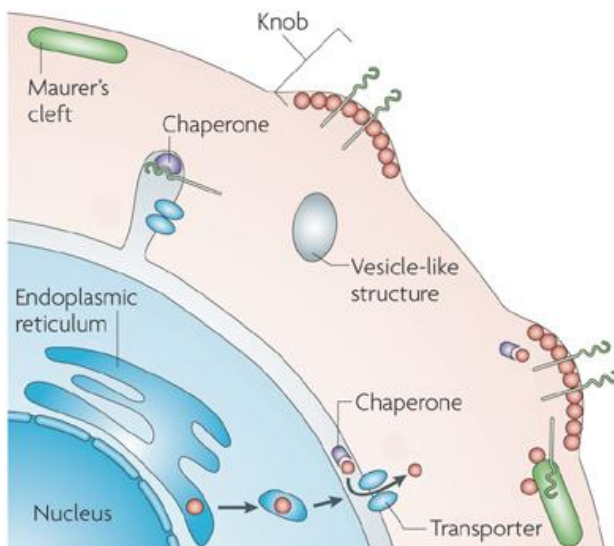


**Figure 1.5**

Maurer's clefts concentrate parasitic secretory proteins before transferring them to the erythrocyte membrane, although none of the proteins associated with these organelles showed significant homologies with enzymes that regulate the trafficking of proteins in higher eukaryotes. It has been hypothesized that the parasite developed a new

system to direct proteins through the cytoplasm of the RBC.<sup>42-44</sup>

Before the proteins can alter the cell membrane, they must cross both the PV and the PVM of the parasite to enter the cell cytosol. A hydrophobic domain at the N-terminal serves as a signal sequence that facilitate the insertion into the endoplasmic reticulum and is required for transfer the proteins through the PV. In many cases, however, the presence of pentameric sequence is required to proceed through the PVM.

The exportation of these proteins, therefore, depends on the presence in the sequence of the *Plasmodium export element* (PEXEL sequence), RxLxE/Q/D, an extremely conserved peptidic motifs identified in many *Plasmodium* species.<sup>45,46</sup> Recognition of the *Plasmodium export element* gave the possibility to predict which proteins should be exported to allow the survival of *Plasmodium* within the erythrocyte, based on its presence within a sequence.

Proteins to be exported are synthesized in the endoplasmic reticulum of *Plasmodium* and, after cleavage at the level of leucine in the PEXEL sequence and acetylation of the N-terminal, are transported into the host cell by an ATP-dependent translocone, known as complex PTEX.<sup>47</sup> Mutations of R or L residues in the sequence lead to an attenuation of the cleavage process and proteins exportation, preventing the proper maturation of the plasmodium, revealing the great importance that the PEXEL sequence has in the parasite development processes.<sup>48,49</sup>

## 1.5 Antimalarial therapies

The first treatment used against malaria was the bark of *Cinchona*, discovered in Perù in 1600 and imported in Europe by the Jesuits. In 1800, chemists Pelletier and Caventou isolated the active ingredient from the *Cinchona* bark, an alkaloid called quinine. To answer the increasing demands of this drug, the Dutch planted large crops of *Cinchona ledgeriana* in their colonies in Indonesia. *Cinchona* bark contains other anti-malarial drugs (quinidine, cinchonine, cinchonidine) but quinine was the most used of them. For centuries, despite its side effects, quinine remained the only anti-malarial drug used in therapy. During World War I, the blockade of ports and

submarine attacks hindered the supply of quinine, and gave new inputs to the research of synthetic antimalarial drugs, generating in new molecules such as pamachine, primaquine and mepacrine. The need to protect the american troops in the Pacific during World War II, encouraged the development of even more potent antimalarial drugs. These research project led to the discovery of chloroquine, amodiaquine, pyrimethamine and proguanil.

As chloroquine resistance appeared in South America and South East Asia in 1960, associations of sulfonamide with pyrimethamine and quinine with tetracycline were used. During the Vietnam War, mefloquine was discovered at the U.S. Army Research Institute "Walter Reed", but unfortunately mefloquine resistance appeared Thailand soon after its first use.

A new therapeutic agents was identified by a government sponsored project aimed to research traditional Chinese medicine to find new molecules to be used against malaria. Extract of *Artemisia annua* was traditional be used for the treatment of fevers for many years. In 1971 artemisinin, a drug with no resemblance to the previous antimalarials, was isolated from *Artemisia annua* extract, and subsequently semisynthetic derivates artemether, artesunate and arteether were synthesized. Continuous studies are currently ongoing in order to discover and synthesize antimalarial drugs more effective and safe.

**Figure 1.6** shows the chemical structures of the most common antimalarial agents.

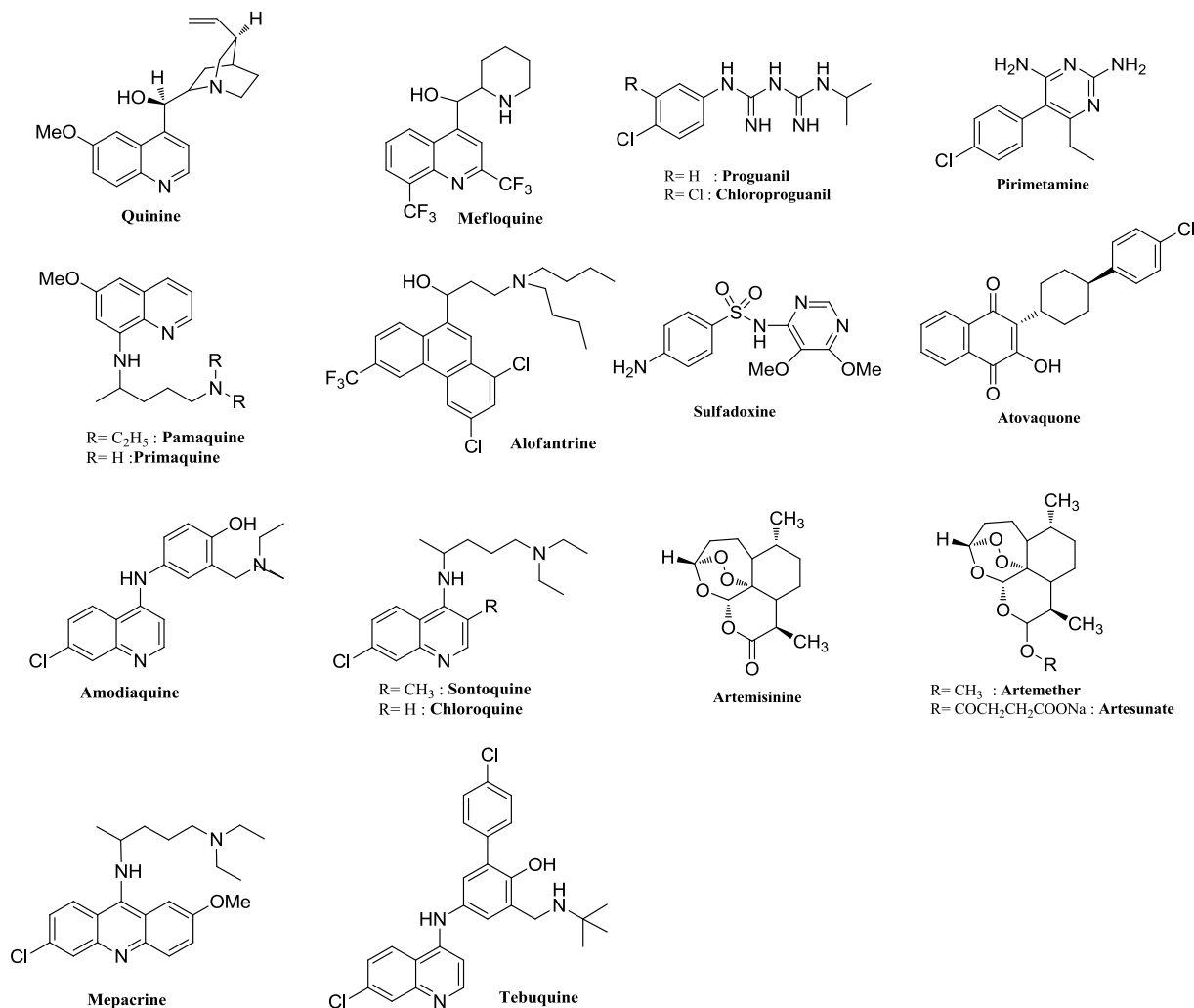


Figure 1.6

In recent years, the widespread and indiscriminate use antimalarials has prompted the development of parasites with high levels of resistance to all classes of drugs. Combining two or more antimalarial drugs, with additive or synergistic action, may be used as a way to overcome parasite resistance. The ultimate goal is the effective elimination of the parasite, that can be achieved with the right combination of drugs with different properties.

The half-life is an important parameter to be considered: if the component with lower half-life can eliminate most of the parasites (such as artemisinin and its derivatives), the second compound, with a longer half-life (eg. mefloquine and lumefantrine) is able to eliminate the few remaining parasites, decreasing the risk of developing resistance.<sup>50</sup>

Studies demonstrated that the synergistic interaction between atovaquone and proguanil (Malarone), is active against *P. falciparum* chloroquine resistant strains. The association between cycloproguanil and dapson (Lapdap) is another combination used in clinical study.

Artemisinin and its analogues are frequently used in combination therapy due to their excellent chemical-physical properties, such as rapid-action, short half-life, limited toxicity and activity towards multi-drug resistant strains.

Artemeter and lumefantrine in combination (Coartem) is effective against *P. falciparum* multidrug resistance and present no serious side effects. Other interesting combinations are artesunate (similar to artemisinin), with mefloquine, sulfadoxine-pyrimethamine or dapson-chloroproguanil.<sup>51;52</sup> However in 2006, the first case of resistance to artemisinin has been reported at the border between Thailand and Cambodia.<sup>53</sup>

In 2011, the European Medicines Agency has approved Eurartisim, association of Diidroartemisin-piperaquine, developed by Sigma-Tau in collaboration with Medicines for Malaria Venture.

## 1.6 Resistance

Resistance of *P. falciparum* against quinolines and in particular chloroquine led to an increase in the number of deaths caused by malaria.<sup>54</sup> The areas characterized by the presence of parasites resistant to chloroquine or mefloquine are showed in **Figure 1.7**.

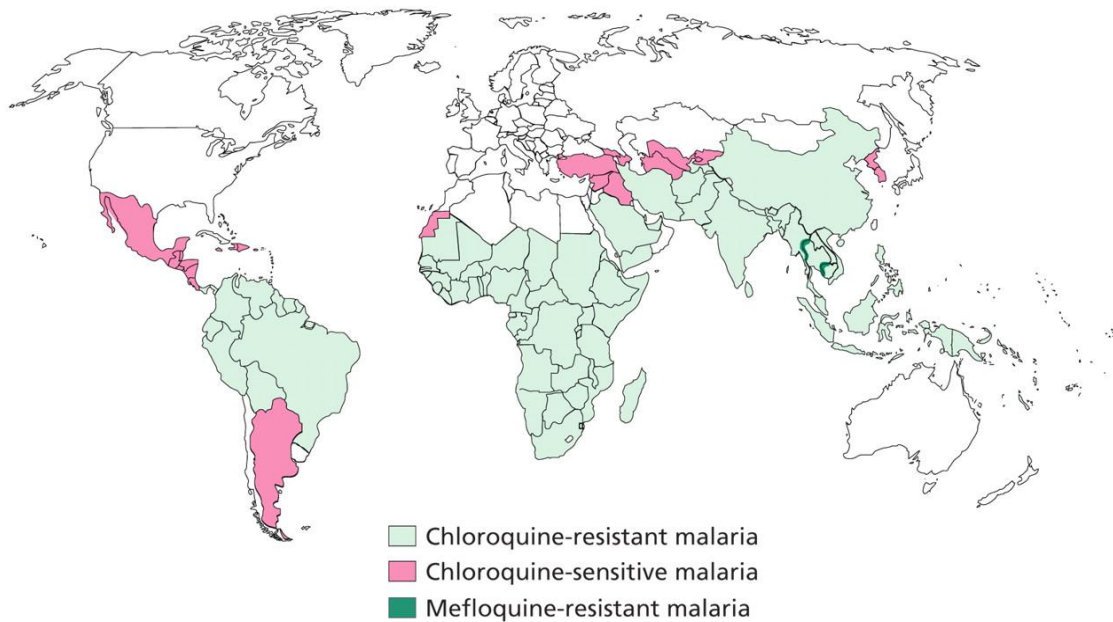


**Figure 1.7**

Chloroquine resistance is associated with a reduction drugs accumulated inside the digestive vacuole.<sup>54</sup>

Both genetic and biochemical studies have attempted to explain the mechanism involved in chloroquine resistance.

These theories include:

- Alteration of the  $\text{Na}^+/\text{H}^+$  pump, causing an increase in cytoplasmic pH and a reduction chloroquine uptake;<sup>55</sup>
- *Pfmdr* amplification, a gene involved in the overexpression of the protein Pgh-1;
- Digestive vacuole membrane mutations: *P. falciparum* chloroquine resistance transporter (PfCRT).



Martin and colleagues, in recent studies, showed the correlation between the PfCRT mutations and the chloroquine resistance.<sup>56</sup> This protein is localized in the digestive vacuole membrane and has ten transmembrane domains.

When a mutation of this protein occurs, in particular at Lys76 (K76T), it causes a modification of the first transmembrane domain and significant increase of chloroquine resistance is observed. Reed *et al.* have shown that the mutation of the protein Pgh-1 contributes not only to the chloroquine resistance but also modulate the resistance to other compounds such as mefloquine, alonfantrine and quinine.<sup>57</sup>

Interestingly compounds strictly analogous to chloroquine are active on chloroquine-resistant strains, demonstrating that the resistance is not due to target changes, but it is compound-specific.

Mitochondrial DNA (mtDNA), with 6 kb of length, is quite unusual in malaria parasites and is the shortest mtDNA known;<sup>58;59</sup> it is highly conserved and encodes for only three proteins (subunits I and II of cytochrome oxidase c and cytochrome b).

Resistance to various cytochrome bc<sub>1</sub> complex inhibitors is characterized by mutations in a defined region coding for the cytochrome b sequence and mutation in these region may explain the different toxicity of different hydroxynaphthoquinonic antimalarial.<sup>58;59</sup> The region of the cytochrome b implicated in the mechanism of resistance is part of the catalytic domain, site Q<sub>0</sub>, in which ubiquinol is oxidized by the complex bc. Mutations observed in *P. yoelii* resistant covers a region of 15 amino acids surrounding the highly conserved sequence of the cytochrome PEWY B.<sup>58;60;61</sup> Mutations alter the hydrophobicity and the volume of part of the binding cavity: therefore even slight variations can affect the affinity of atovaquone towards cytochrome bc<sub>1</sub>.<sup>58</sup> Resistance to atovaquone is rapidly observed in *P. falciparum* infections when it is used as a single agent, and experimental evidence have shown that parasites that become resistant to atovaquone are also resistant to the synergistic effects of proguanil, to which atovaquone is usually associated.<sup>58</sup>

Combination therapy based on derivatives of artemisinin or ACT (artemisinin combination therapy) provides an important alternative to quinoline derivatives.

In the last decade almost all countries with endemic malaria adopted this ACT for the treatment of *P. falciparum* malaria. Artemisinin has a very short half-life and is

rapidly eliminated from the body due to glucuronidation by CYP 2B6.<sup>3</sup> For this reason, this molecule is usually associated with long half-life antimalarial drugs such as piperazine or amodiaquine.<sup>3</sup> In 2006 the first case of resistance to artemisinin was reported in Ta Sanhal, a small city near the border between Thailand and Cambodia. The cause of resistance to artemisinin in South-East Asia has been attributed to the widespread use of this drug as monotherapy.<sup>62</sup>

The World Health Organization (WHO), even before the artemisinin resistance was reported, banned artemisinin monotherapy to delay the development of resistance and protect these important derivatives for antimalarial therapy.

In Vietnam, artemisinin is used to control malaria since 1989, and although current national guidelines recommend the use ACT, artemisinin and artesunate monotherapy are still widely available through the private sector. Vietnam is also one of the few countries where artemisinin monotherapy led to a highly successful program for the malaria control, with reported cases of malaria falling sharply from 1,672,000 with 4,650 deaths in 1991, 91,635 clinical cases with 43 deaths in 2006.<sup>62</sup>

Current data suggest that resistance to artemisinin is simply a natural consequence of the massive use of ACTs in South East Asia.<sup>53</sup>

## **1.7 Natural products privileged scaffolds in drug discovery**

Parasite resistance to many of agents currently employed in therapy is one of the main issues that hinder malaria eradication.

In the quest for new therapeutics, natural products (NPs) have been an invaluable source of drug leads over many years.<sup>63-66</sup> Natural products have played a dominant role in the cancer therapeutic area where, over the last 30 years, 74.8% of approved drugs are either natural products, based on natural products, or mimics of natural products.<sup>67</sup> Up to 2006, 24 unique chemotypes from natural products produced 49 marketed drugs.<sup>68</sup> Numerous scaffolds identified in natural products have led to approved drugs or drug candidates for a range of diseases. Examples include antibacterials ( $\beta$ -lactams, tetracyclins, erythromycins), antivirals (modified

nucleosides), anticholesterolemic (lovastatin), and anti-tumour agents (rapamycins, epothilones).<sup>69</sup>

Two recent reviews highlight the past achievements of natural products in providing new drugs, while at the same time providing a realistic evaluation of commitment within the pharmaceutical industry in the area of discovering new natural product drugs.<sup>70,71</sup>

Harvey highlights the seminal work of Snader on drug prototypes.<sup>65</sup> This work on the prototypes, the initial lead molecule developed to a candidate drug and then a marketed therapeutic, indicated that more than 80% of drug substances were natural products or inspired by natural products.

While Harvey articulates the perceived disadvantages of NPs as difficulty in access and supply, complexities of natural product chemistry, inherent slowness of working with natural products, concerns about intellectual property rights and hopes associated with the use of collections of compounds prepared by combinatorial chemistry methods, the review demonstrates the need to develop new approaches to take advantage of NPs. Shoichet *et al.* have examined the systematic absences in chemical biology/screening libraries and found that 83% (12,977) of core ring scaffolds present in natural products were absent from commercial collections.<sup>72</sup> Their analysis suggests that collections that include molecules containing scaffolds present in natural products will provide better opportunities to find both screening hits and chemical biology probes.

---

## 2. Aim of the Research

Malaria causes 300 to 500 million clinical cases and more than 2.7 million deaths annually, almost entirely localized in Africa tropical regions and mostly involving children under the age of 5.<sup>73</sup> There are four species that can cause this disease in humans: *Plasmodium falciparum* (Pf), *Plasmodium vivax* (Pv), *Plasmodium ovale* (Po) and *Plasmodium malariae* (Pm). Pf is the most virulent and is responsible for the high infant mortality. One estimate puts 40% of the world population in areas at risk of contagion and the threat is increasing in recent years due to global climate changes, insurgence of parasite strains resistant to drugs traditionally used and an increase in international travels.

Despite the existence of effective therapies, the living conditions in most of the areas affected by the disease limit their use. Also, given their widespread use, low-cost drugs currently available are those against which the parasite has developed resistance, so there is a dire need of new antimalarial able to overcome the disadvantages of the drugs still in use, such as resistance and high costs.

Plasmepsin V (PMV), the enzyme responsible for cutting the sequence PEXEL, plays a critical role in the maturation of merozoites during the early blood stages,<sup>74,75</sup> regulating the translocation of parasite proteins on the membrane of the red blood cells. Due to this central role in the onset and propagation of the disease, the inhibition of its activity appears to be a promising therapeutic target. The belonging of this enzyme to the family of aspartic proteases allows the use a classic approach in the development of new inhibitors.

### 2.1 Plasmepsins

The aspartic proteases present in the *Plasmodium* are considered one of the most promising target for the development of new antimalarial.<sup>76</sup> To date, four homologous aspartic proteases have been characterized in detail, called plasmepsins (PMs). These four plasmepsins (PMI, PMII, PMIV and HAP), are digestive vacuole enzymes that are actively involved in hemoglobin degradation<sup>77,78</sup> and may also been

involved in the degradation of spectrin II and plasmepsin IV.<sup>79,80</sup> The inhibition of these enzymes effectively blocks the parasite growth, and for this reason, plasmepsin have been considered as a possible therapeutic target.<sup>78,81,82</sup> Six additional genes coding for plasmepsin<sup>76</sup> and the mRNA of three of these genes (PMV, IX and X) are present in early stages of *Pf* infection.<sup>78</sup> Immunofluorescence analysis showed that these plasmepsin are not localized in the digestive vacuole and, therefore do not take part in hemoglobin degradation.<sup>78</sup> Recently, plasmepsin V (PMV) role has been clarified.<sup>74,75</sup> This enzyme, localized in the endoplasmic reticulum, cleaves the PEXEL sequence that signals the need to export a protein. Aligning the sequence of PMV with other aspartic proteases of eukaryotic organisms showed many regions of high homology, revealing conserved structural and catalytic residues.<sup>83</sup> In **Figure 2.1**, aspartate residues of the catalytic site are highlighted in yellow. A cysteine-rich region (**Figure 2.1**, blue), whose function has yet to be elucidated, has been identified in many aspartic proteases of plant origin.<sup>84</sup> The C-terminal portion of the sequence contains a sequence of 25 hydrophobic aminoacids, whose function is to anchor the enzyme to the endoplasmic reticulum (**Figure 2.1**, red), and 15 other hydrophobic aminoacids are present in the N-terminal region, which serve as a signal sequence for the secretory system (**Figure 2.1**, green).<sup>83</sup>

10	20	30	40	50	60
MNNYFLRKEN	<b>FFILFCFVFV</b>	<b>SIFFV</b> SNVTI	IKCNNVENKI	DNVGKKIENV	GKKIGDMENK
70	80	90	100	110	120
NDNVENKNDN	VGNKNDNVKN	ASSDLYKYKL	YGDIDEYAYY	FLDIDIGKPS	QRISLILDTG
130	140	150	160	170	180
SSSLSFPCNG	CKDCGIHMEK	PYNLNYSKTS	SILYCNKSNC	PYGLKCVGNK	CEYLQSYCEG
190	200	210	220	230	240
SQIYGFYFSD	IVTLPSYNNK	NKISFEKLMG	CHMHEESLFL	HQQATGVLGF	SLTKPNGVPT
250	260	270	280	290	300
FVDLLFKHTP	SLKPIYSICV	SEHGGELIIG	GYEPDYFLSN	QKEKQKMDKS	DNNSSNKGNV
310	320	330	340	350	360
SIKLNNDKN	DDEENNSKDV	IVSNNVEDIV	WQAITRKYYY	YIKIYGLDLY	GTNIMDKKEL
370	380	390	400	410	420
DMLVD <b>D</b> SGSTF	THIPENIYNQ	INYYLDILCI	HDMTNIYEIN	KRLKLTNESL	NKPLVYFEDF
430	440	450	460	470	480
KTALKNIIQN	ENLCIKIVDG	VQCWKSLENL	PNLYITLSNN	YKMIWKPSSY	LYKKESFWCK

---

```

      490          500          510          520          530          540
GLEKQVNNKP ILGLTFFKNK QVIFDLQQNQ IAFIESKCPN NLTSSRPRTF NEYREKENIF

      550          560          570          580          590
LKVSYINLYC LWLLLALTIL LSLILLYVRKM FYMDYFPLSD QNKSPIQEST

```

**Figure 2.1**<sup>83</sup>

Experiments conducted by Klemba and Goldberg and have confirmed that the PMV is an integral membrane protein.<sup>83</sup> Despite PMV is related to the other nine plasmepsin present in *P. falciparum*, there is only a 17% identity with the sequence of mature PMII, while the identity between PMII and PMIV, both vacuolar plasmepsin, reaches 70%.<sup>76,85</sup> During the course of the 44 hours necessary to complete a replication cycle of *P. falciparum*, the PMV is observed in small amounts during the first 12 hours. Its concentration increases during trophozoite (between 24 and 31 hours) and schizont (between 31 and 41 hours) maturation. This increase of protein levels during development is similar to that observed for the digestive vacuole plasmepsin.<sup>78</sup> In many aspartic proteases a specific region blocks the catalytic site and maintains the enzyme in an inactive state during translocation until it reaches its final destination.<sup>86</sup> Plasmepsin I, II, IV and HAP possess a proregion including a transmembran dominion that anchor the proenzyme to the membrane during translocation into the digestive vacuole. The analysis of PMV proregion (**Figure 1.6**, underlined) of different Plasmodium species has revealed a high variability of the sequence, indicating the lack of important requirements for the structural or functional features of this region and supports the hypothesis that PMV is transported into the endoplasmic reticulum in unfolded and, therefore, does not require a mechanism to inhibit its activity.<sup>83</sup> This mechanism has been observed in other aspartic proteases, including BACE, in which the proregion contributes to the correct folding of the catalytic site,<sup>87</sup> and may have a similar role in PMV. In vitro inhibition of this enzyme was obtained using high concentrations of HIV protease inhibitors or pepstatin A, while other classes of inhibitors were ineffective. BACE inhibitors have little effect on the activity of PMV, probably due to the large evolutionary distance present between these two enzymes.<sup>75</sup>

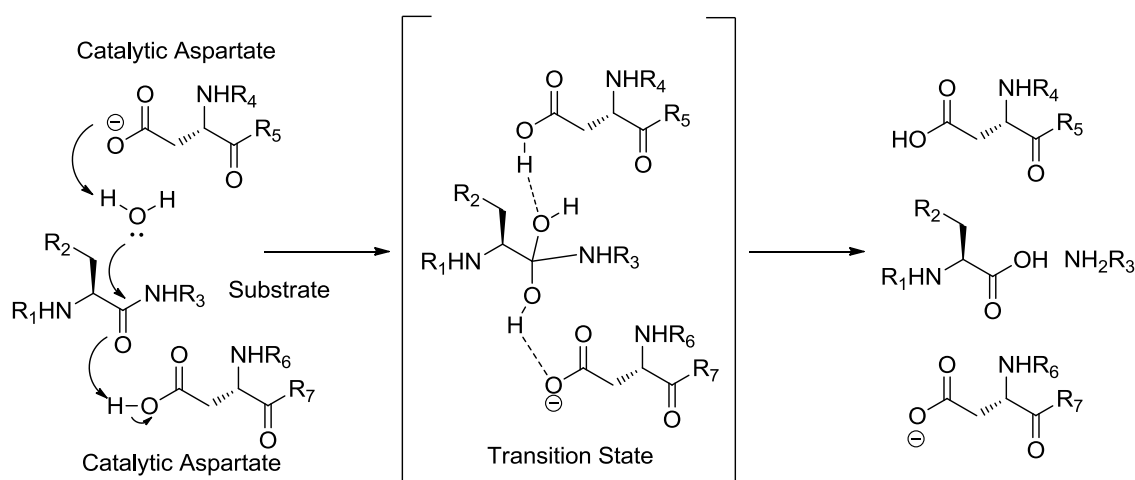
Further studies have shown that PMV is a essential protease present in the endoplasmic reticulum and *P. falciparum* parasite modified with a deletion of the

transmembrane portion were unable to mature.<sup>83</sup> While these results are promising, the lack of an efficient inhibitor of this enzyme limits the studies that could be performed to assess the viability of PMV as a new antimalarial target. With this work, we aim to synthesize peptidomimetic inhibitors to assess the structural and chemical requirements of the enzyme catalytic site, and compare them to the features present in recognized natural sequences. Data obtained will be used to design a set of compounds with reduced peptidic nature, that may be used as a starting point for a new series of antimalarial compounds. The main goal is to understand the therapeutic potential of PMV inhibition.

### 3. Discussion

#### 3.1 Aspartic proteases inhibition

The aspartic proteases are a family of proteolytic enzymes, mainly active at acid pH. The mechanism of action of these enzymes consist of the establishment of an acid-base system which involves the two aspartates of the active site and a water molecule positioned between the two. The two aspartic acid residues act as a proton acceptor and donor, respectively, catalyzing the hydrolysis of the protein substrate. The water molecule is partially activated by an aspartate and performs a nucleophilic addition on a specific carbonyl of the peptide sequence: the carbonyl oxygen, in turn, captures a proton from the second aspartic acid of the active site, generating the tetrahedral intermediate, which converts into a stable product, resulting in the cleavage of the peptide sequence (**Scheme 3.1**).<sup>88</sup>



Scheme 3.1

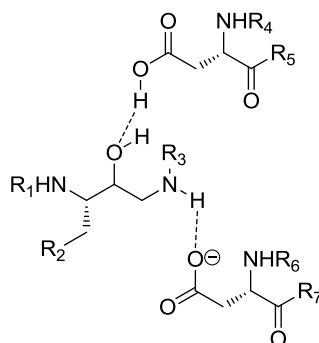
Being part of fundamental processes in the development of various pathologies, the aspartic proteases have been for a long time the subject of study for the development of inhibitors that could block their activity and thus reduce the onset or development of diseases. Among the most known and studied there are renin, an integral part of the renin-angiotensin-aldosterone system that regulate blood pressure; BACE, responsible for the amyloid precursor protein cleavage, and HIV viral aspartic



proteases. The inhibition of these proteases has become an important therapeutic approach for the treatment of erectile disfunction, Alzheimer and AIDS.<sup>89</sup>

The primary method used to inhibit the aspartic proteases is the use of bioisoster of the peptide bond that mimic the tetrahedral intermediate generated during the hydrolysis of the amide bond. The design of inhibitors of aspartic proteases exploits the formation of the transition state by introducing within the molecule an isosteric group that mimics the conformation of the intermediate, but it is not subject to the proteolytic activity of the enzyme. Isosteric groups as hydroxyethylaminic, hydroxyethylsulphidic and hydroxyethylureidic have successfully been used in the development of renin, viral protease and BACE inhibitors.<sup>88</sup>

Following the identification of the PMV as a promising therapeutic target in the treatment of malaria, prof. Romeo's group synthesized peptidic inhibitors of the enzyme, mimicking the PEXEL sequence but introducing an hydroxyethylamine moiety in place of the labile peptide bond, capable of effectively mimic the substrate transition state (**Scheme 3.2**).



**Scheme 3.2**

The HEA group was introduced within a sequence PEXEL replacing the peptide bond between the leucine and alanine. The first compound designed wanted to imitate as much as possible the sequence of the PMV substrate, RxLxE/Q/D (**Figure 3.1**).

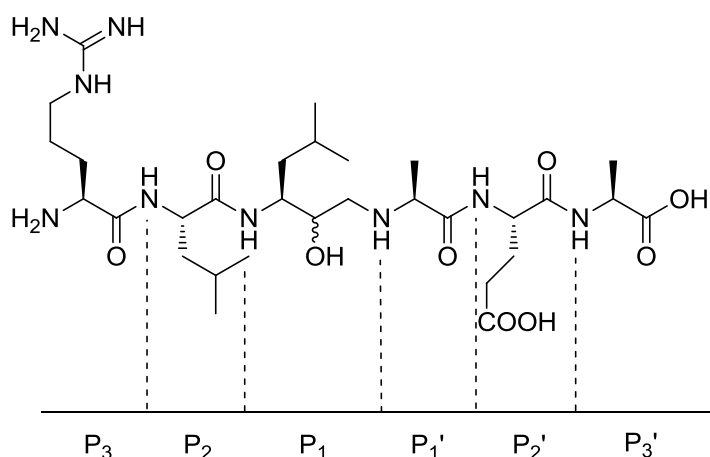


Figure 3.1

The amino acids present in the various positions have been modified to study the interactions required to effectively inhibit the enzyme. Leucine(HEA) was maintained constant and multiple substitutions in other positions in the sequences were introduced. Since the localization of plasmodium within the red blood cell implies that PMV inhibitors should be able to cross biological membranes, the amount of charged residues in the sequences were kept to a minimum to allow the penetration of lipophilic membrane. The position **P3** was the most studied due to its extreme conservation in the natural PEXEL sequences. Arginine is a basic amino acid with a long side chain, with a positive charge delocalized on the guanidine group at physiological pH, and these studies demonstrate how most modifications in the **P3** position led to inactive compounds. The compounds synthesized are shown in **Table 3.1**.

The compounds generated by prof. Romeo's group are the first reported PMV inhibitors, but they were unable to inhibit parasite growth probably due to their unfavorable pharmacokinetic properties.<sup>90</sup>

Compound	N-terminal	P <sub>3</sub>	P <sub>2</sub>	P <sub>1</sub>	P <sub>1</sub> '	P <sub>2</sub> '	P <sub>3</sub> '	C-terminal	PMV IC <sub>50</sub> (nM)
LG21	H	Arg	Leu	Leu-HEA	Ala	Glu	Ala	OH	4
LG25	H	Met	Leu	Leu-HEA	Ala	Glu	Ala	OH	inactive
LG26	H	Gln	Leu	Leu-HEA	Ala	Glu	Ala	OH	4900
LG20	H	Arg	Leu	Leu-HEA	Ala	Glu	Ala	NH <sub>2</sub>	1.6
LG22	H	Arg	Ile	Leu-HEA	Ala	Glu	Ala	NH <sub>2</sub>	228
LG23	H	Lys	Leu	Leu-HEA	Ala	Glu	Ala	NH <sub>2</sub>	3300
LG29	H	His	Leu	Leu-HEA	Ala	Glu	Ala	NH <sub>2</sub>	174
LG30	H	Trp	Leu	Leu-HEA	Ala	Glu	Ala	NH <sub>2</sub>	3
LG37	H	Tyr	Leu	Leu-HEA	Ala	Glu	Ala	NH <sub>2</sub>	3000
SV01	H	Arg	Leu	Leu-HEA	Ala	Gln	Ala	NH <sub>2</sub>	1.04
LG32	H	Lys	Leu	Leu-HEA	Ala	Gln	Ala	NH <sub>2</sub>	14000
LG48	H	Trp	Leu	Leu-HEA	Ala	Gln	Ala	NH <sub>2</sub>	700
LG33	Bz	Lys	Leu	Leu-HEA	Ala	Gln	Ala	NH <sub>2</sub>	inactive
LG34	Ac	Arg	Leu	Leu-HEA	Ala	Gln	Ala	NH <sub>2</sub>	75.6
LG38	H	Arg	Leu	Leu-HEA	Tyr	Glu	Ala	NH <sub>2</sub>	0.8
LG44	H	Arg	Leu	Leu-HEA	Tyr	Gln	Ala	NH <sub>2</sub>	10
LG45	H	His	Leu	Leu-HEA	Tyr	Gln	Ala	NH <sub>2</sub>	5000
LG35	Ac	Lys	Leu	Leu-HEA	Pro	Gln	Ala	NH <sub>2</sub>	inactive
LG40	H	Lys	Leu	Leu-HEA	Ala	Glu	X	NH <sub>2</sub>	1140
LG46	H	X	Trp	Leu-HEA	Tyr	Gln	Ala	NH <sub>2</sub>	inactive

Table 3.1

### 3.2 Compounds stereochemistry

Compounds generated using SPPS procedures present an undefined stereocenter due to the unselective reduction used in the HEA synthesis. During purification of compounds **2**, **3**, **4**, **6**, **8** and **9** it was possible to isolate a main peak and a secondary peak with the expected mass, probably corresponding to the two diastereoisomers.

Biological testing revealed that the secondary peak possess, in all the instances, an inhibitorial activity lower than the main one. This different activity was already been observed by different research group working with HEA inhibitors of BACE-1. In these cases, the (R)-HEA moiety always showed a better activity compared against the same compound containing the (S)-HEA group.<sup>91</sup>

Literature data, also, report that unselective reduction of a carbonyl moiety during solid-phase synthesis preferentially generate the (R)-HEA over the (S)-HEA with a *syn-anti* ratio of 80:20 similar to the one observed in the synthesis of these class of compounds.<sup>92,93</sup>

Experiments to determine the absolute configuration of these compounds are currently ongoing.

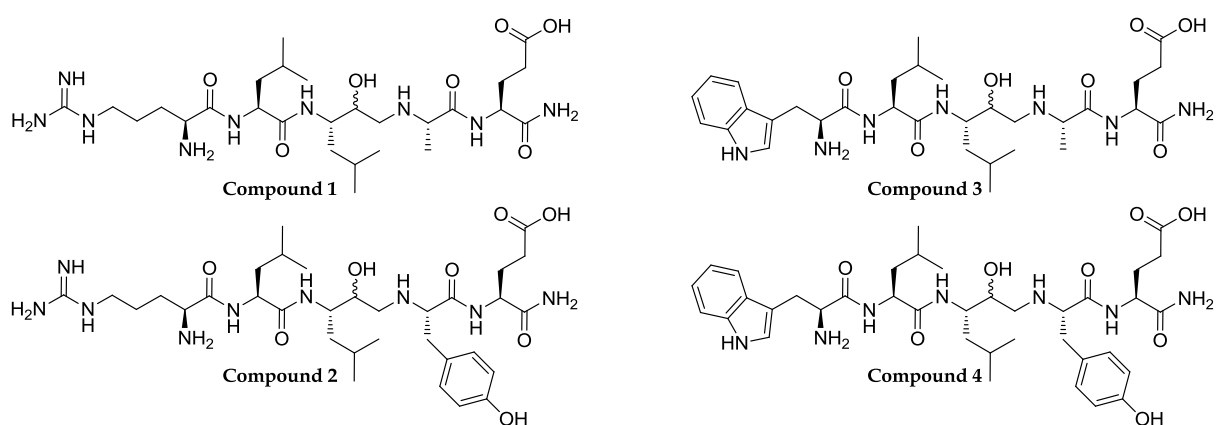
### 3.3 SAR studies on peptidomimetics

The first step in this research project was to increase the amount of structure-activity relationships of this class of compounds. Previous work was mainly focused on sampling the enzyme tolerance to different aminoacidic residues in the **P3** position of the sequence. This position is the most conserved, and as expected very few modifications led to sequences recognized by the enzyme. Building upon that knowledge, my work aimed to assess the other position on the sequence in order to reduce the peptidic nature of this inhibitors and trying to achieve an inhibition of plasmodium growth.

### 3.3.1 P3' position

In compounds **1-4** (Figure 3.2) the C-terminal alanine was removed. This amino acid was originally added to balance the compounds length, and it is not part of any specific PEXEL sequences.

P3' modifications does not seem to affect the activity of compounds **1** and **2**, presenting an arginine in **P3**, but a complete loss of activity has been observed in previously active sequences containing a Trp in **P3** (Compound **3** and **4**). As observed in previous sequences, introduction of Tyr in **P1'** slightly decrease the IC<sub>50</sub>, but it's still considered a favorable modification since allows an easier purification process.



Compound	<i>Pf</i>	<i>Pf</i>
	PMV IC <sub>50</sub> [nM]	3D7 IC <sub>50</sub> [μM]
1	0.25	>200
2	1.1/19.9	>200
3	inactive	ND
4	inactive	ND

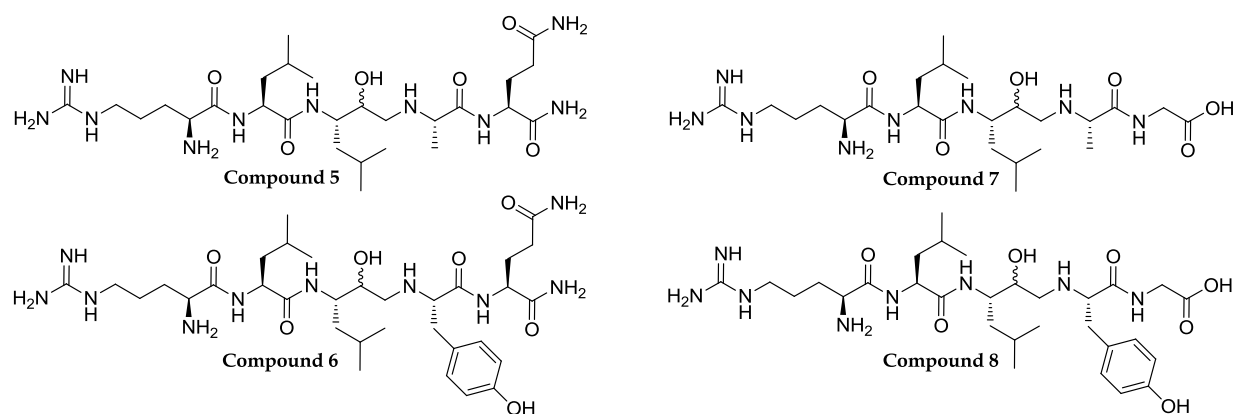
Figure 3.2

### 3.3.2 P2' position

Compounds **5-8** (Figure 3.3) were synthesized in order to test the requirements present in **P2'**. Looking at the PEXEL sequences found in nature, the residue present

in this position is less conserved than the one occupying **P3** and **P1**, but usually sports an acidic sidechain. Glutamic acid, aspartic acid and glutamine are equally found in this position when analyzing natural PEXEL sequences. Trying to understand the role of the acid group presents on the aminoacid sidechain, compounds **5** and **6**, presenting a Gln residue in position **P2'**, were synthesized. While active, these compounds showed a nine-fold and a twenty-fold reduction in activity when compared with compounds **1** and **2**. This shows that, while not necessary, the strong interaction of a glutamate residue in the **S2'** is important for the activity of this class of compounds.

To further explore the requirements of this pocket, a Gly residue was introduced (compounds **7** and **8**). In order to maintain an acidic moiety in that position, the peptidomimetics were synthesized using 2-chlorotritylic resin, in order to obtain a carboxyterminal sequences. These compounds showed a good IC<sub>50</sub> against PMV, and performed slightly better than compounds **5** and **6**, while still being less active than compounds **1-2**.

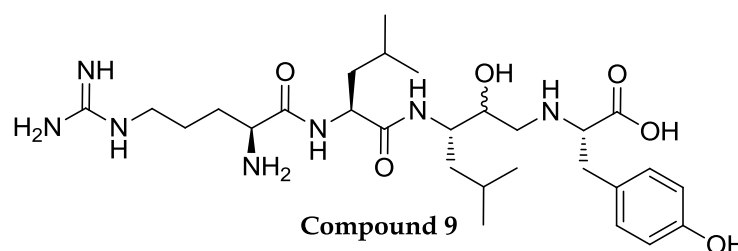


Compound	<i>Pf</i> PMV IC <sub>50</sub> [nM]	<i>Pf</i> 3D7 IC <sub>50</sub> [μM]
<b>5</b>	9	>200
<b>6</b>	20/138	>200
<b>7</b>	10	>200
<b>8</b>	2/78	>200

Figure 3.3

The last modification introduced was the complete removal of the aminoacid from the **P2'** position (**Figure 3.4**). For synthetic reasons, the sequence synthesized was the one containing a carboxyterminal Tyr, easier to purify. This compound maintains only the two highly conserved residue Arg (in **P3**) and Leu (in **P1**), but lacks the acidic residue in **P2'**.

As expected, compound **9** is almost unable to inhibit PMV activity, with an  $IC_{50}$  in the micromolar range, opposed to the other member of this class of inhibitor, that are usually in the low nanomolar range.



Compound	<i>Pf</i> PMV $IC_{50}$ [nM]	<i>Pf</i> 3D7 $IC_{50}$ [μM]
9	2500/9200	>200

Figure 3.4

### 3.4 Antiplasmodial activity of compounds 1-9

Compounds **1-9** were tested for antimalarial activity against *P. falciparum* cultures. Despite their high inhibitory activities against PMV, these compounds were unable to block parasite proliferation, as it was observed in compounds of the same class previously synthesized. This could be attributed to the highly peptidic nature of these molecules, which can hinder the peptidomimetic ability to cross biological membranes. In order to reach its site of action localized in the endoplasmic reticulum, the compounds need to cross three different biological membranes (RBC membrane, PV membrane and finally the parasite membrane), each with different physiological properties that may not allow the diffusion of a multiple-charged compound. Also, both the erythrocytes and the parasites contain various kinds of

proteolytic enzymes, which may be able to cleave the sequences before they reach PMV.

These factors could help to explain the poor performances of these compounds when tested against *Pf* cultures. Since these problems are linked to the peptidic nature of these class of compounds, and further modifications usually led to a loss of PMV inhibition properties, a new strategy was devised in order to design a new class of compounds that could target the PMV pathway, but without all the inherent complications arising from working with peptides. A natural product privileged scaffold was selected and used as a starting point upon which a small compound library was built in order to find a better candidate for drug development.

### 3.5 Azaspirodecane scaffold

It has been observed that 83% of the cyclic scaffolds found in nature are not represented in commercially available products. These scaffolds have a complex three-dimensional structure, which could be exploited for biological interactions. An analysis performed by the research group of prof. Quinn (Eskitis Institute, Brisbane, Australia) has shown that these scaffolds, which are often main structural features of the molecule, are found in many natural products extracted from different biological sources. These structures, therefore, offer a versatility that can be exploited to obtain a suitably substituted compound possessing the characteristics of the molecules from which they derive, and thus eliminating the problems resulting from the total synthesis of individual natural products. One of the structures identified by the group of prof. Quinn is the 1-azaspiro[5.5]undecane scaffold (**Figure 3.5**).

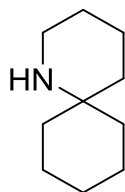


Figure 3.5



Such scaffold is contained by a diverse set of natural products. There are at least 5 distinct natural product chemical classes that have this scaffold embedded (**Figure 3.6**). The spiro-scaffold is the clear three-dimensional determinant for all these molecules. 201 known lycopodium alkaloids, of which 70 belong to the quinolizidine class, contains this scaffold. An example of this structural class is lycopodine (**Figure 3.6**).

Erythrinane alkaloids, such as erythralin (**Figure 3.6**), have been isolated from a variety of plants belonging to the genus *Erithrina*, widely used in traditional medicine to treat a number of health problems including anxiety, insomnia and inflammation. This family of compounds has been reported to have anticonvulsant, hypotensive, hypnotic, analgesic and cytotoxic effects.<sup>94-96</sup>

Cylindricines were isolated from the Tasmanian ascidian *Clavelina cylindrical*,<sup>97</sup> and the related marine natural product, fascicularin (**Figure 3.6**) has selective activity against a DNA repair-deficient yeast strain.<sup>98</sup>

Eudistone A (**Figure 3.6**) was isolated from the Seychelles tunicate *Edistoma sp.*,<sup>99</sup> while karachine (**Figure 3.6**) is a protoberberine alkaloid from *Beberis arisata*, used in the Unani system of medicine for the treatment of jaundice and skin diseases.

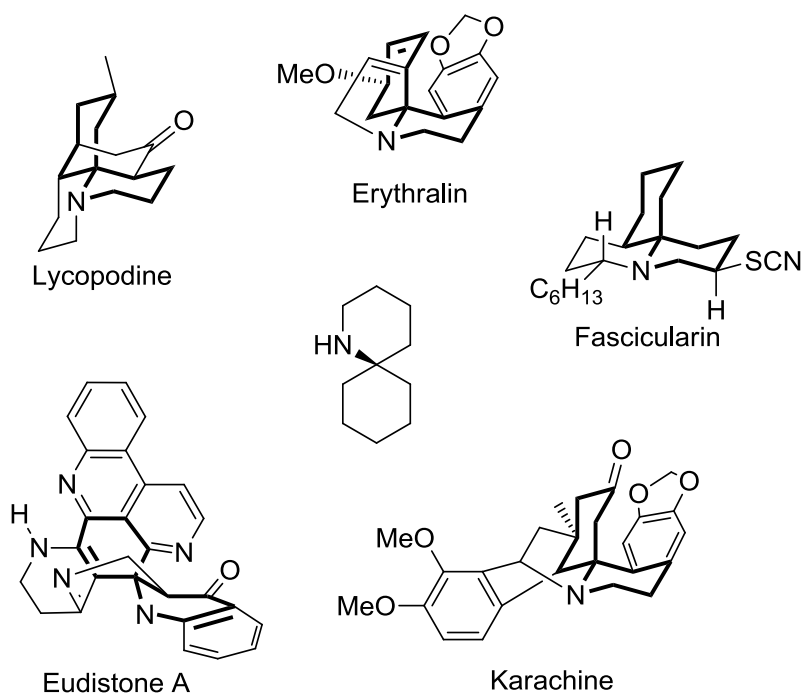


Figure 3.6

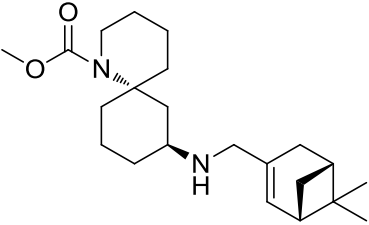
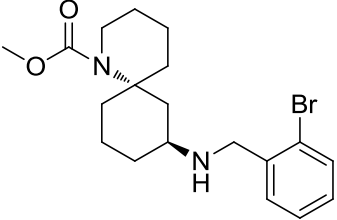
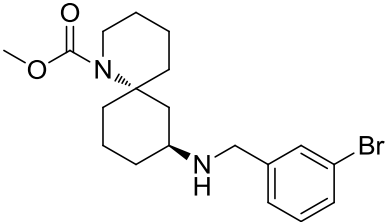
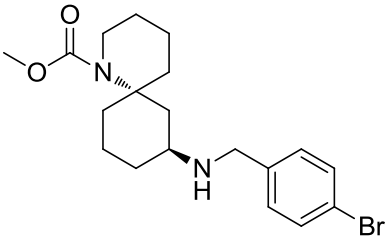
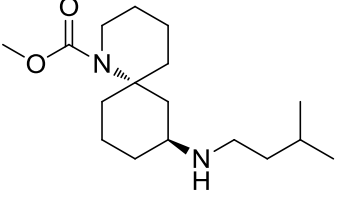
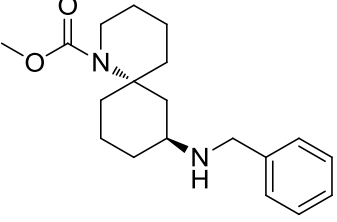
### 3.6 Scaffold library

Prof. Quinn work shows that the 1-azaspiro[5,5]undecane scaffold controls the 3D geometry of the compounds in which it is embedded. The orientation provided by the 3D geometry of the core scaffold seems to facilitate the interaction with the biological space, showed by the high proportion of active compounds in their synthetic library. Embedded 3D scaffolds occurring in natural products offer the potential to retain the biological relevant chemical space of natural products into libraries designed on these scaffolds. Starting from these observation, we used the same library used by prof. Quinn group to assess the adaptability of this scaffold in our project. Compounds **10-29** have been synthesized using the synthetic strategy devised during my stay in prof. Quinn group at the Eskitis Insitute, and they were tested in a single dose assay against *Pf* 3D7 cultures to assess their ability to inhibit plasmodium growth.

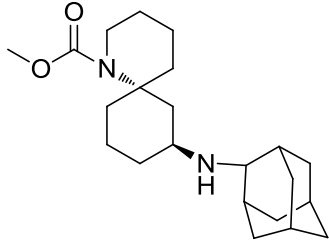
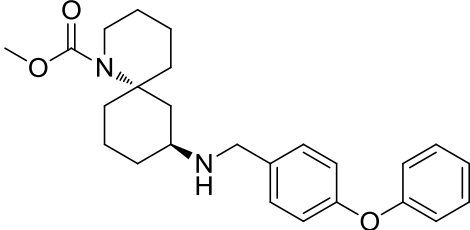
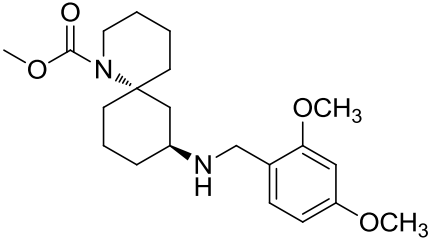
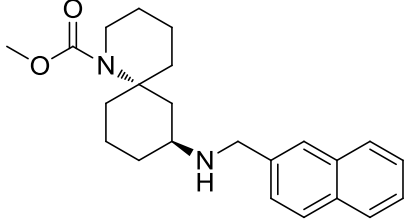
Due to the extreme difficulty to assess PMV inhibition, compounds **10-19** were tested for their antimalarial properties before further investigation, using a single dose assay at high concentration (50  $\mu$ M) against chloroquine-sensitive and chloroquine-resistant strains of *Pf* was used as a preliminary screening.

In this way we were able to screen the compounds in order to select only the one possessing antimalarial activity for further studies on PMV inhibition.

**Table 3.2** shows the activity of compounds **10-19**, while the activity of compounds **20-29** is currently under assessment.

Compound	<i>Pf</i> 3D7 (D10) Growth inhibition % @ 50 $\mu$ M	<i>Pf</i> 3D7 (W2) Growth inhibition % @ 50 $\mu$ M
<b>Scaffold A</b>	Inactive	Inactive
	89.03	88.91
	25.41	36.34
	27.76	37.20
	28.44	30.76
	88.62	91.30
	85.68	78.94

---

	99.48	98.80
	99.93	97.39
	85.19	85.63
	80.93	81.18

---

Table 3.2

### 3.7 Activity of compounds 10-19

All compounds, beside **11-13** containing a bromine atom, showed a good inhibitorial activity when tested at 50  $\mu$ M, while the unsubstituted scaffold A was unable to stop parasite growth. This is important since allow to rule out an unspecific activity due to the presence of the azaspiroundecane scaffold. Since the test was conducted using high concentration, it was not possible to observe significant differences in compounds activity and identify structure-activity relationships, but the presence of inactive compounds (**11-13**) suggest that a specific target with defined structural requirements may be at the base of their activity.

These observations led us to design two more compounds, using the SAR obtained working on the peptidomimetics in order to synthesize tailored compounds with better chances to interact with PMV.

### 3.8 Design and activity of compounds 30-32

In order to select the appropriate substituent, we looked at the SAR of peptidomimetics. Position **P3** was the most critical and the only aminoacid accepted in this position, with limited exception consisting in other basic aminoacids like Trp or Lys. Therefore, in compounds **30-32**, the NP scaffold has been functionalized with L-arginine or 6-carboxyindole, in order to mimic the two most effective side-chain substitutions found in the SAR study. 6-Carboxyindole was selected in order to move away from peptide-like structures. Another advantage of using the spiro-scaffold is that the two nitrogen atoms were maintained at a similar distance when compared with the peptidomimetic inhibitors (6 bonds, **Figure 3.5**), and the cleavable bond was substituted with a carbamate, another bioisoster of the peptide bond already used in other aspartic proteases inhibitors, as Darunavir (**Figure 3.5**).<sup>100</sup>

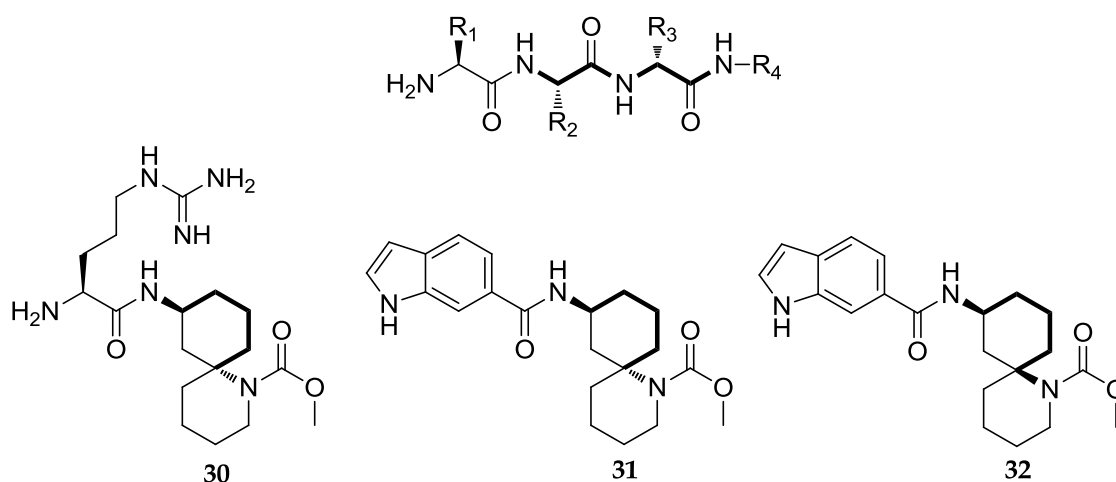


Figure 3.5

When tested on Plasmodium cultures, compound **30**, containing an arginine residue, showed no activity up to 50  $\mu\text{M}$ , while both compounds **31** and **32** showed an activity in the low micromolar range (**Table 3.3**).

The reason of this could be due to the multiple charges present on the arginine residue, that could hinder the ability of this molecule to cross biological membrane, as observed in the peptidomimetic compounds.

Compounds **31** and **32**, the two diastereoisomer of the same molecule, showed different activities related to the different stereochemistry.

Compound	<i>Pf</i> 3D7 (D10)	<i>Pf</i> 3D7 (W2)
	IC <sub>50</sub> (μM)	IC <sub>50</sub> (μM)
<b>30</b>	>50	>50
<b>31</b>	12.8	16.5
<b>32</b>	>20	>20

Table 3.3

Compounds **31** and **32**, possessing an acceptable IC<sub>50</sub> will soon be tested against PMV to assess their ability to inhibit this enzyme.

---

## 4. Synthesis

### 4.1 Solid-Phase Peptide Synthesis

The solid-phase peptide synthesis (SPPS) was conceived in 1963 by Merrifield in an attempt to solve the problems encountered in peptide synthesis using traditional methodology.

This technique relies on an insoluble polymer matrix, suitably functionalized, acting as a physical support for the sequential growth of the peptide. The resin allows for an easy removal of unreacted reagents by simple filtration, avoiding laborious purification procedures after each synthetic steps. Bypassing the purification steps allow for the optimization of parallel synthesis strategies, and also the automation of the process.

This approach evolved in recent years, allowing not only the synthesis of peptides, but to introduce modification in the peptidic sequences, such as disulfide bridge or unnatural aminoacids.

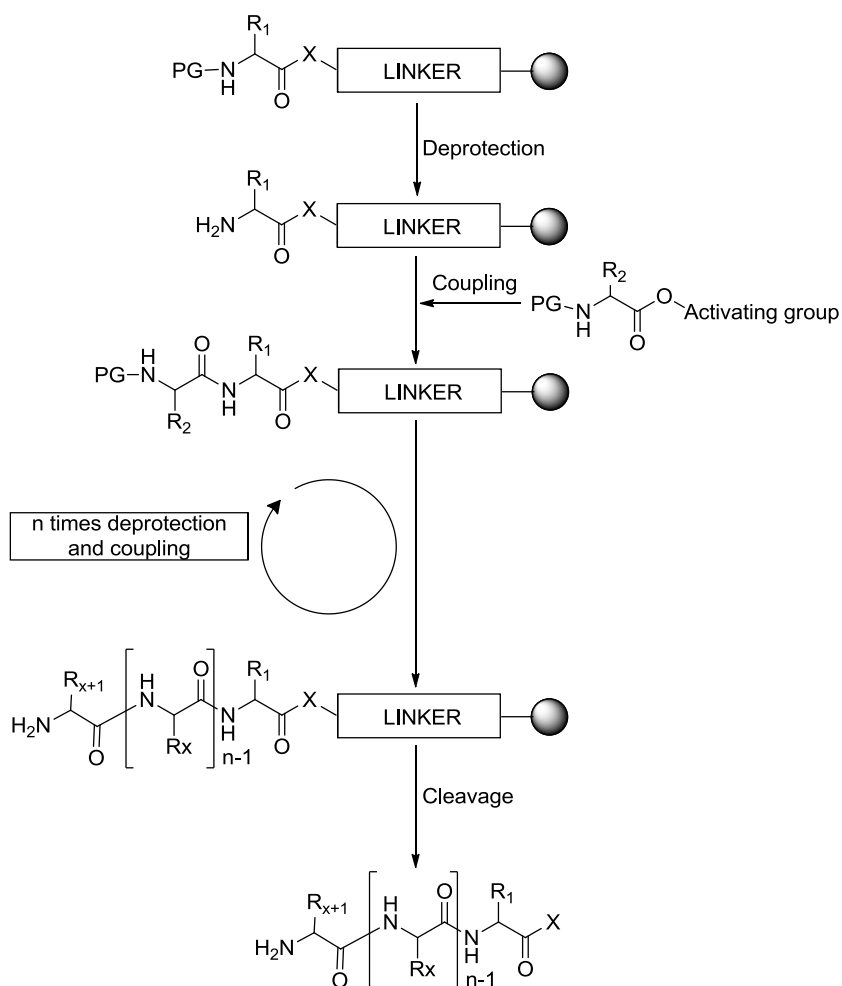
During solid-phase synthesis, solubilized reagents reach the free functional groups present on the surface and in the inner part of the polymer granules only by diffusion: therefore the reaction is conducted using a large excess of reagents. Repeated washings and filtrations are then employed to remove the unreacted fraction.

The synthesis (**Scheme 4.1**) begins with the formation of a covalent bond between the carboxy- terminal amino acid and the resin linker, followed by its deprotection and the insertion of the next amino acid, a loop that continues until the desired sequence is completed. The side chains of amino acids inserted must be protected with groups stable in the conditions used in the synthesis, but easily removable in selected conditions. The whole process is thus reduced to a series of cycles of coupling-deprotection that continue until the desired sequence is obtained, which will be finally cleaved from the resin.

The nature of the terminal group can be selected using different type of linker.

The most common protecting groups used primarily the terminal amino groups are the t-butylcarbamate (Boc-) and the 9-fluorenylmethyl carbamate (Fmoc) groups. These two protecting groups require completely different synthetic strategies, as they are labile under different conditions and require specific orthogonal protections.

The peptide bond formation is made possible by the presence of coupling reagent, such as carbodiimides or benzotriazoles. The cleaving methods used to detach the peptide sequences from the resin will vary depending on the type of resin, but they are usually carried out using a mixture containing different scavengers that mimic the functional groups present on the side chains, reducing the risk of parasite reactions during the cleavage step.



Scheme 4.1



### 4.1.1 SPPS features and requirements

The solid phase synthesis has many advantages compared to traditional synthesis:

- simple work-up;
- removal of secondary products, cleaved protecting groups and the excess reagents at the end of each reaction by simple filtration;
- Possibility to increase reactions yields by working with large excess of reagents;
- Avoid problems involving decreased solubility of the peptide during synthesis;
- Easily automated process.

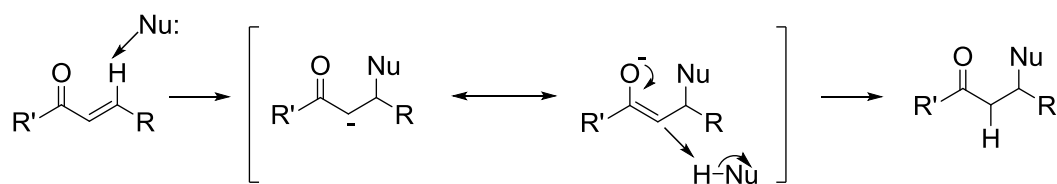
The support used in the synthesis must be insoluble and chemically inert, with granule-size sufficient to allow the fast removal of the solvent by filtration. The support must swell quickly, to facilitate the reagents diffusion into its pores, and this reaction may be facilitated introducing a spacer that separates the inert matrix and the reactive sites. The solvent used in the reaction must be of intermediate polarity, such as  $\text{CH}_2\text{Cl}_2$  or DMF.

In optimal conditions, the coupling reaction should always be completed, in order to avoid the formation of peptides bearing deletions in the sequence that can complicate the final purification step. It is possible to perform, at the end of the coupling, a capping of unreacted amino groups by acylation, thus obtaining truncated sequences that no longer take part in subsequent coupling reactions. However, there is no guarantee that this operation will improve the overall yield, and therefore is often avoided.

## 4.2 Organic Reactions

### 4.2.1 Aza-Michael Addition

The Michael reaction, discovered in 1887, is one of the most important reactions in organic chemistry, consisting in the conjugated addition of a nucleophile on an unsaturated carbonyl compound, defined Michael acceptor. It consists in the nucleophilic attack at the  $\beta$  carbon of an  $\alpha,\beta$ -unsaturated carbonyl compound<sup>33</sup>. Kohler better define the reaction as a 1,4 addition of a doubly stabilized nucleophilic carbon to a  $\alpha,\beta$ -unsaturated carbonyl compound. If the functional group which acts as the nucleophile is an amine or another nitrogen containing moiety, such as carbamates, the reaction is classified as an aza-Michael. The mechanism of the reaction is illustrated below (**Scheme 4.2**).



Scheme 4.2

For many years the method used for the conjugated-addition between the carbonyl and the amino group required acidic or basic conditions and a catalyst. The reaction carried out in such environment was not applicable to industrial level, due to the numerous secondary products that could be formed in acidic or basic conditions. High yields are usually observed in this reaction when applied to strong nucleophiles; while weak one, such as carbamates, are less prone to react and need a much more reactive catalyst. For the aza-Michael reactions involving a carbamate, metal catalysts have been studied and bismuth salts have showed a remarkably ability to catalyze this kind of reaction.

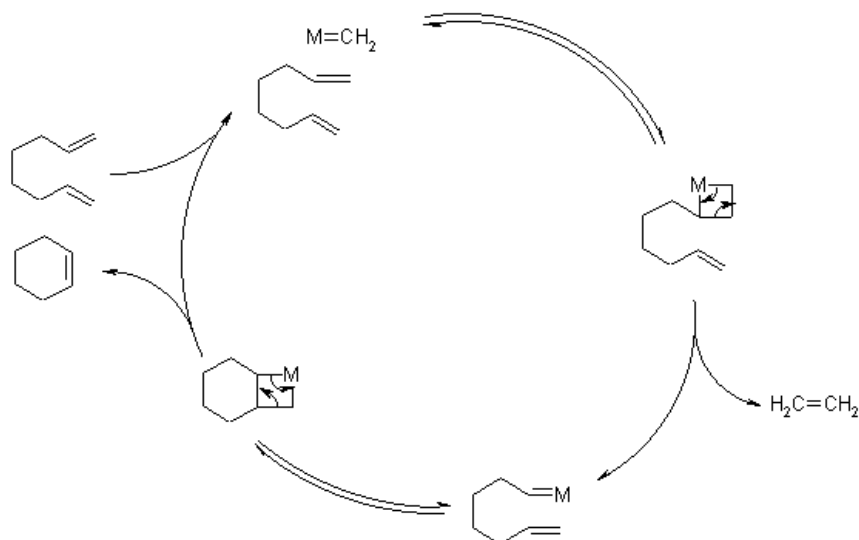
### 4.2.2 Bismuth role as a catalyst

The success of the Michael reactions in the presence of bismuth nitrate stimulated researcher to try to understand the reaction mechanism.<sup>101</sup> In absence of bismuth nitrate reagents are not completely converted and low product yields are observed. Bismuth nitrate produces small amount of nitric acid, which leads to an acid environment required for this type of reactions, although substituting bismuth nitrate led to decreased yields. These results suggested that the role of this catalyst is not only related to the formation of acid, but may be due to its action also as a complexing agent. The low yields obtained when the same reaction is catalyzed by other nitrate salts, such as sodium nitrate, iron nitrate and zinc nitrate, confirm the important role played by bismuth nitrate. The failure of these salts in promoting the reaction could be indicative of their inability to release sufficient amount of acid or create specific reactive-catalyst coordination complex. In conclusion, bismuth nitrate seems to be the catalyst with the ideal characteristics for the success of an aza-Michael reaction.

### 4.2.3 Ring-closing metathesis

The ring-closing metathesis (RCM) involves the formation of a ring by the intramolecular reaction of two double bonds. The metathesis reaction was discovered around 1960 and the search for efficient catalysts led to the synthesis of many reagents. The efforts made for the development of this reaction led Robert H. Grubbs, Yves Chauvin and Richard R. Schrock to share the Nobel Prize for chemistry in 2005.

**Scheme 4.3** illustrates the reaction mechanism.



Scheme 4.3

The formation of the cycle is usually entropically favored and the equilibrium can be shifted towards the product removing the ethylene liberated in the reaction. The amount of solvent used in the RCM is important, since an excessive or reduced dilution could lead to the formation of secondary products. The catalysts used in RCM reactions are metal-carbene compounds, and one of the most used the first generation Grubbs catalyst, containing ruthenium. Grubbs I catalyst (**Figure 4.1**) is a derivative of Ru(IV) with 16 electrons and, being less reactive than other catalysts, need to be used in a slightly higher quantity, usually 0.5-1%. The increasingly widespread use of this compound it is due to its excellent compatibility with most of the functional groups, except Lewis bases, and its greater air stability compared to other catalyst.<sup>102</sup>

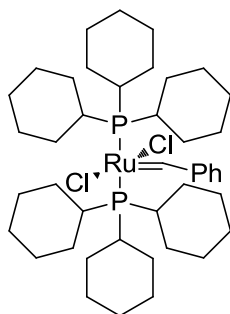
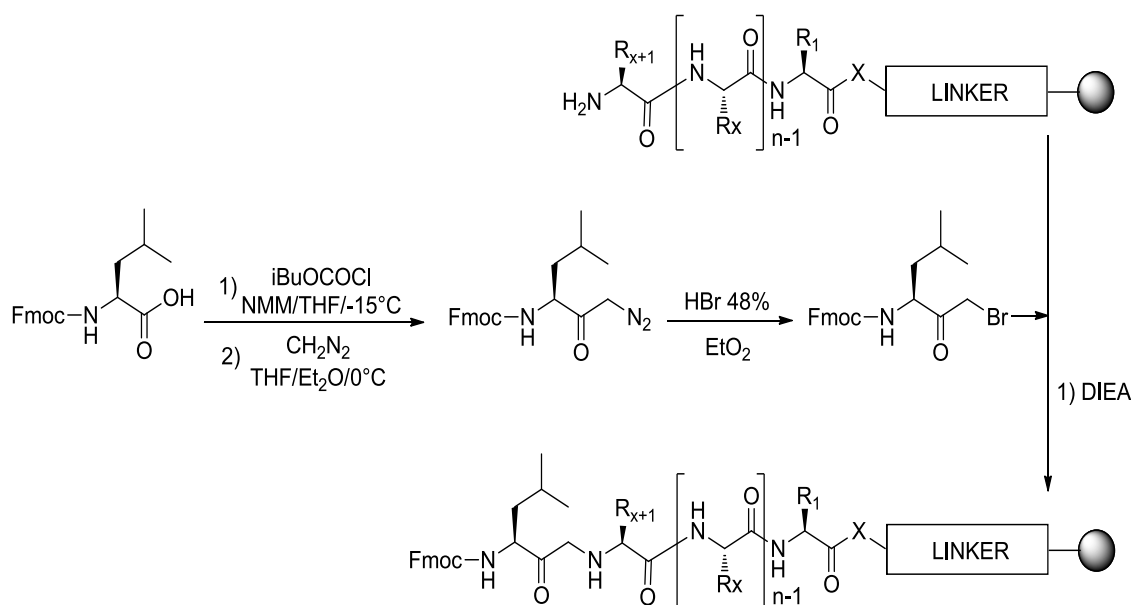


Figure 4.1

### 4.3 Reactions schemes

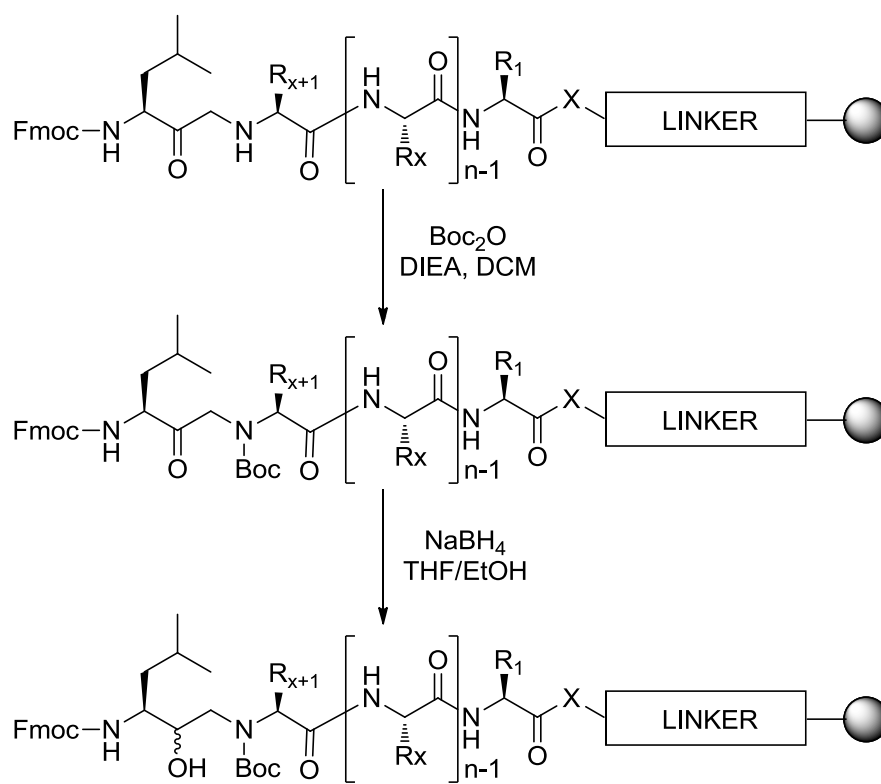
Compounds **1-9** described above present an HEA core, a peptide bond isoster. The introduction of this group in a solid-phase synthesis approach is different from the normal procedures usually applied in this kind of synthesis, which mainly consists in the formation of peptide bonds between the amino acid residues. The HEA group was generated after reduction of the carbonyl moiety of an aminomethylketone, obtained by alkylation on the N-terminal amine of the peptide anchored to the resin. The alkylation was performed exploiting a nucleophilic substitution, which allows the formation of the bond between the methyl ketone of Fmoc-3-amino-1-bromo-5-methylhexan-2-one and the amine of the last amino acid introduced (**Scheme 4.4**). The bromomethylketone (intermediate **1**) was obtained by reaction of Fmoc-leucine with  $\text{CH}_2\text{N}_2$  and subsequent treatment with HBr 48%, as described in literature.<sup>91</sup>



Scheme 4.4

Using an alkylation reaction instead of an acylation generate a secondary amine, a group able to further reacts in the later stages of the synthesis, due to the large excess of reagents used in SPPS. This problem was solved by the introduction of a Boc protecting group, labile under the cleavage conditions. The reduction step was then

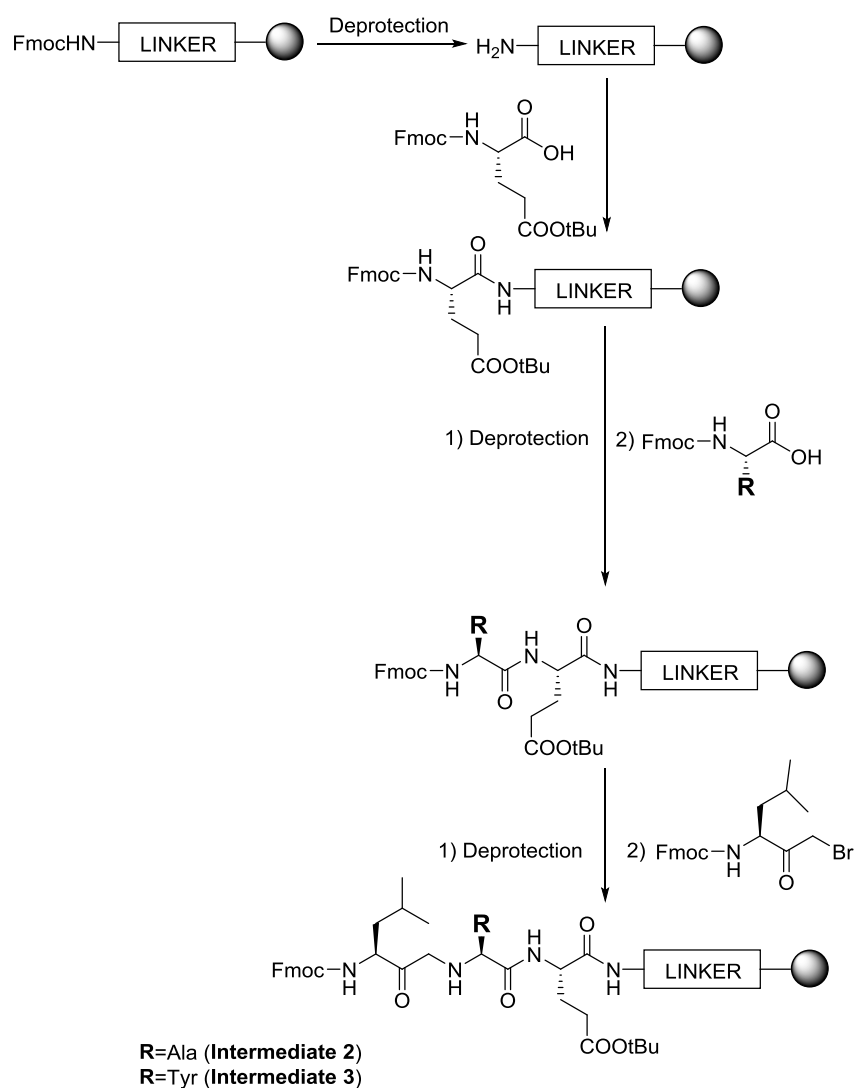
conducted in a solution of THF/EtOH (1:1), adding a large excess of NaBH<sub>4</sub> (**Scheme 4.5**). Not being stereoselective, the reduction produced both the diastereoisomers.



Scheme 4.5

### 4.3.1 Synthesis of peptidomimetics 1-4

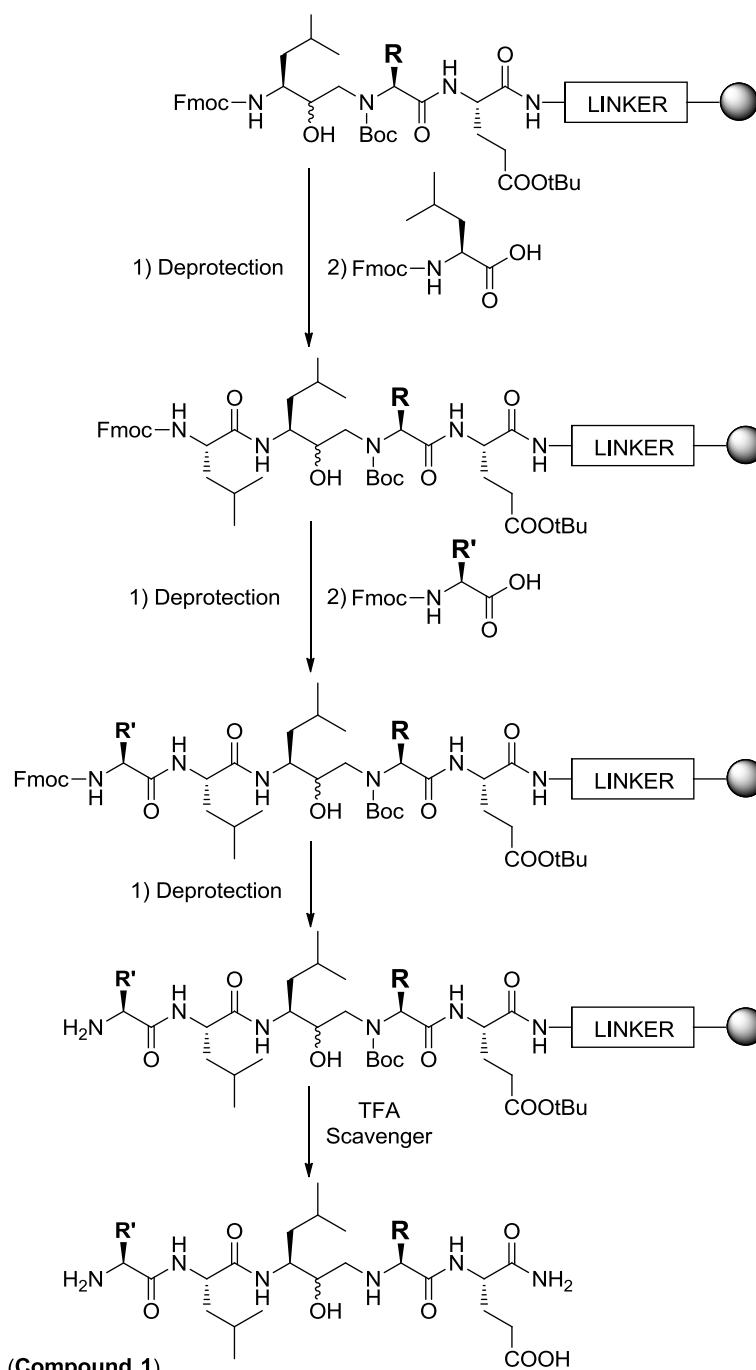
Compounds **1-4**, synthesized using Rink amide resin, are characterized by a terminal dipeptide Ala-Glu or Tyr-Glu that reacts with Fmoc-3-amino-1-bromo-5-methylhexan-2-one to generate intermediates **2** and **3**, the HEA group precursor (Scheme 4.6).



Scheme 4.6

HEA group was generated in situ following the procedure showed in **Scheme 4.5**.

**Scheme 4.7** illustrates the final steps necessary to obtain compounds **1-4**.



**R=Ala; R'=Arg (Compound 1)**

**R=Tyr; R'=Arg (Compound 2)**

**R=Ala; R'=Trp (Compound 3)**

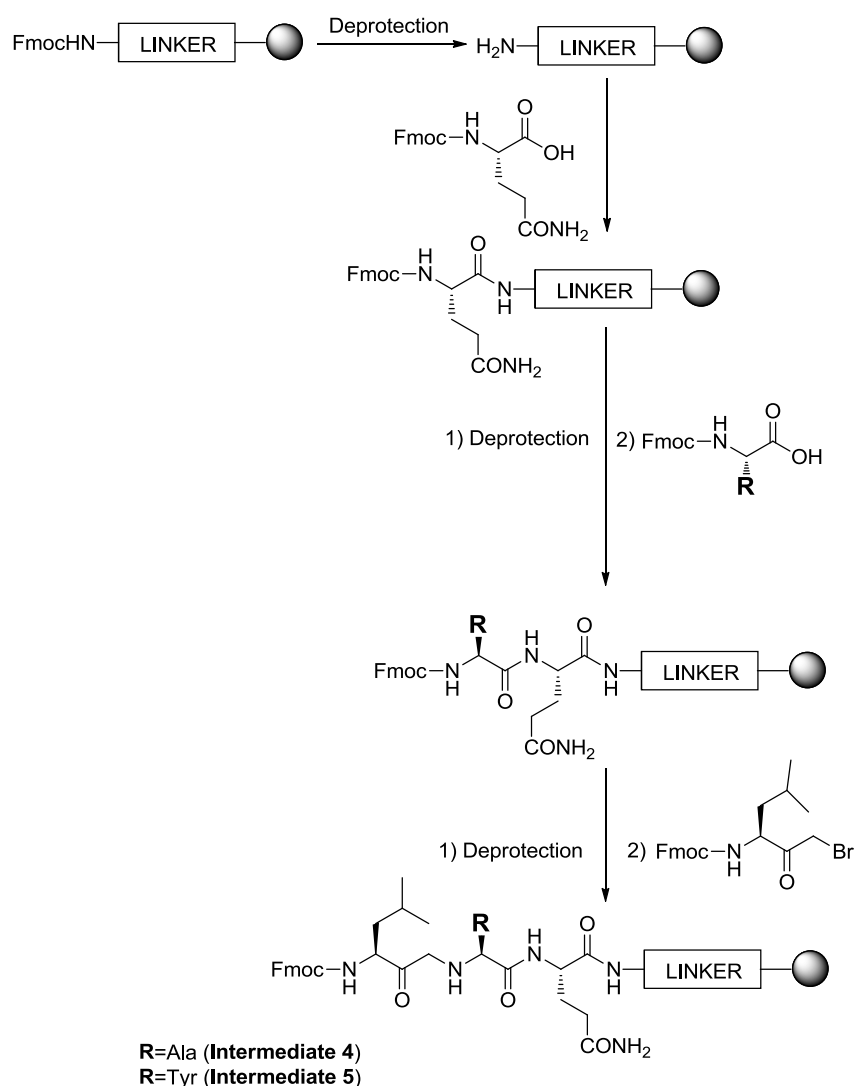
**R=Tyr; R'=Trp (Compound 4)**

**Scheme 4.7**



### 4.3.2 Synthesis of peptidomimetics 5 and 6

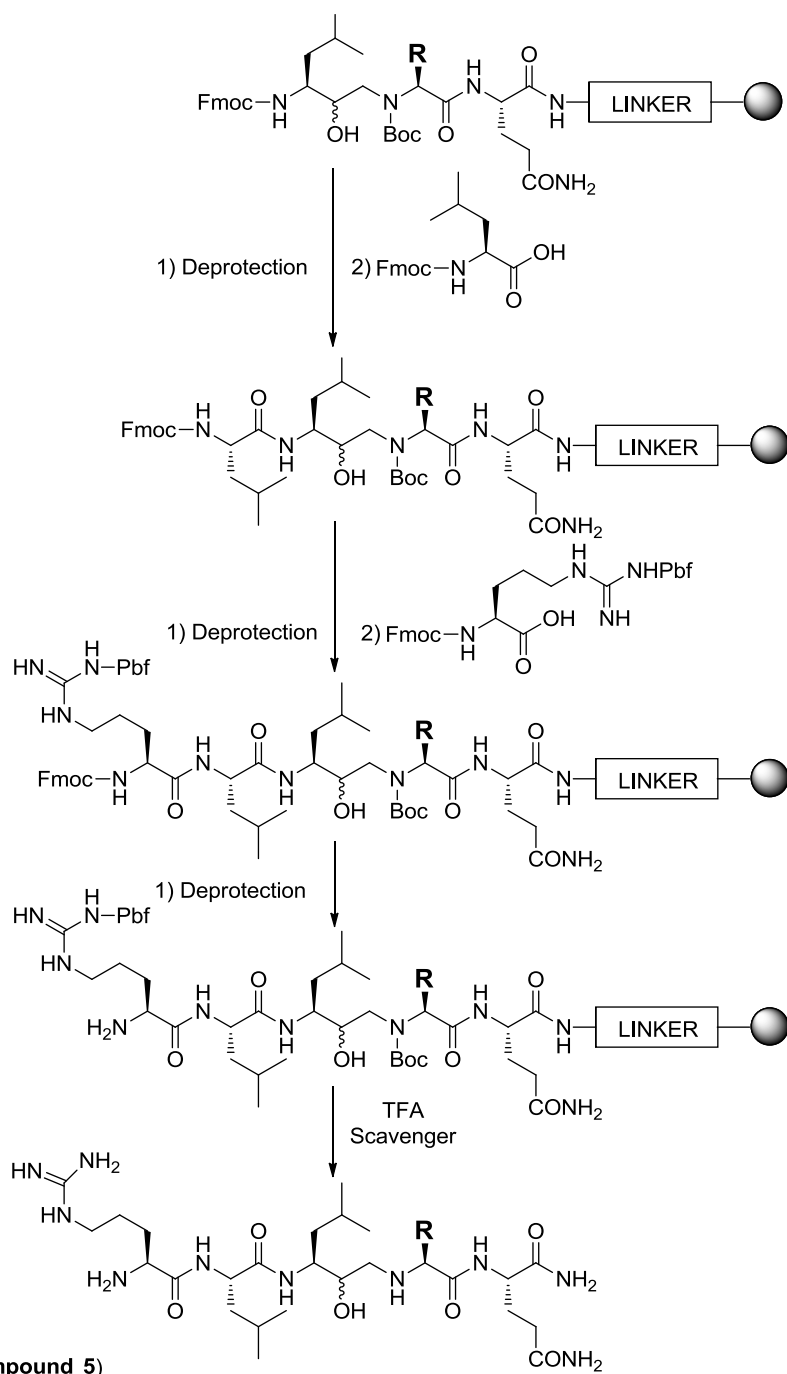
Compounds **5** and **6**, synthesized using Rink amide resin, are characterized by a terminal dipeptide Ala-Gln or Tyr-Gln that reacts with Fmoc-3-amino-1-bromo-5-methylhexan-2-one to generate intermediates **4** and **5**, the HEA group precursor (Scheme 4.8).



Scheme 4.8

HEA group was generated in situ following the procedure showed in Scheme 4.5.

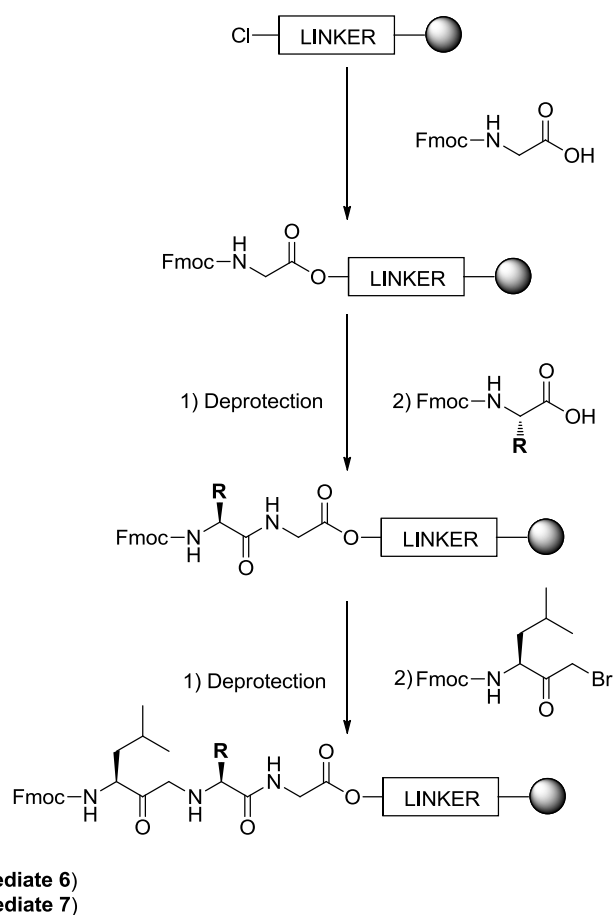
Scheme 4.9 illustrates the final steps necessary to obtain compounds **5** and **6**.



Scheme 4.9

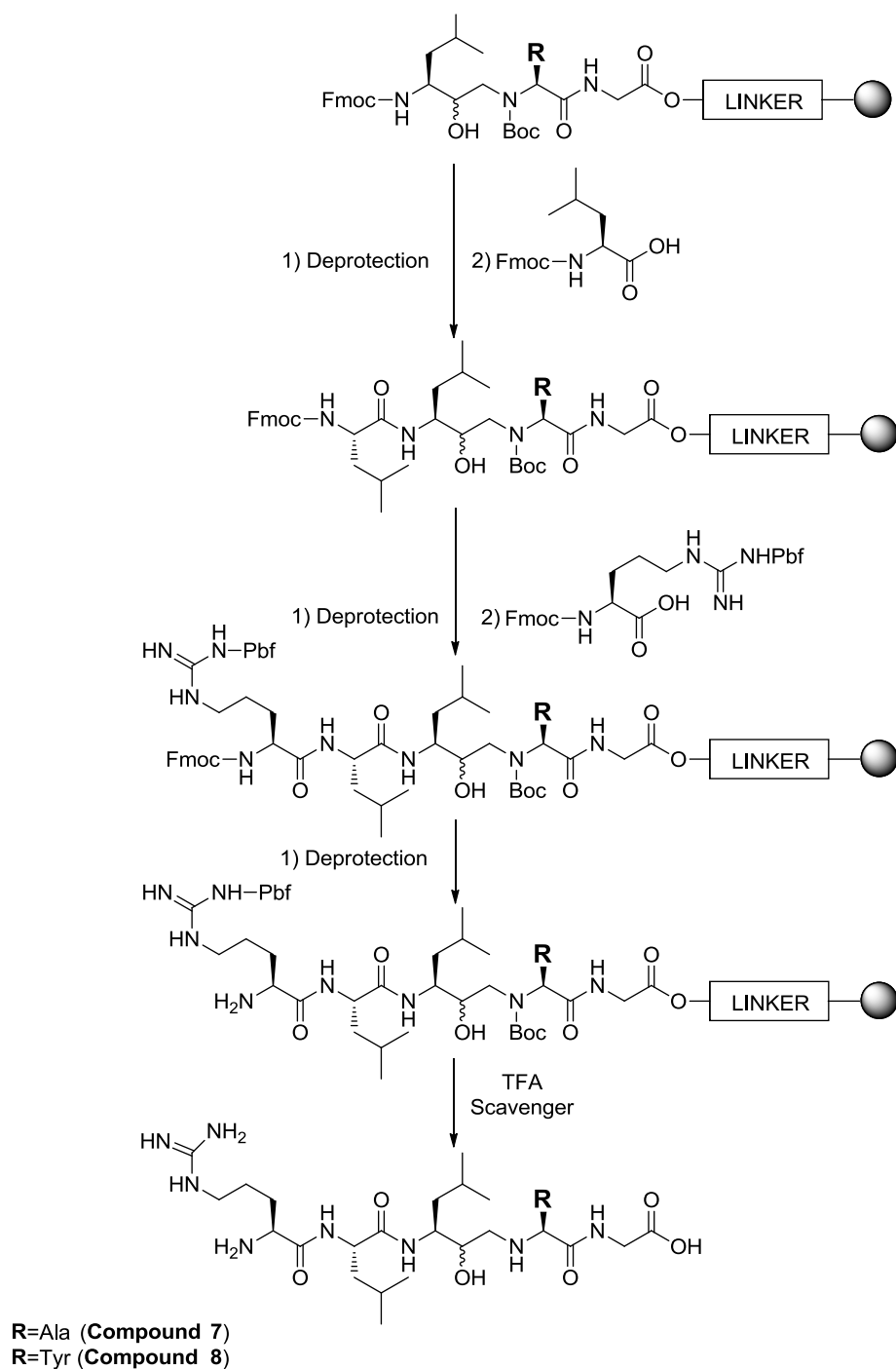
### 4.3.3 Synthesis of peptidomimetics 7 and 8

Compounds **7** and **8**, synthesized using 2-Chlorotrytil resin, are characterized by a terminal dipeptide Ala-Gly or Tyr-Gly that reacts with Fmoc-3-amino-1-bromo-5-methylhexan-2-one to generate intermediates **6** and **7**, the HEA group precursor (Scheme 4.10).



Scheme 4.10

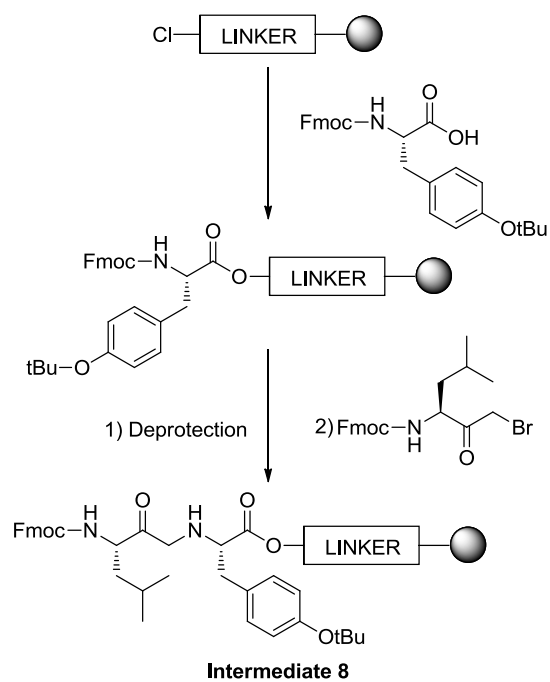
HEA group was generated in situ following the procedure showed in Scheme 4.5. Scheme 4.11 illustrates the final steps necessary to obtain compounds **7** and **8**.



Scheme 4.11

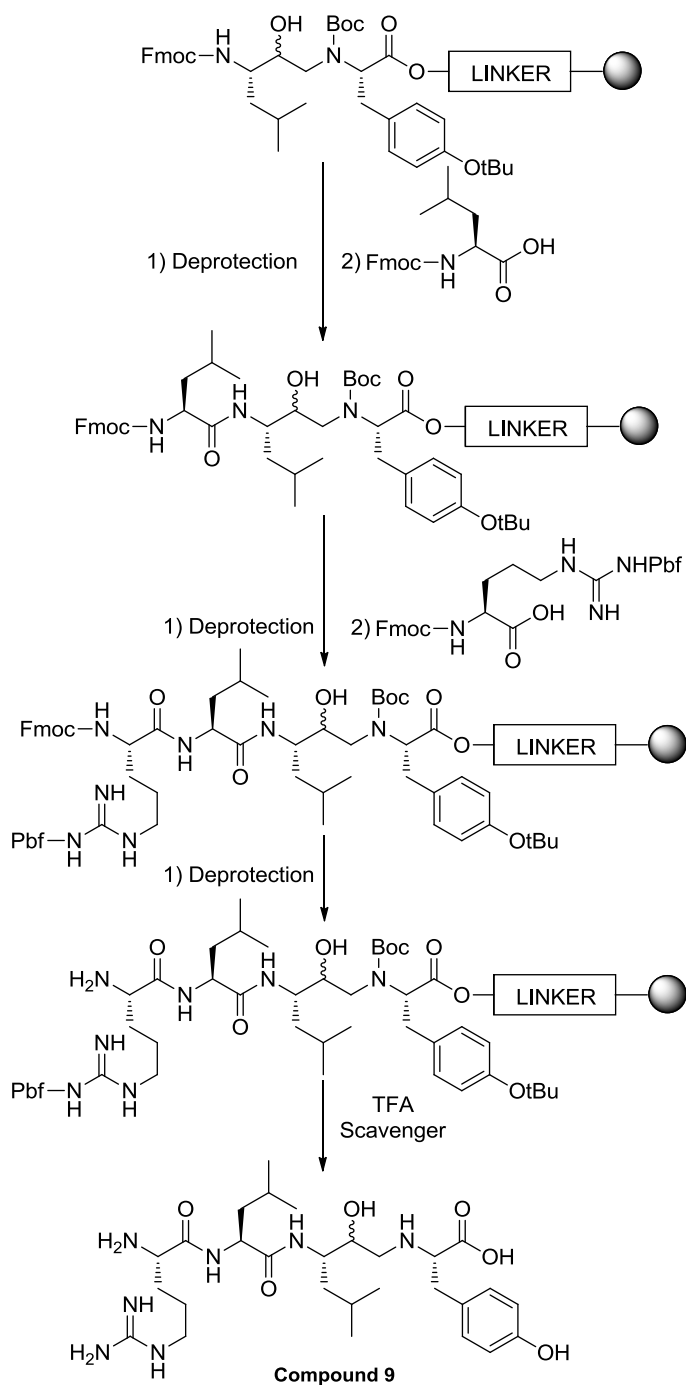
#### 4.3.4 Synthesis of peptidomimetic 9

Compound 9, synthesized using 2-Chlorotrytil resin, is characterized by a single aminoacid in position P1' that reacts with Fmoc-3-amino-1-bromo-5-methylhexan-2-one to generate intermediate 8, the HEA group precursor (Scheme 4.12).



Scheme 4.12

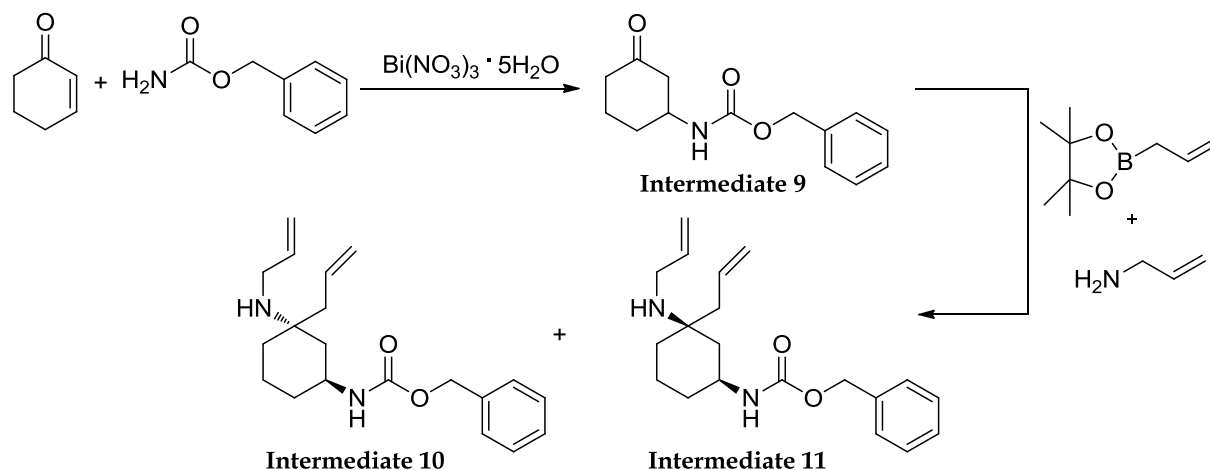
HEA group was generated in situ following the procedure showed in **Scheme 4.5**. **Scheme 4.13** illustrates the final steps necessary to obtain compound **9**.



Scheme 4.13

### 4.3.5 Synthesis of intermediates 10 and 11

Intermediate **10** and **11** were synthesized according to the synthetic pathway illustrated below (Scheme 4.14).



Scheme 4.14

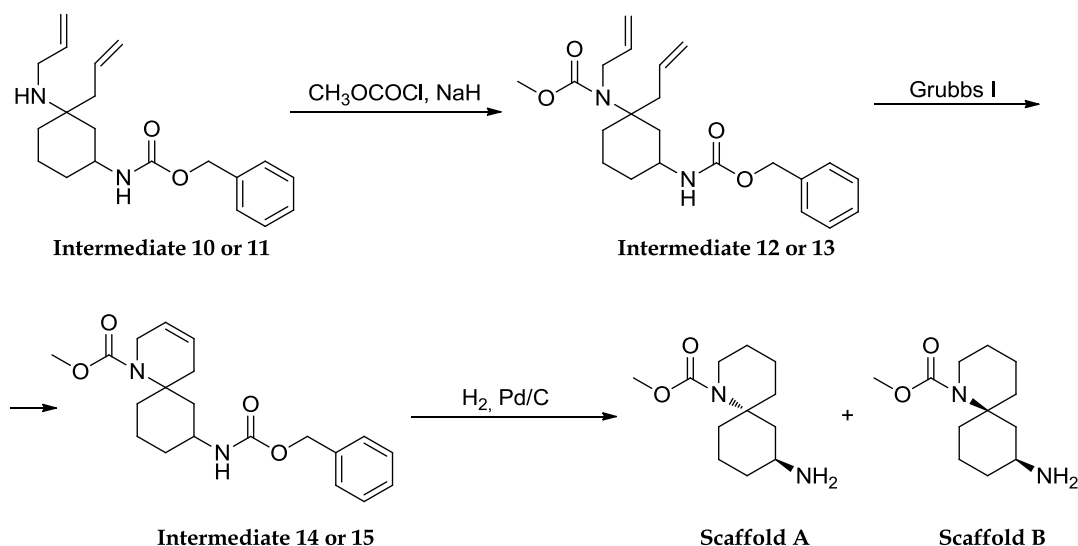
The scheme involves a reaction between the 2-cyclohexenone and benzylcarbamate giving intermediate **9**, and subsequent one-pot double allylation with formation of intermediates **10** and **11**. The intermediates **10** and **11** are obtained in a ratio of about 75:35, calculated on purified compounds. Table 4.1 shows the reactions yields.

Intermediate	IUPAC name	Yield
<b>9</b>	benzyl (3-oxocyclohexyl)carbamate	90.4%
<b>10</b>	benzyl ((1S±1R,3R±3S)-3-allyl-3-(allylamino)cyclohexyl)carbamate	50.6%
<b>11</b>	benzyl ((1S±1R,3S±3R)-3-allyl-3-(allylamino)cyclohexyl)carbamate	27%

Table 4.1

### 4.3.6 Synthesis of scaffolds A and B

Scaffolds **A** and **B** were synthesized according to the synthetic pathway illustrated below (Scheme 4.15).



Scheme 4.15

The scheme consists of three steps: the protection of the amine with formation of intermediate **12** or **13** starting from intermediate **10** or **11**, respectively; cyclization of those intermediates using first generation Grubbs reagent, generating the intermediates **14** and **15**; and catalytic hydrogenation with formation respectively of scaffolds **A** and **B**. Table 4.2 shows the reactions yields.

Intermediate	IUPAC name	Yield
<b>12</b>	allyl(1R±1S,3S±3R)-1-allyl-3-(((benzyloxy)carbonyl)amino)cyclohexyl)methylcarbamate	72.7%
<b>13</b>	(allyl((1S±1R,3S±3R)-1-allyl-3-(((benzyloxy)carbonyl)amino)cyclohexyl)methylcarbamate	67.8%
<b>14</b>	(6R±6S,8S±8R)-methyl 8-(((benzyloxy)carbonyl)amino)-1-azaspiro[5.5]undec-3-ene-1-carboxylate	91%
<b>15</b>	(6S±6R,8S±8R)-methyl 8-(((benzyloxy)carbonyl)amino)-1-azaspiro[5.5]undec-3-ene-1-carboxylate	84.9%

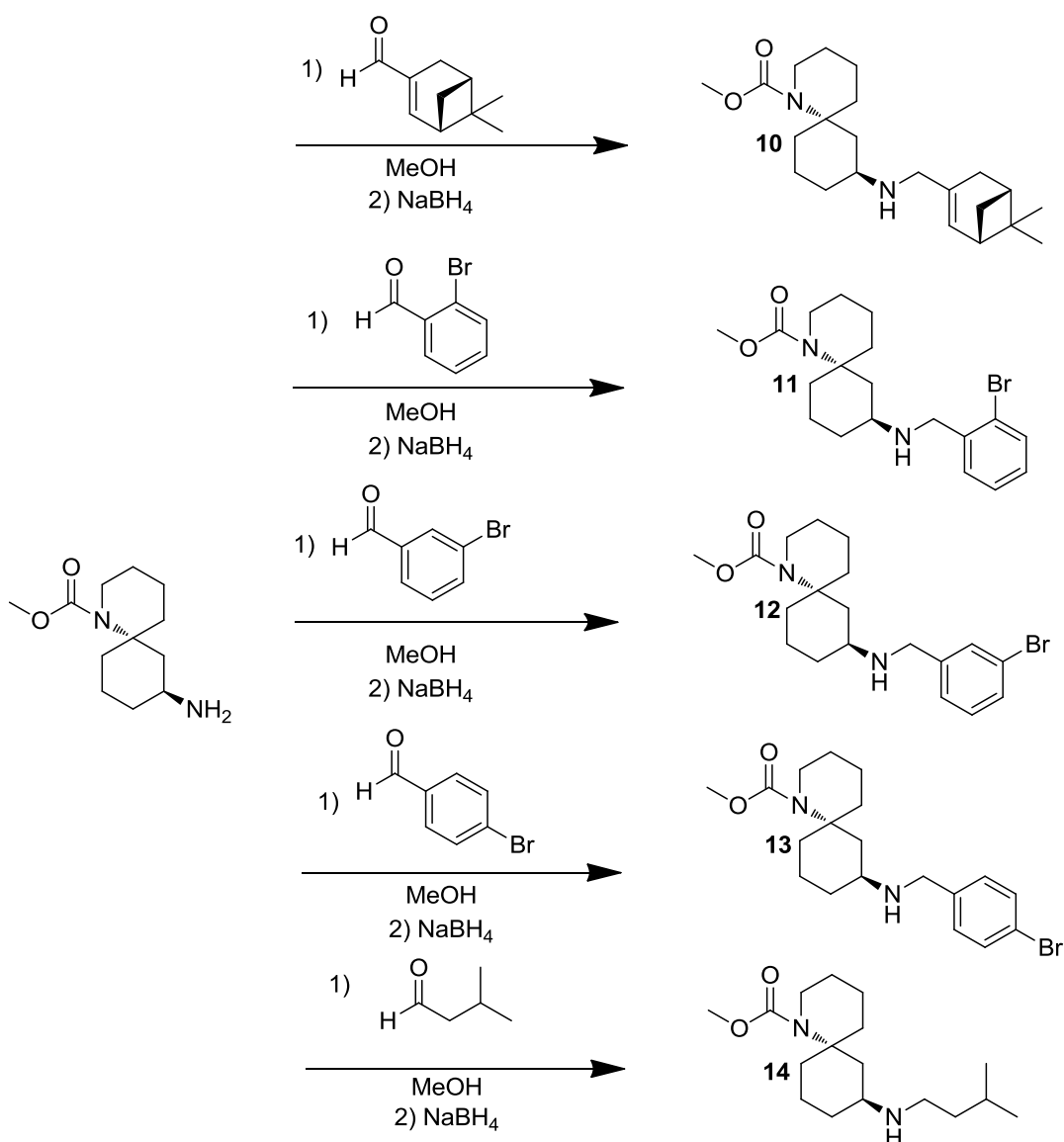


<b>A</b>	((6R±6S,8R±8S)-methyl 8-amino-1-azaspiro[5.5]undecane-1-carboxylate	99.8%
<b>B</b>	((6R±6S,8S±8R)-methyl 8-amino-1-azaspiro[5.5]undecane-1-carboxylate	68.6%

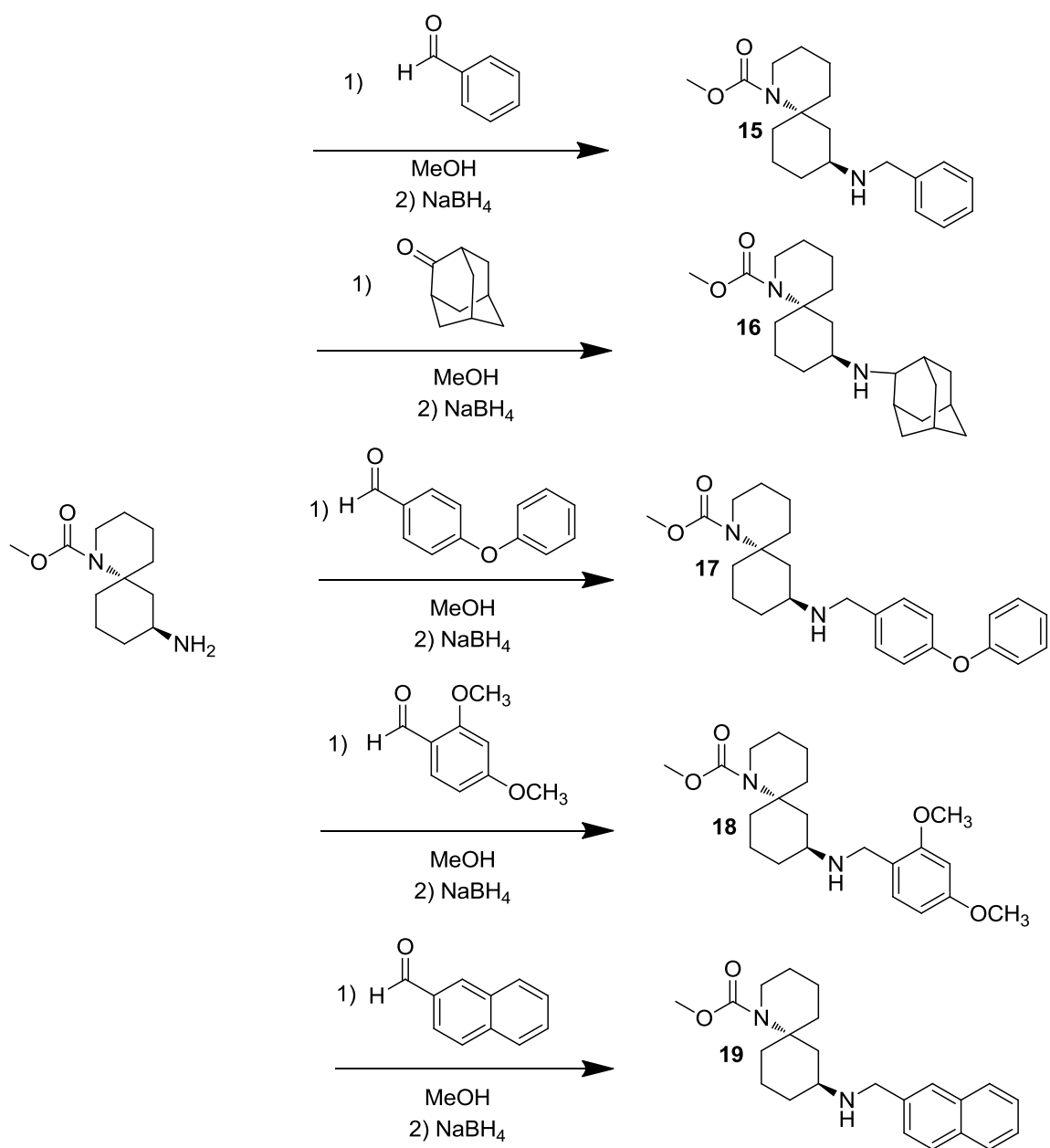
Table 4.2

### 4.3.7 Synthesis of compounds 10-19

Compounds **10-19** were synthesized through a reductive amination reaction starting from Scaffold A (Scheme 4.16).



Scheme 4.16



Scheme 4.16 (continued)

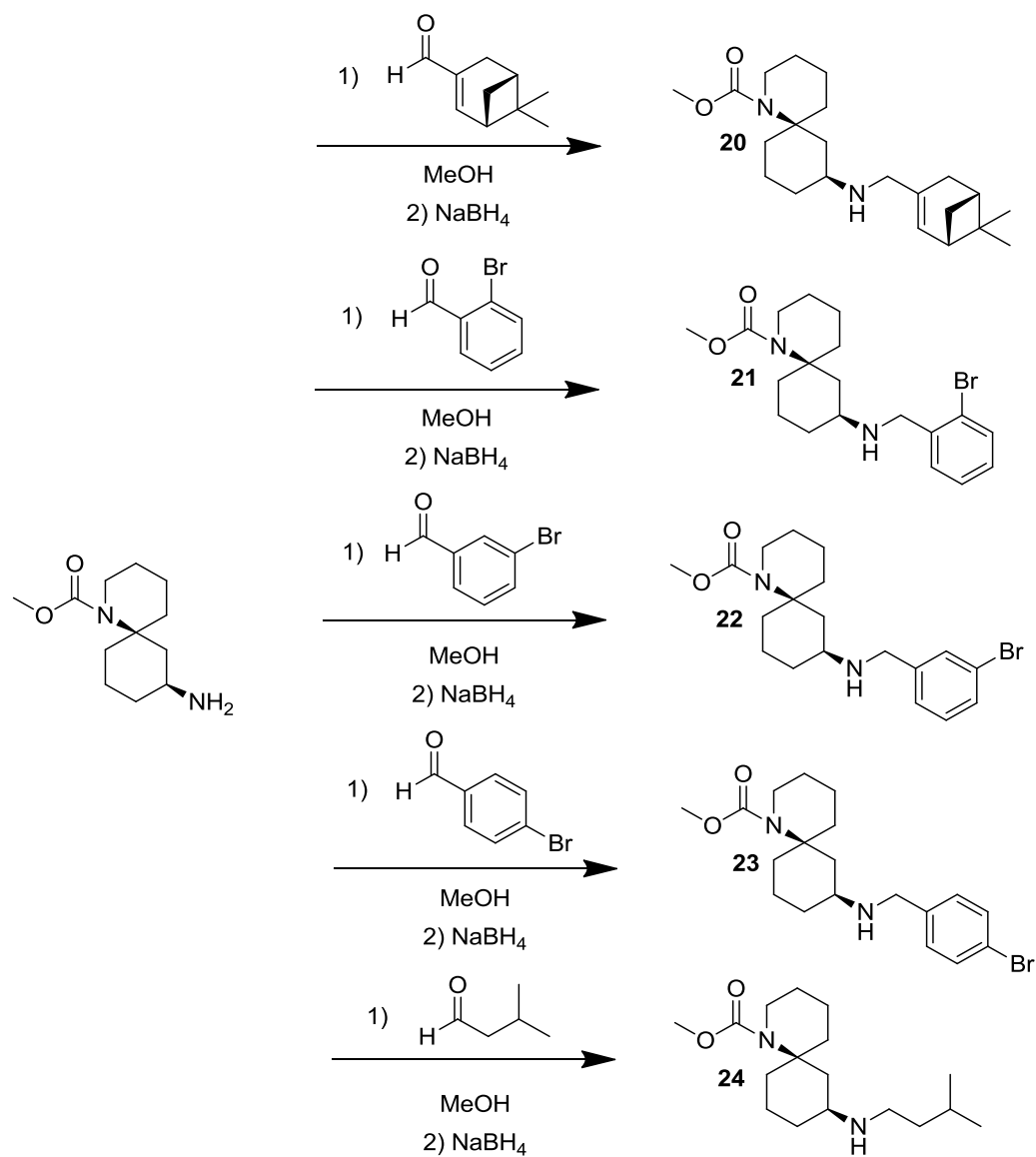
Table 4.3 illustrates the reaction yields of each compound.

Compound	IUPAC name	Yield
10	(6R±6S,8R±8S)-methyl 8-(((6,6-dimethyldicyclo[3.1.1]ept-2-en-3-yl)methyl)amino)-1-azaspiro[5.5]undecane-1-carboxylate	18.2%
11	(6R±6S,8R±8S)-methyl 8-((2-bromobenzyl)amino)-1-azaspiro[5.5]undecane-1-carboxylate	95.7%
12	(6R±6S,8R±8S)-methyl 8-((3-bromobenzyl)amino)-1-azaspiro[5.5]undecane-1-carboxylate	94.5%
13	(6R±6S,8R±8S)-methyl 8-((4-bromobenzyl)amino)-1-azaspiro[5.5]undecane-1-carboxylate	90.9%
14	(6R±6S,8R±8S)-methyl 8-(isopentylamino)-1-azaspiro[5.5]undecane-1-carboxylate	77.8%
15	(6R±6S,8R±8S)-methyl 8-(benzylamino)-1-azaspiro[5.5]undecane-1-carboxylate	51.8%
16	(6R±6S,8R±8S)-methyl 8-(adamantan-2-yl)amino)-1-azaspiro[5.5]undecane-1-carboxylate	63%
17	(6R±6S,8R±8S)-methyl 8-((4-phenoxybenzyl)amino)-1-azaspiro[5.5]undecane-1-carboxylate	74.1%
18	(6R±6S,8R±8S)-methyl 8-((2,4-dimethoxybenzyl)amino)-1-azaspiro[5.5]undecane-1-carboxylate	66.7%
19	(6R±6S,8R±8S)-methyl 8-((naphthalen-2-ylmethyl)amino)-1-azaspiro[5.5]undecane-1-carboxylate	49.6%

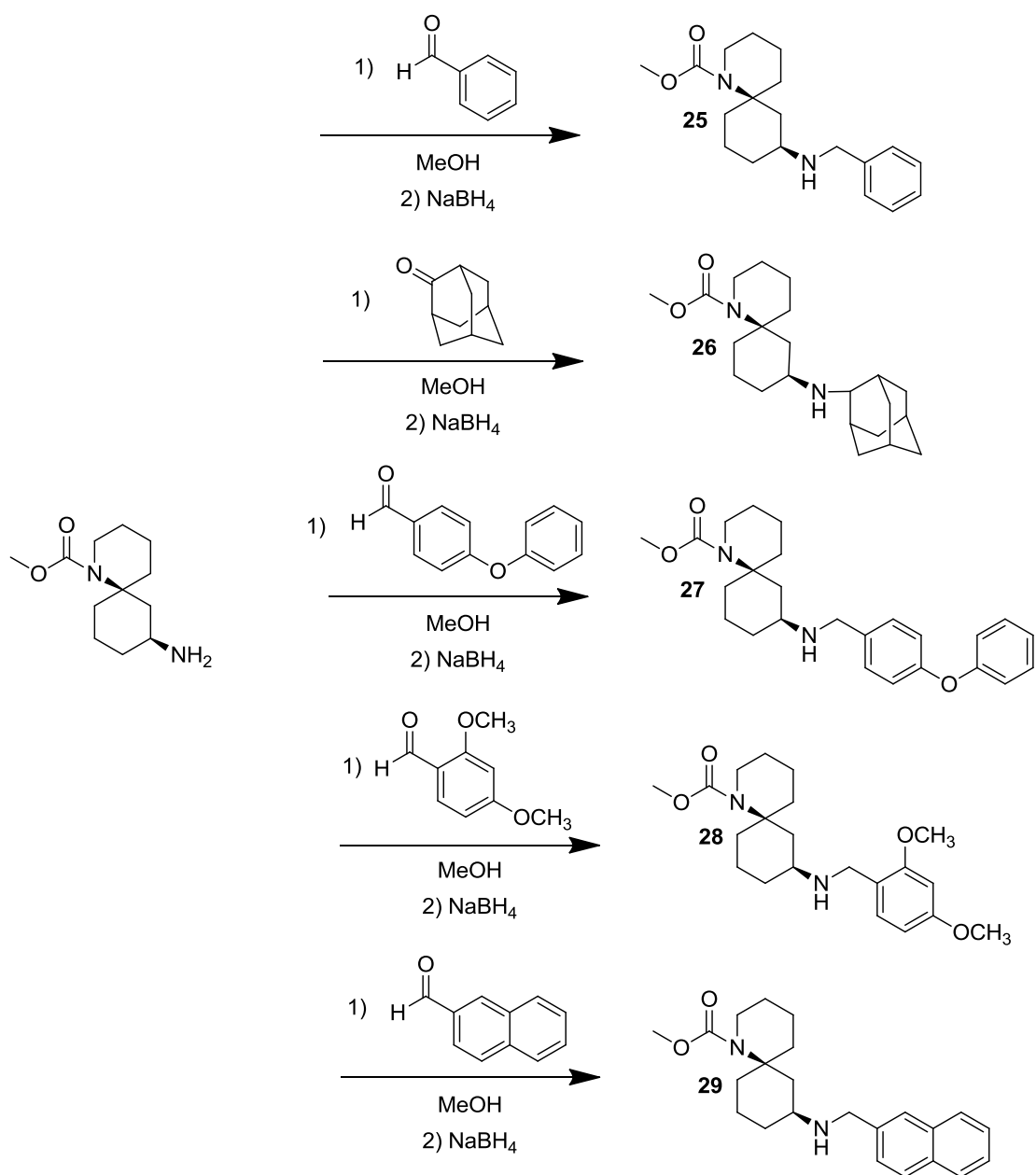
Table 4.3

## 4.3.8 Synthesis of compounds 20-29

Compounds **20-29** were synthesized through a reductive amination reaction starting from Scaffold **B** (Scheme 4.17).



Scheme 4.17



Scheme 4.17 (continued)

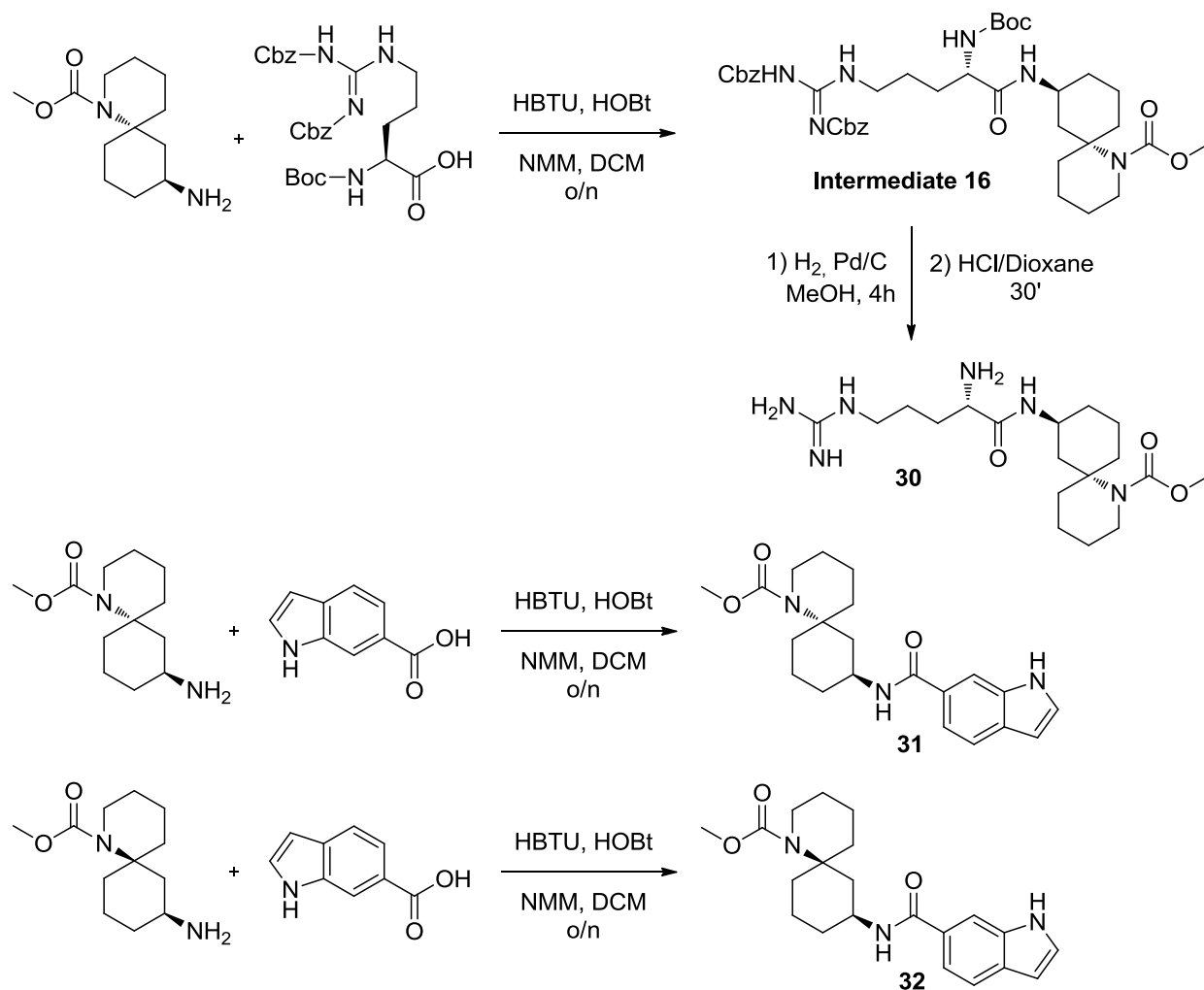
Table 4.4 illustrates the reaction yields of each compound.

Compound	IUPAC name	Yield
20	(6R±6S,8S±8R)-methyl 8-(((6,6-dimethyldicyclo[3.1.1]ept-2-en-3-yl)methyl)amino)-1-azaspiro[5.5]undecane-1-carboxylate	10%
21	(6R±6S,8S±8R)-methyl 8-((2-bromobenzyl)amino)-1-azaspiro[5.5]undecane-1-carboxylate	3.85%
22	(6R±6S,8S±8R)-methyl 8-((3-bromobenzyl)amino)-1-azaspiro[5.5]undecane-1-carboxylate	38.5%
23	(6R±6S,8S±8R)-methyl 8-((4-bromobenzyl)amino)-1-azaspiro[5.5]undecane-1-carboxylate	10.8%
24	(6R±6S,8S±8R)-methyl 8-(isopentylamino)-1-azaspiro[5.5]undecane-1-carboxylate	23.1%
25	(6R±6S,8S±8R)-methyl 8-(benzylamino)-1-azaspiro[5.5]undecane-1-carboxylate	4.6%
26	(6R±6S,8S±8R)-methyl 8-(adamantan-2-yl)amino)-1-azaspiro[5.5]undecane-1-carboxylate	11.5%
27	(6R±6S,8S±8R)-methyl 8-((4-phenoxybenzyl)amino)-1-azaspiro[5.5]undecane-1-carboxylate	18.6%
28	(6R±6S,8S±8R)-methyl 8-((2,4-dimethoxybenzyl)amino)-1-azaspiro[5.5]undecane-1-carboxylate	13.1%
29	(6R±6S,8S±8R)-methyl 8-((naphthalen-2-ylmethyl)amino)-1-azaspiro[5.5]undecane-1-carboxylate	5.4%

Table 4.4

## 4.3.9 Synthesis of compounds 30-32

Compounds **30-31** were synthesized through a coupling reaction starting from Scaffold **A**, while compound **32** originate from scaffold **B** (Scheme 4.18).



Scheme 4.18

Table 4.5 illustrates the reaction yields of each compound.

Compound	IUPAC name	Yield
<b>Intermediate 16</b>	(6S±6R,8S±8R)-methyl 8-((S)-5-(2,3-bis((benzyloxy)carbonyl)guanidino)-2-((tert-butoxycarbonyl)amino)pentanamido)-1-azaspiro[5.5]undecane-1-carboxylate	60.7%
<b>30</b>	(6S±6R,8S±8R)-methyl 8-((S)-2-amino-5-guanidinopentanamido)-1-azaspiro[5.5]undecane-1-carboxylate	88.2%
<b>31</b>	(6S±6R,8S±8R)-methyl 8-(1H-indole-6-carboxamido)-1-azaspiro[5.5]undecane-1-carboxylate	34.6%
<b>32</b>	(6S±6R,8R±8S)-methyl 8-(1H-indole-6-carboxamido)-1-azaspiro[5.5]undecane-1-carboxylate	19%



---

## 5. Conclusions

In developing countries, endemic malaria epidemics preclude the possibility of economic progress and impose a high cost in terms of lost human life.<sup>103</sup> The rapid onset of the *Plasmodium* resistance to therapeutic agents is forcing the research to develop new molecules and identify alternative targets to devise an effective method to eradicate the parasite from infested areas. Thanks to the discovery the *Plasmodium export element* function,<sup>14</sup> the characterization of the aspartic protease plasmepsin V<sup>83</sup> and the interaction between these two elements, which allows the plasmodium development,<sup>74,75</sup> a new therapeutic target may be now available. Inhibition of PMV could stop the modification taking place on the erythrocytes membrane, which is necessary to make the RBC capable of supporting the parasite replication process.<sup>10</sup>

In this work, I evaluated the potential of PMV inhibition as a new target for malaria treatment. The advantages in targeting this enzyme are due to its role in plasmodium maturation and its presence in gametocytes, that could allow inhibitors to act at different stages of the parasite life cycle.

In order to assess the viability of this target, peptidomimetics compounds were synthesized to study the catalytic pocket of the enzyme, and to compare these findings with the natural sequences recognized by PMV (**Figure 6.1**).

MESA	DIYTNCE <span style="color:red">S</span> PTYSYSSIKNNNDRYV <span style="color:red">R</span> IL <span style="color:blue">S</span> E <span style="color:green">T</span> EP <span style="color:purple">P</span> MSLEEIM	90	(1434)
STEVOR	ENYLNNDY <span style="color:red">N</span> V <span style="color:blue">S</span> FIQ <span style="color:green">N</span> NTK <span style="color:purple">R</span> TTIKS <span style="color:red">R</span> LLA <span style="color:blue">Q</span> T <span style="color:green">Q</span> IHNPHYHND	63	( 297)
PfEMP3	-YFTVVK <span style="color:red">N</span> YNKIDNVYNI <span style="color:blue">F</span> EIRL <span style="color:green">K</span> RS <span style="color:purple">L</span> A <span style="color:red">Q</span> VLGNTRLSSRG	75	(2441)
11.1	--CSNGKYKSTLYIVGNHLRFRGFRILAENEYEMKTKYKT	109	(1948)
HRPII	---NNSAFNNNLC <span style="color:red">S</span> KNAKGLN <span style="color:blue">L</span> NK <span style="color:green">R</span> LLY <span style="color:purple">E</span> TQAHVDDA <span style="color:red">H</span> HA	60	( 305)
R45	----NEVIY <span style="color:red">N</span> KYDYSSKSIQ <span style="color:blue">H</span> YCI <span style="color:green">R</span> NL <span style="color:purple">S</span> E <span style="color:red">C</span> FRGKSALNDD	103	(1222)
RESA	----GNLGYNGSSSSGVQFTDRCS <span style="color:red">R</span> NLY <span style="color:blue">G</span> ETLPVNPYADS	101	(1085)
GBP130	-----YICGDKYEKAVDYGFRES <span style="color:red">R</span> ILAE <span style="color:blue">G</span> EDTCARKEKT	99	( 824)
RIFIN	-----VYSKNKPSITPHHTQ <span style="color:red">T</span> N <span style="color:blue">R</span> SL <span style="color:green">C</span> E <span style="color:purple">C</span> DTQSTNYNND	51	( 336)
KAHRP	-----CNNGNGSGDSFDFRNK <span style="color:red">R</span> TLA <span style="color:blue">Q</span> KQHEHHHHHHH	69	( 654)

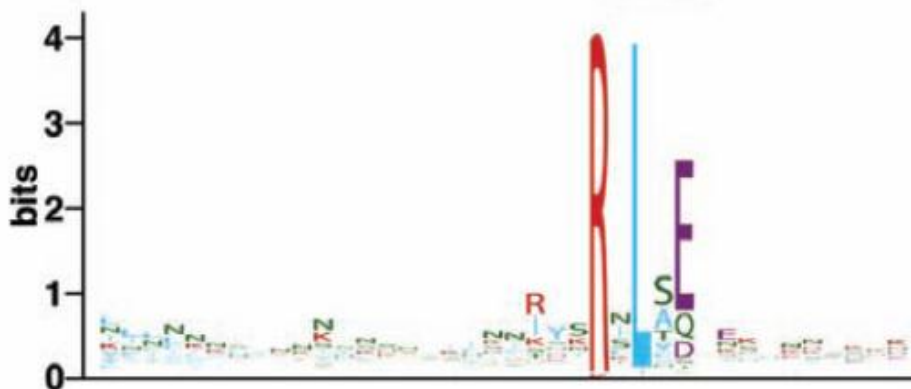


Figure 6.1

As described previously, the arginine and the leucine in the sequence are conserved among all the sequences that share this exportation mechanism.

While usually, it is possible to observe some degree of difference among recognized natural sequences and the inhibitor sequences, our findings highlight that only other basic aminoacids could substitute the arginine residue. All other substitutions led to molecules with an activity greatly reduced, or inactive compounds. Only in six-aminoacids peptidomimetics (Compounds 1-4, and previously synthesized compounds) modification of P3 position generated active compounds.

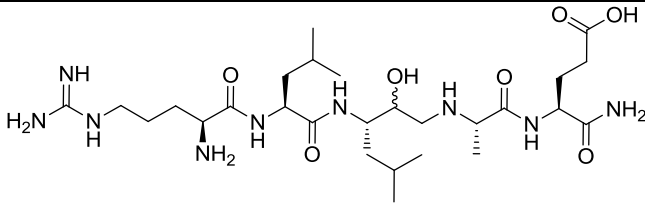
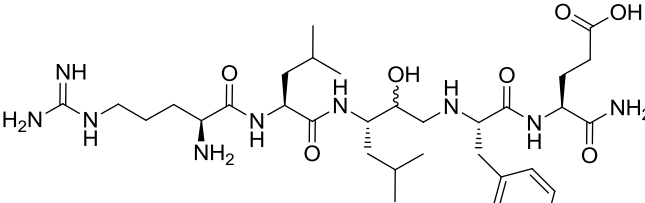
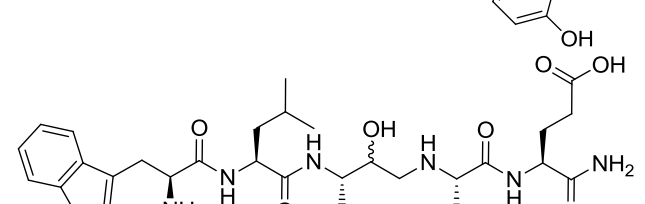
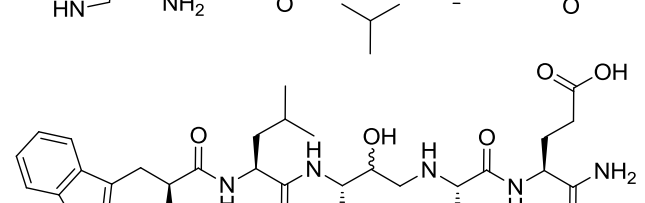
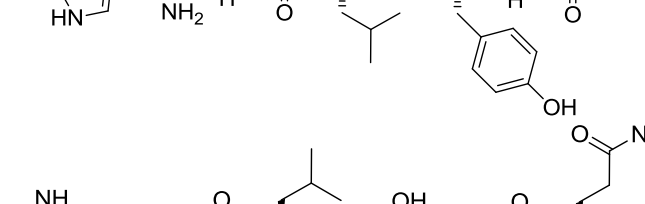
Since positions **P2** and **P1'** do not show any degree of conservation, they were not explored except for synthetic reasons, introducing a Tyr residue in position **P1'** to simplify the purification process.

Position **P2'**, while requiring an acidic sidechain, it is less strict about the identity of the residue: glutamate is the most observed aminoacid in natural PEXEL sequences, but aspartate and glutamine are also tolerated. The same behavior was found in the peptidomimetic inhibitors, where switching from Glu to Gln gave active compounds, albeit with a 100-fold loss of activity (Compounds 1 and 5, Compounds 2 and 6). The

need for an acidic sidechain was confirmed substituting the glutamate with a carboxyterminal glycine: the free carboxylic acid can still interact with the aminoacids in the S2' subsite, and both compounds possess a low micromolar IC<sub>50</sub>.

While less conserved, though, the interaction of this residue with the subsite is necessary for the inhibitorial activity of the compounds, as showed by the lack of activity of compound 9.

Structure and activity of compounds 1-9 are reported in **Table 5.1**.

Compound	Structure	<i>Pf</i> PMV IC <sub>50</sub> [nM]
1		0.25
2		1.1/19.9
3		Inactive
4		Inactive
5		9

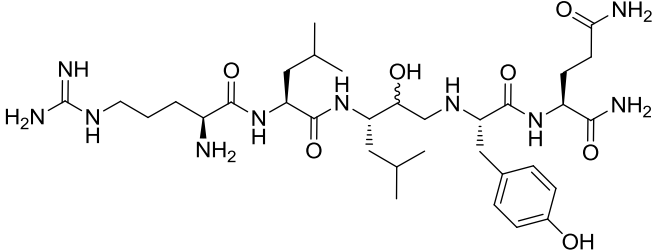
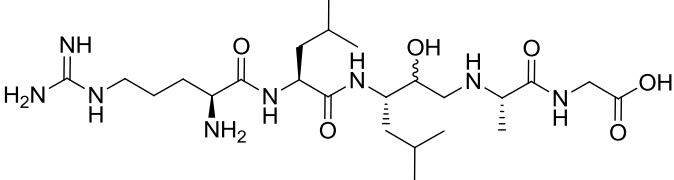
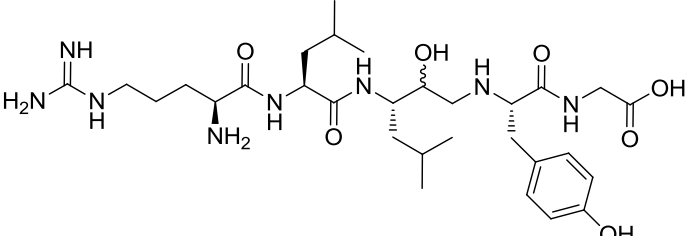
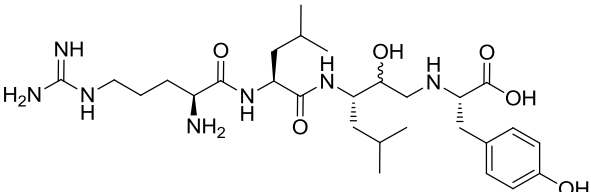
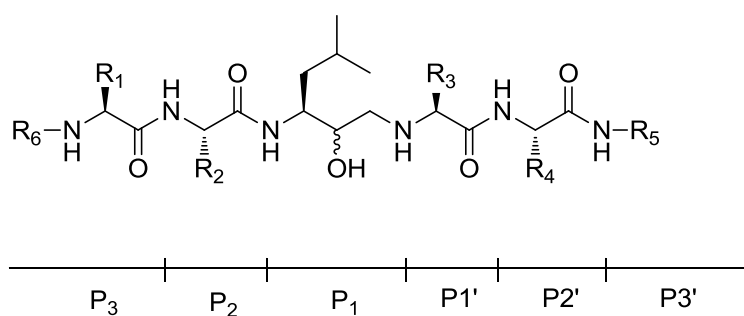
6		20/138
7		10
8		2/78
9		2500/9200

Table 6.1

Structure-activity relationships of this class of compounds, obtained in this thesis and during previous work, could be summarized as following:



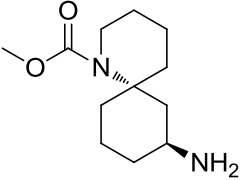
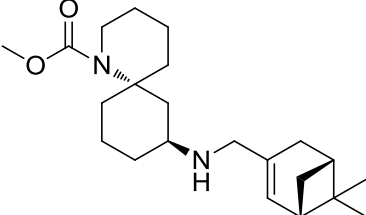
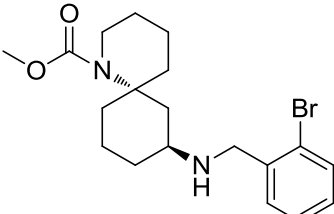
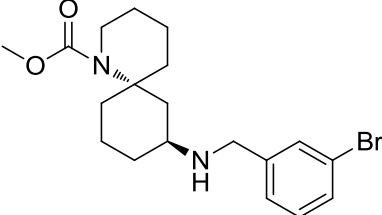
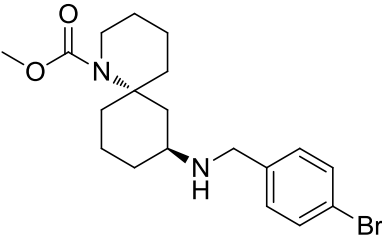
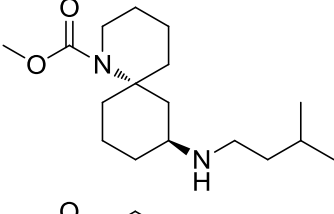
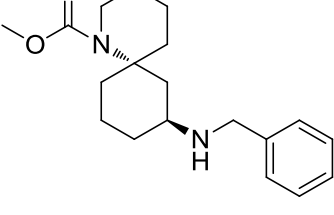
- R<sub>1</sub>: Residues different from arginine are not well tolerated and lead to inactive compounds;
- R<sub>2</sub>: Leucine or Isoleucine are equally accepted in this position;
- R<sub>3</sub>: Tyr slightly decreases the activity of the peptidomimetic sequences but simplify the purification process;

- R<sub>4</sub>: Gln may replace Glu without significant loss of activity, and a -COOH terminal Gly is able to mimic the Glu sidechain;
- R<sub>5</sub>: Removing this aminoacid from the sequence does not significantly affect the activity of the peptidomimetics;
- R<sub>6</sub>: Alifatic capping groups maintain or increase the activity, while aromatic groups kill PMV inhibition.

Since position **P3**, **P1** and **P2'** need to be occupied for this class of compounds, it is evident that five aminoacids is the minimum length to generate an active compound. This is an issue, since it complicates the task of reducing the peptidic nature of the molecules, and the charged sidechains seriously hinder the compounds ability to cross biological membranes. Due to localization of PMV, the lack of antiplasmodial activity of compounds **1-9** could be easily explained as an inability to reach their target at an effective concentration.

Since this problem is intrinsically correlated to their peptidic nature, we decided to look into natural products in order to find a suitable scaffold to be used as a starting point for a new class of compounds. The existence of three-dimensional skeletons overrepresented in many natural products gave us the idea to exploit one of those structures, the 1-azaspiro[5,5]undecane, as a core scaffold.

A small library of compounds was synthesized, and tested against *P.f.* cultures to evaluate their role as a useful starting point. The molecules presenting the azaspiroundecane scaffold (Scaffold A) demonstrate a remarkable ability to inhibit plasmodium growth at 50  $\mu$ M, with just three compounds unable to go above 40% inhibition (**Table 5.2**), while the free scaffold is ineffective. These compounds are equally active against both chloroquine-resistant and sensitive strains, an important feature in the identification of new antimalarial.

Compound	Structure	<i>Pf</i> 3D7 (D10)	<i>Pf</i> 3D7 (W2)
		Growth inhibition % @ 50 $\mu$ M	Growth inhibition % @ 50 $\mu$ M
Scaffold A		Inactive	Inactive
10		89.03	88.91
11		25.41	36.34
12		27.76	37.20
13		28.44	30.76
14		88.62	91.30
15		85.68	78.94

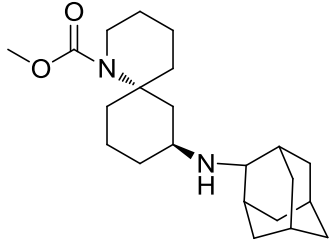
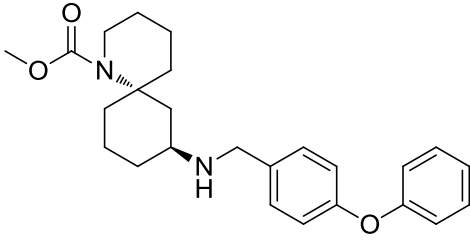
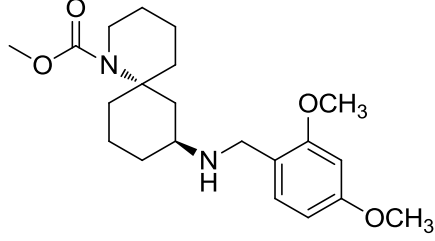
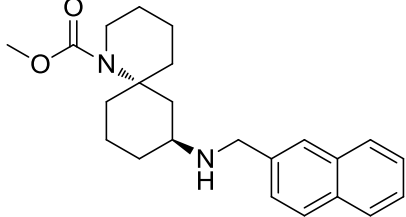
16		99.48	98.80
17		99.93	97.39
18		85.19	85.63
19		80.93	81.18

Table 5.2

The high activity of these compounds at this concentration make it difficult to extrapolate any kind of structure-activity relationship, but the presence of low active molecules (compounds **11-13**) and the inactive scaffold seem to suggest the presence of a defined mechanism of action.

These data were used to design new molecules with more specific substituents. The SAR study performed using the peptidomimetic sequences provided the essential requirements for PMV inhibitors, and we decided to introduce a suitable substituent able to interact with **S3** pocket of the catalytic site. Arginine was an obvious choice, but still marred by the presence of multiple positive charges on the guanidine group. 6-carboxyindole was selected trying to overcome this problem, introducing a basic moiety less flexible and with less charges compared to arginine.

In the scaffold, the distance (in bond length) between the two nitrogens match the bond distance occupied by the aminoacids usually found in position **P2-P1**, putting

the methylcarbamate moiety close to the cleaving position of the natural substrate. Carbamates have already been used as bioisosters of the peptide bond, as in the HIV aspartic protease inhibitor Darunavir, thus providing an optimal substituent for the endocyclic amine of the scaffold.

Compounds **30** and **31** were synthesized and preliminary screened against PMV culture in order to assess their  $IC_{50}$ . Compound **30**, presenting some of the liability of the peptidomimetic compounds, resulted inactive, while compound **31** showed a low micromolar  $IC_{50}$ . Its diastereoisomer, compound **32**, was less active (Table 5.3).

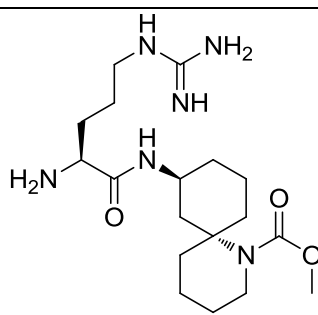
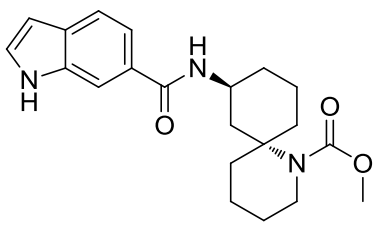
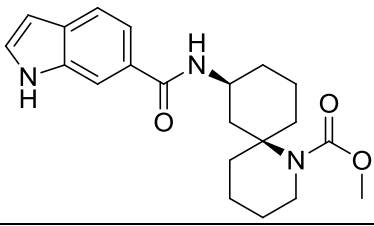
Compound	Structure	<i>Pf</i> 3D7 (D10) $IC_{50}$ ( $\mu$ M)	<i>Pf</i> 3D7 (W2) $IC_{50}$ ( $\mu$ M)
30		>50	>50
31		12.8	16.5
32		>20	>20

Table 5.3

At this stage, unfortunately, there is no direct correlation between the activity of these compounds and PMV inhibition; however, they are based on deductive design built on SAR data of previously synthesized PMV inhibitors.

Our collaborators are currently undergoing the assessment of PMV inhibition, but this work is hindered by difficulties in purifying the functional enzyme.



## 5.1 Closing remarks

PMV is an interesting enzyme that regulate the trafficking of plasmodium proteins during the RBC membrane remodeling stage. Due to its central role in one of the fundamental steps of parasite infection, being able to interfere with PMV activity may provide a new strategy to fight the insurgence of plasmodium strains resistant to conventional therapies.

While at this stage I could not positively identify PMV as a drugable target, my work on this enzyme shed light to some of the structural requirements that potential inhibitors should possess in order to efficaciously interact with the catalytic site. Moreover, the merging of this information with the exploitation of a natural product scaffold led to the identification of a new series of compounds that, while possessing an  $IC_{50}$  of low therapeutically interest, do not seem to share the same mechanism of action of chloroquine, and could be optimized during further studies to achieve a better activity.

## 6. Experimental Section

### 6.1 Abbreviations

**A:** Alanine; **E:** Glutamic acid; **H:** Histidine; **I:** Isoleucine; **K:** Lysine; **L:** Leucine; **M:** Methionine; **N:** Asparagine; **P:** Proline; **Q:** Glutamine; **R:** Arginine; **W:** Tryptophan; **Y:** Tyrosine; **TBTU:** 2-(1H-benzotriazol-1-yl)-1,1,3,3-tetramethyluronium tetrafluoroborate; **HOBt:** 1-Hydroxybenzotriazole hydrate; **DMF:** N,N-Dimethylformamide; **DCM:** Dichloromethane; **NMP:** N-Methyl pyrrolidone; **DIEA:** Diisopropyl ethylamine; **Pip:** Piperidine; **MeOH:** Methanol; **Ac<sub>2</sub>O:** Acetic anhydride; **Boc<sub>2</sub>O:** Di-tert-butylidicarbonate; **THF:** Tetrahydrofuran; **EtOH:** Ethanol; **TFA:** Trifluoroacetic acid; **NMM:** N-methyl morpholine; **SPPS:** Solid phase peptide synthesis.

## 6.2 Reagents and Instrumentations

NMR spectra were recorded at 30°C on either a Varian 500 or 600 MHz Unity INOVA spectrometer, the latter spectrometer equipped with a triple resonance cold probe (Eskitis Institute, Griffith University) or a Varian 300 MHz Mercury spectrometer (Dipartimento di Scienze Farmaceutiche, Università degli Studi di Milano), and referenced using the residual non-deuterated solvent peak.

LR-ESIMS were recorded on a Mariner time-of-flight spectrometer equipped with a Gilson 215 eight-probe injector.

LC-MS were recorded on a ZQ Waters ESI quadrupole LC-MS system.

Spectrophotometric measurements were performed on a UV-VIS Perkin-Elmer LAMDA 11.

HR-ESIMS were recorded on a Bruker Daltonics Apex III 4.7e Fourier-transform mass spectrometer.

Alltech DAVISIL 40–60  $\mu\text{m}$  60 Å C18 bonded silica was used for preadsorption work. A Waters 600 pump equipped with a Waters 996 PDA detector and a Waters 717 autosampler were used for HPLC.

A Thermo-Electron C<sub>18</sub> Betasil 143Å column (5  $\mu\text{m}$ , 21.2 × 150 mm) was used for semipreparative HPLC separations. All solvents used for chromatography and MS were HPLC grade (RCI Lab-Scan, Sigma-Aldrich), and the H<sub>2</sub>O was Millipore Milli-Q PF filtered. Natural products used to test activity were isolated in previous work at the Eskitis institute and are part of its collection. All reagents were commercially obtained (Sigma-Aldrich, Acros, Boron Molecular, IRIS Biotech GmbH, Carlo Erba Reagenti) at highest commercial quality and used without further purification. Air- and moisture-sensitive liquids and solutions were transferred with a syringe. All reactions were carried out under anhydrous conditions with within an argon atmosphere in dry solvents, unless otherwise noted. Yields refer to chromatographically and spectroscopically (<sup>1</sup>H NMR, LC, MS) homogeneous materials, unless otherwise stated. Reactions were monitored by thin-layer chromatography carried out on 0.25 mm Merck silica gel plates (60F-254) with UV light as the visualizing agent and permanganate stain solution as developing agent. Merck silica gel (60, particle size 0.040–0.063 mm) was used for flash chromatography.

Resins, Fmoc-aminoacids, solvents and reagents used for SPPS were obtained from IRIS Biotech GmbH (Schnelldorf, Germany), Carlo Erba Reagenti (Rodano, Italia) and Sigma-Aldrich (Schnelldorf, Germany) and used without further purification. Peptides were manually synthesized using polypropylene syringes (10 ml) with polyethylene frits bought from Grace Discovery.

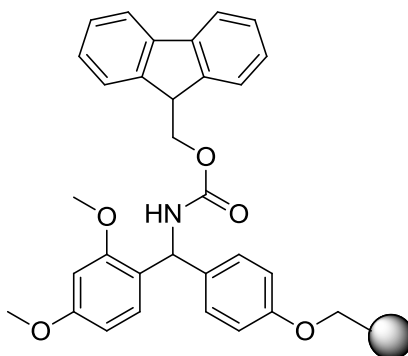
### 6.3 SPPS General Procedures

The peptide synthesis was performed on solid phase, using the Rink amide resin (150 mmol; loading: 0.46 mmol/g) or the 2-chlorotrityl resin (150 mmol; loading 1.55 mmol/g).

#### 6.3.1 Resin-specific Solid-Phase Procedures

- **Rink amide resin**

- 

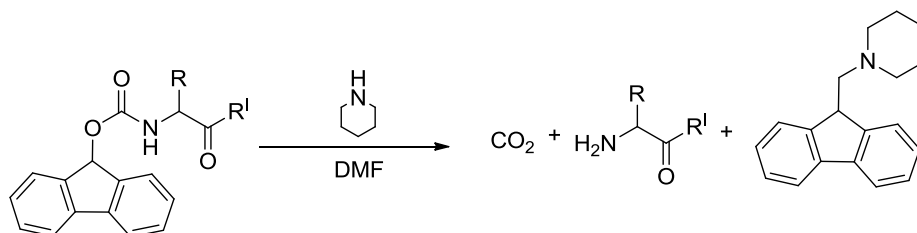


The rink amide resin presents a Fmoc-protected amine that need to be cleaved in order to activate the resin.

#### a) Swelling

The resin is suspended in a solution of NMP (1 ml per 150  $\mu$ mol of resin) and DCM (7.5 ml) and left in a ultrasound bath for 5 minutes. The swollen resin is moved in a reactor, washed 3 times with DCM and filter under vacuum to obtain the dry resin.

## b) Fmoc Cleavage



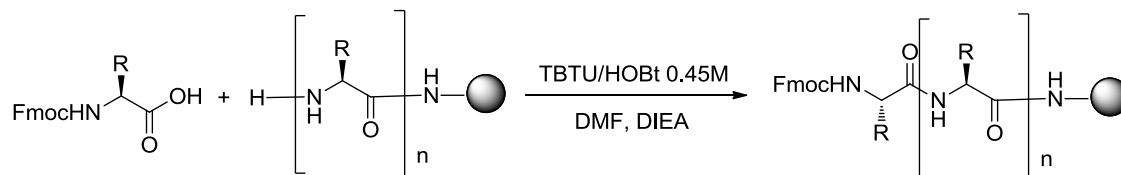
The resin is suspended in a solution of Pip (20% in DMF) and stirred for 5 minutes, filtered and the procedure repeated, increasing the stirring time to 15 minutes. After that, the resin was filtered and washed 6 times with DMF. The filtered DMF is collected in order to quantify the amount of Fmoc cleaved by the deprotection step, which is proportional to the amount of amino acid bound to the resin.

Measuring the absorbance of the fluorene formed after Fmoc cleavage is possible to evaluate the quantity of Fmoc eliminated in the reaction. A sample of the washing DMF is dissolved in a known amount of DMF (usually 3 ml) and its UV absorbance at 300.8 nm is measured.

The mol of fluorene are derived from the absorbance using the following formula:

$$\mu\text{mol} = (\text{abs}_{(\text{Sample})} - \text{abs}_{(\text{Blank})}) \cdot V_s \cdot V_c / (C \cdot V_p)$$

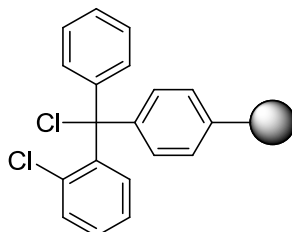
- $\text{Abs}_{(\text{Sample})}$ : Sample absorbance at 300,8 nm.
- $\text{Abs}_{(\text{Blank})}$ : Blank absorbance at 300,8 nm.
- $V_s$ : DMF washing volume.
- $V_c$ : Cuvette volume.
- $V_p$ : Sample volume.
- $C$ : Molar extinction coefficient ( $C_{\text{fluorene}} = 7.8 \text{ ml}/\mu\text{mol}$ ).

**c) Coupling Reaction**

A solution of Fmoc-AA (3 eq) in TBTU/HOBt (0.45M in DMF, 4 eq) was treated with DIEA (8 eq) and added to the resin. The resulting suspension was left shaking for 50 minutes. Once the reaction is complete, the resin filtered and washed 6 times with DMF.

At this stage, if more aminoacids need to be introduced in order to complete the sequence, step **b)** and **c)** are repeated until the last residue is bound to the resin and deprotected. At this point, the resin is washed 3 times with DCM and dried thoroughly before proceeding with the peptide cleavage from the resin.

- **2-Chlorotritylic Resin**

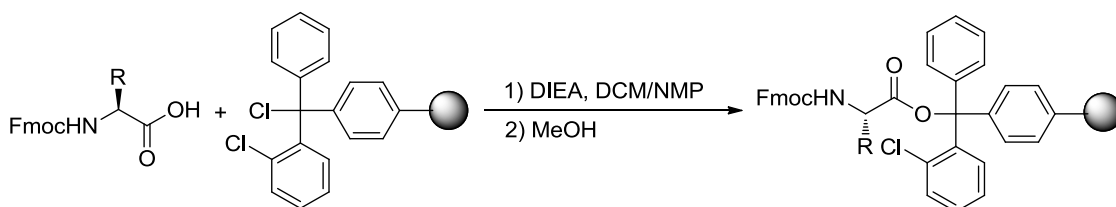


2-Chlorotritylic resin is devoid of protecting group and does not need an activation step before the introduction of the first amino acid.

**a) Swelling**

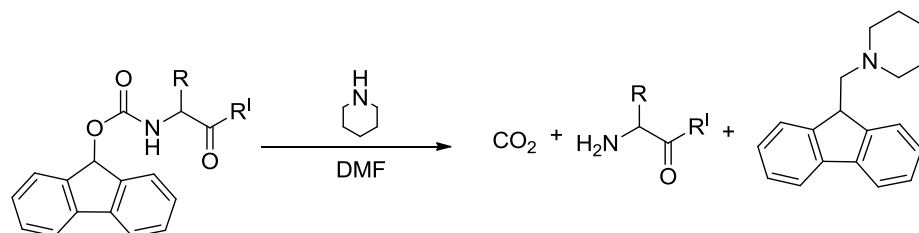
The resin is suspended in a solution of NMP (1 ml per 150  $\mu$ mol of resin) and DCM (7.5 ml) and left in a ultrasound bath for 5 minutes. The swollen resin is moved in a reactor, washed 3 times with DCM and filter under vacuum to obtain the dry resin.

**b) Coupling of the first amino acid to the resin**



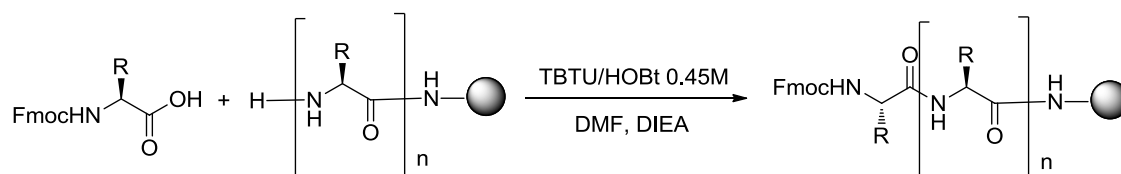
A solution of the Fmoc-AA (150  $\mu$ mol, 1 eq) in DCM/NMP (2:1, 1 ml) was treated with DIEA (2 eq) and added to the resin. The reactor was left shaking for 50 minutes, after which 400  $\mu$ l of MeOH were added in order to cap all the reacting groups left on the resin, and the reaction was left shaking for additional 5 minutes. At the end, the resin was filtered and washed 6 times with DMF.

## c) Fmoc Cleavage



The resin is suspended in a solution of Pip (20% in DMF) and stirred for 5 minutes, filtered and the procedure repeated, increasing the stirring time to 15 minutes. After that, the resin was filtered and washed 6 times with DMF. The filtered DMF is collected in order to quantify the amount of Fmoc cleaved by the deprotection step, which is proportional to the amount of amino acid bound to the resin.

## d) Coupling Reaction



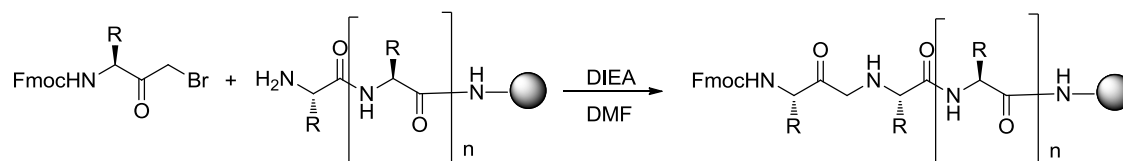
A solution of Fmoc-AA (3 eq) in TBTU/HOBt (0.45M in DMF, 4 eq) was treated with DIEA (8 eq) and added to the resin. The resulting suspension was left shaking for 50 minutes. Once the reaction is complete, the resin filtered and washed 6 times with DMF.

At this stage, if more amino acids need to be introduced in order to complete the sequence, step c) and d) are repeated until the last residue is bound to the resin and deprotected. At this point, the resin is washed 3 times with DCM and dried thoroughly before proceeding with the peptide cleavage from the resin.



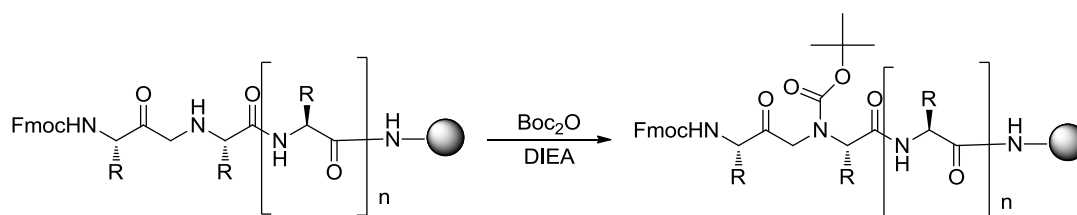
### 6.3.2 Common Solid-Phase Procedures

#### a) Ketomethylamine Synthesis



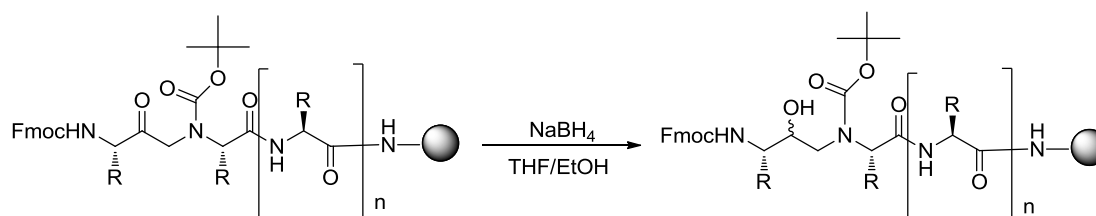
A solution of Fmoc-AA (1 eq) in DMF was treated with DIEA (1 eq) and added to the resin. The reactor was left shaking overnight. After that, the resin was filtered and washed 6 times with DMF.

#### b) Boc- Protection



A solution of  $\text{Boc}_2\text{O}$  (5 eq) in DCM was treated with DIEA (10 eq) and added to the resin. The suspension was left shaking for 1 hour, after which was filtered and washed 6 times with DCM.

#### c) Hydroxyethylamine Synthesis



The resin was suspended in THF/EtOH (1:1) and treated with 10 mg of  $\text{NaBH}_4$ . After 4 hours the resin was filtered, washed 3 times with THF, 6 times with THF/  $\text{H}_2\text{O}$  (1:1), 2 times with THF and 3 times with MeOH.

### d) Peptide Cleavage

After removing the N-terminal Fmoc group, the resin was washed 4 times in DCM and dried under vacuum. The cleavage cocktail was prepared according to the sequence that need to be cleaved and the resin suspended in 3 ml of it for 2 hours, after which the liquid was filtered in the chosen precipitation media. The suspension created was centrifugated and the surnatant removed, and new precipitation media was added to the precipitate. These operations were repeated two times to remove all the cocktail scavengers, after which the precipitate was solubilized in 1 ml of DMSO and purified by preparative HPLC.

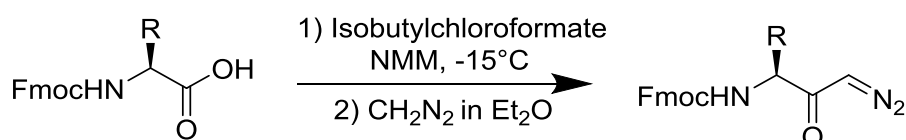
### e) Peptide Purification

Synthesized peptides were purified by reverse-phase HPLC, using a linear gradient from H<sub>2</sub>O/MeOH/TFA 95:5:0.1 to MeOH/TFA 100:0.1 at 14 ml/min.

Fractions containing the compound were collected, concentrated to remove the MeOH, the TFA salt exchanged with HCl (1M) to obtain the hydrochloride salt and freeze-dried to remove the water.

## 6.4 General Synthetic Procedures

### a) Diazomethylketone Synthesis

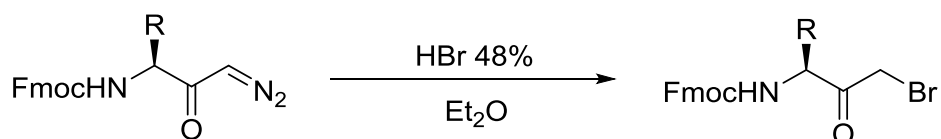


A solution of Fmoc-AA in anhydrous THF (4.7 ml/mmol of Fmoc-AA) was cooled to -15°C and kept under inert atmosphere. Isobutylchloroformate (1.1 eq) and NMM (1.1 eq) were added to the solution and the mixture stirred for 15 minutes. The crude was then filtered to remove the NMM-salt and the solution cooled to -70°C. The

mixture was kept under inert atmosphere, under vigorous stirring, and an excess of  $\text{CH}_2\text{N}_2$  in  $\text{Et}_2\text{O}$  was slowly added dropwise, keeping the reaction below  $-60^\circ\text{C}$ , and the left reacting overnight at  $0^\circ\text{C}$ .

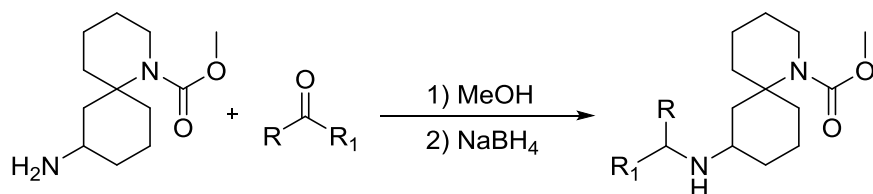
Once completed, the diazomethane excess was evaporated and quenched with  $\text{AcOH}$ , and the crude mixture evaporated under reduced pressure. The crude was then solubilized with  $\text{AcOEt}$ , extracted 3 times with water and 1 time with brine. The organic phase was collected, dried over  $\text{Na}_2\text{SO}_4$  and evaporated under reduced pressure.

### b) Bromomethylketone Synthesis



A solution of Fmoc-diazomethylketone in  $\text{Et}_2\text{O}$  (3.5 ml/mmol) was cooled to  $0^\circ\text{C}$  and  $\text{HBr}$  48% (1 eq) was added dropwise. After complete disappearance of the starting material (TLC) the reaction was diluted in  $\text{AcOEt}$  and washed 3 times with a saturated solution of  $\text{NaHCO}_3$ , once with water and once with brine. The organic phase was collected, dried over  $\text{Na}_2\text{SO}_4$  and dried under vacuum. The product was used without further purification.

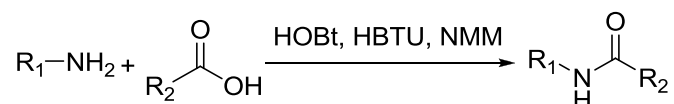
### c) Reductive Amination



A mixture of the chosen aldehyde or ketone (1 eq) and scaffold **A** or **B** (1 eq) in methanol was left stirring overnight. To this reaction mixture  $\text{NaBH}_4$  (2 eq) was added portion-wise. After 30 minutes the reaction mixture was preadsorbed on  $\text{C}_{18}$

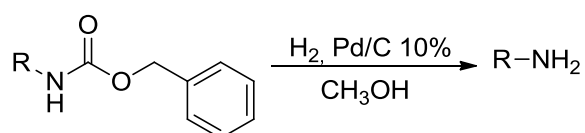
bonded silica and chromatographed on a semipreparative C<sub>18</sub> HPLC column using a 30 minutes gradient from H<sub>2</sub>O/MeOH 95:5 to H<sub>2</sub>O/MeOH (0.1% TFA) 0:100 to give the desired product.

#### d) Coupling Reaction

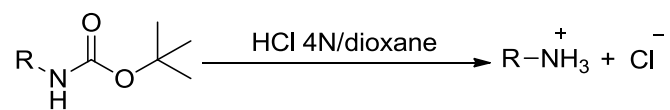


A solution of the carboxylic acid (1.1 eq) and the amine (1.0 eq) in an appropriate solvent (DMF or dichloromethane) (5mL/mmol), was cooled to 0°C and hydroxybenzotriazole (HOBt) (1.5 eq) and *O*-(benzotriazol-1-yl)-*N,N,N',N'*-tetramethyluronium hexafluorophosphate (HBTU) was added (1.1 eq). NMM was added until pH 8 was reached. The mixture was then stirred at room temperature overnight. Dichloromethane was then added and the organic phase washed with HCl 1N, saturated NaHCO<sub>3</sub>, water, brine, dried, filtered and concentrated. The crude was purified using normal or reverse phase chromatography.

#### e) Removal of the Cbz- protecting group



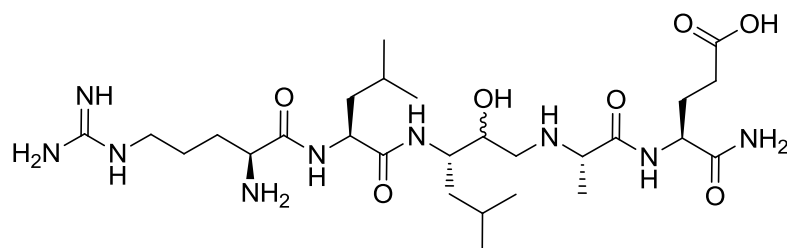
The Cbz protected compound was dissolved in methanol (10 mL/mmol) and then Pd/C (10%) (80 mg/mmol) was added. The mixture was left under H<sub>2</sub> atmosphere for 2h, checking the progress with TLC after which the mixture was filtrated, washed with methanol and the residue concentrated and used in the next step without any further purification or characterization.

**f) Removal of the Boc- protecting group**

Boc protected compound was cooled to 0°C ND HCl 4N in dioxane was added (10 mL/g of compound). The mixture was stirred at room temperature for 30 minutes, after which it was concentrated and the residue washed 3 times with ethyl ether and purified using reverse phase HPLC.

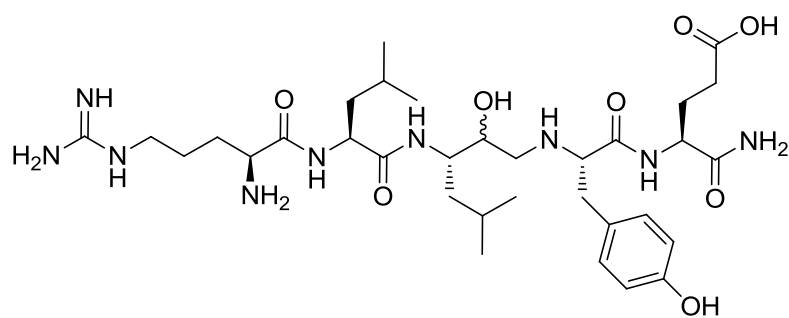
## 6.5 Specific Synthetic Procedures

### Compound 1



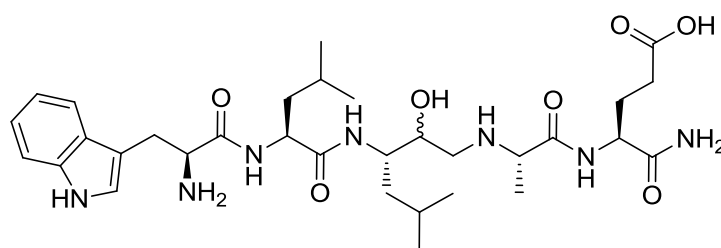
The peptide was synthesized on rink amide resin using SPPS procedure. Cleavage for resin was performed using TFA (10 ml), TIS (0.5 ml), thioanisole (0.25 ml) and phenol (75 mg), and the peptide precipitated in a solution of Methyl-t-Butyl ether/Petroleum ether 1:1. Only one stereoisomer was recovered as a white solid (7.1 mg, 7.7%).

HRMS-ESI  $m/z$   $[M+H]^+$  calcd for  $C_{27}H_{53}N_9O_7$ : 616.4068, found: 616.41392.

**Compound 2**

The peptide was synthesized on rink amide resin using SPPS procedure. Cleavage for resin was performed using TFA (10 ml), TIS (0.5 ml), thioanisole (0.25 ml) and phenol (75 mg), and the peptide precipitated in a solution of Methyl-t-Butyl ether/Petroleum ether 1:1. Both stereoisomers were recovered as a white solids (7.0 mg, 7.7%; 3.4 mg, 3.2%).

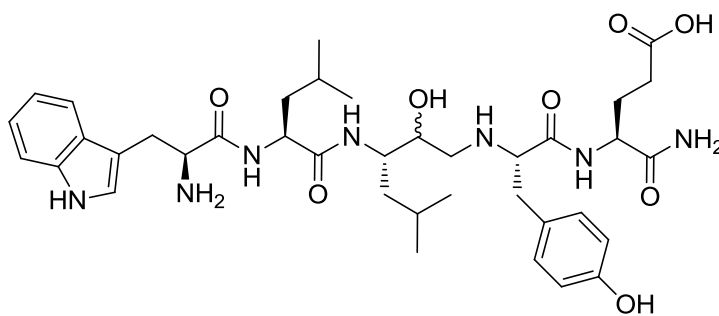
HRMS-ESI  $m/z$   $[M+H]^+$  calcd for  $C_{33}H_{57}N_9O_8$ : 708.4330, found: 708.44080 and 707.43929.

**Compound 3**

The peptide was synthesized on rink amide resin using SPPS procedure. Cleavage for resin was performed using TFA (10 ml), TIS (0.5 ml), thioanisole (0.25 ml) and phenol (75 mg), and the peptide precipitated in a solution of Methyl-t-Butyl ether/Petroleum ether 1:1. Both stereoisomers were recovered as a white solids (13.3 mg, 13.7%; 7.2 mg, 7.5%).

HRMS-ESI  $m/z$   $[M+H]^+$  calcd for C<sub>32</sub>H<sub>51</sub>N<sub>7</sub>O<sub>7</sub>: 646.3850, found: 646.39136 and 646.39127.

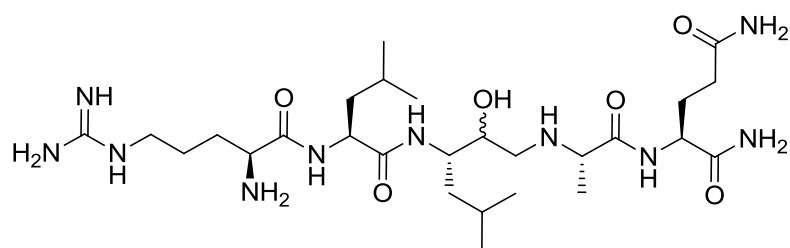


**Compound 4**

The peptide was synthesized on rink amide resin using SPPS procedure. Cleavage for resin was performed using TFA (10 ml), TIS (0.5 ml), thioanisole (0.25 ml) and phenol (75 mg), and the peptide precipitated in a solution of Methyl-t-Butyl ether/Petroleum ether 1:1. Both stereoisomers were recovered as a white solids (7.3 mg, 6.6%; 4.6 mg, 3.1%).

HRMS-ESI  $m/z$   $[M+H]^+$  calcd for  $C_{38}H_{55}N_7O_8$ : 738.4112, found: 738.41315 and 738.41421.

## Compound 5



The peptide was synthesized on rink amide resin using SPPS procedure. Cleavage for resin was performed using TFA (10 ml), TIS (0.5 ml), thioanisole (0.25 ml) and phenol (75 mg), and the peptide precipitated in a solution of Methyl-t-Butyl ether/Petroleum ether 1:1. Only one stereoisomer was recovered as a white solid (26.7 mg, 28.9%).

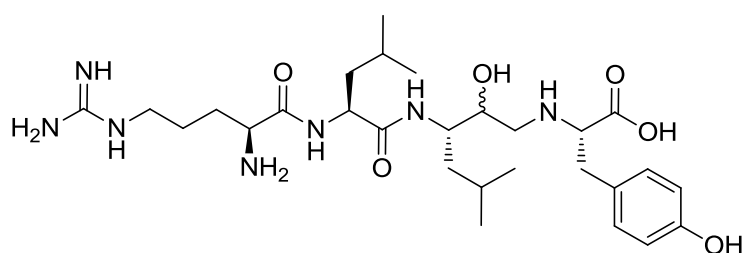
HRMS-ESI  $m/z$   $[M+H]^+$  calcd for  $C_{27}H_{54}N_{10}O_6$ : 615.4228, found: 615.43040 and 615.42946.







## Compound 9



The peptide was synthesized on 2-Chlorotritylic resin using SPPS procedure. Cleavage for resin was performed using TFA (10 ml), TIS (0.5 ml), thioanisole (0.25 ml) and phenol (75 mg), and the peptide precipitated in a solution of Methyl-t-Butyl ether/Petroleum ether 1:1. Both stereoisomers were recovered as a white solids (12.3 mg, 14.1%; 10.3 mg, 11.8%).

HRMS-ESI  $m/z$   $[M+H]^+$  calcd for  $C_{28}H_{49}N_7O_6$ : 580.3744, found: 580.38127 and 580.38125.

## Intermediate 9

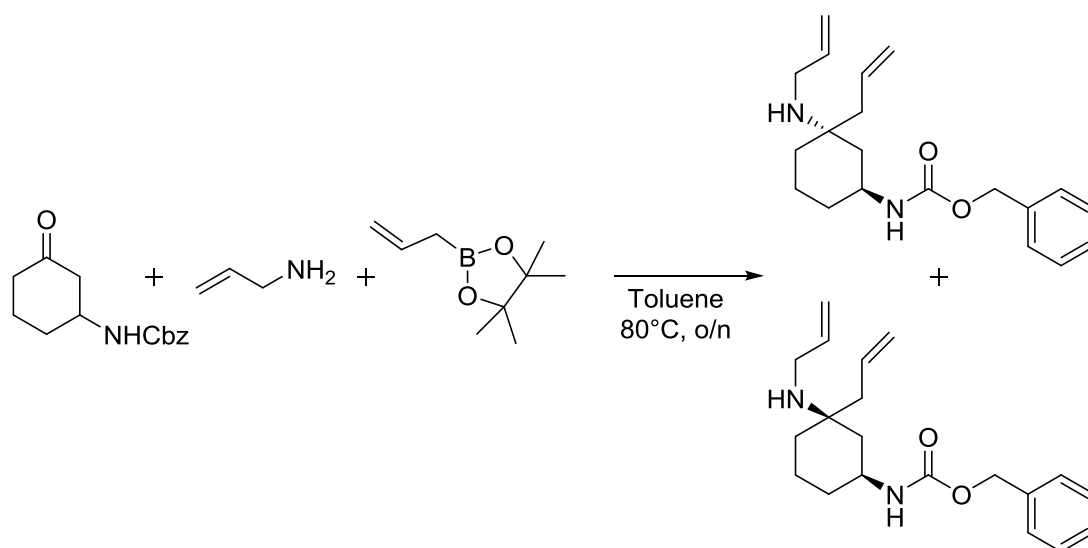


A mixture of benzylcarbamate (1 g, 6.6 mmol) and Bi(NO<sub>3</sub>)<sub>3</sub> (1.92 g, 3.96 mmol) was suspended in cyclohex-2-enone (630  $\mu$ l, 6.6 mmol) and stirred overnight at room temperature. After complete consumption of the starting material (TLC chromatography), the mixture is diluted using DCM and filtered to remove the catalyst. The filtrated solution was then concentrated under pressure, followed by flash chromatography (Cyclohexene/AcOEt 100:0 to 50:50). Intermediate **9** was isolated as an orange solid (1.46 g, 5.97 mmol, 90.4%).

$R_f=0.44$  (Cyclohexane/AcOEt 5:5)

<sup>1</sup>H NMR (500 MHz, CDCl<sub>3</sub>)  $\delta=7.39 - 7.30$  (m, 5H), 5.09 (s, 1H), 4.77 (s, 1H), 3.99 (s, 1H), 2.70 (dt,  $J = 17.2, 8.6$  Hz, 1H), 2.41 - 2.34 (m, 1H), 2.31 - 2.22 (m, 2H), 2.15 - 2.06 (m, 1H), 2.02 - 1.93 (m, 1H), 1.83 - 1.55 (m, 1H).

## Intermediate 10 and 11



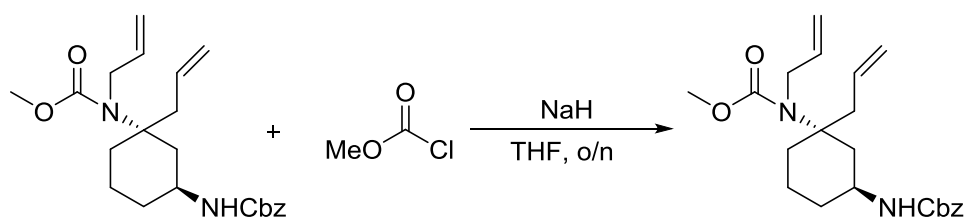
A solution of intermediate **9** (1.46 g, 5.97 mmol) in dry toluene over 3Å molecular sieves (0.3 g/mmol) was treated with allylamine (1.3 ml, 17.91 mmol) and allylboronic acid pinacol ester (5.6 ml, 29.85 mmol) and stirred overnight at 80°C. The reaction crude was then filtered to remove the molecular sieves and concentrated under vacuum, followed by flash chromatography (Cyclohexane/AcOEt 100:0 to 50:50). It was possible to separate the two diastereoisomer **10** (0.95 g, 3.02 mmol) and **11** (0.51 mg, 1.61 mmol) as dark yellow oils due to their different retention ( $R_f=0.67$  and  $R_f=0.32$  in cyclohexane/AcOEt 7:3). The overall yield of the reaction was 77.5%.

$^1\text{H}$  NMR of **10** (500 MHz,  $[\text{D}_6]$ DMSO)  $\delta=8.37$  (s, 1H), 7.50 – 7.20 (m, 5H), 6.01 – 5.91 (m, 1H), 5.79 (td,  $J = 17.2, 7.3$  Hz, 1H), 5.50 (d,  $J = 17.0$  Hz, 1H), 5.41 (d,  $J = 10.2$  Hz, 1H), 5.24 (d,  $J = 7.2$  Hz, 1H), 5.21 (s, 1H), 5.03 (s, 2H), 3.83 – 3.72 (m, 2H), 3.64 (s, 1H), 2.45 (d,  $J = 7.2$  Hz, 2H), 2.00 (d,  $J = 14.0$  Hz, 1H), 1.86 – 1.75 (m, 2H), 1.71 – 1.60 (m, 2H), 1.49 – 1.37 (m, 2H), 1.19 – 1.10 (m, 1H).

$^1\text{H}$  NMR of **11** (500 MHz,  $[\text{D}_6]$ DMSO)  $\delta=8.56$  (d,  $J = 27.9$  Hz, 1H), 7.46 – 7.26 (m, 5H), 5.95 – 5.75 (m, 2H), 5.49 (d,  $J = 17.1$  Hz, 1H), 5.37 (t,  $J = 14.2$  Hz, 2H), 5.27 (d,  $J = 9.8$  Hz, 1H), 5.02 (s, 2H), 3.60 (s, 2H), 3.56 – 3.48 (m, 1H), 2.65 – 2.52 (m, 2H), 2.11 (d,  $J = 11.7$  Hz, 1H), 1.90 – 1.76 (m, 2H), 1.74 – 1.65 (m, 1H), 1.56 – 1.32 (m, 3H), 1.25 – 1.06 (m, 1H).



## Intermediate 12

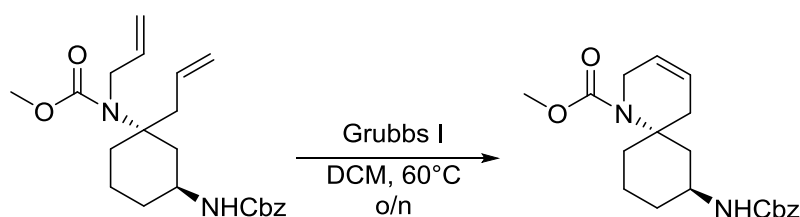


A solution of intermediate **10** (1.75 g, 5.56 mmol) in dry THF was cooled at  $-78^{\circ}\text{C}$  and treated with NaH (0.67 g, 27.8 mmol). After the solution had been stirred for 30 min at  $-78^{\circ}\text{C}$  the reaction was brought to room temperature and methylchloroformate was added dropwise (2.15 ml, 27.8 mmol) and left reacting overnight. At the end of the reaction (TLC chromatography) the crude was diluted with DCM and quenched with HCl 1M. The organic layer was separated and extracted three times with HCl 1M, once with brine and then collected, dried ( $\text{NaSO}_4$ ) and evaporated under vacuum. The residue was purified by flash chromatography (Cyclohexane/AcOEt 100:0 to 80:20) to give intermediate **12** (1.56 g, 4.04 mmol, 72.6%) as a yellow oil.

$R_f=0.57$  (Cyclohexane/AcOEt 7:3).

$^1\text{H}$  NMR (500 MHz,  $[\text{D}_6]\text{DMSO}$ )  $\delta=7.42 - 7.25$  (m, 5H), 7.17 (d,  $J = 6.5$  Hz, 1H), 5.93 - 5.80 (m, 1H), 5.79 - 5.66 (m, 1H), 5.18 (d,  $J = 17.2$  Hz, 1H), 5.10 - 4.93 (m, 6H), 4.02 - 3.91 (m, 2H), 3.55 (s, 3H), 3.47 - 3.38 (m, 1H), 2.70 - 2.61 (m, 1H), 2.41 (d,  $J = 6.9$  Hz, 2H), 1.78 (d,  $J = 10.5$  Hz, 1H), 1.53 (d,  $J = 13.2$  Hz, 1H), 1.39 - 1.26 (m, 1H), 1.25 - 1.04 (m, 3H).

## Intermediate 14

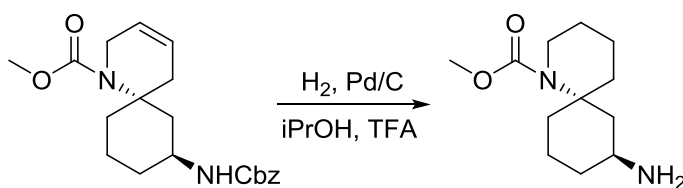


To a solution of intermediate **12** (1.56 g, 6.04 mmol) in DCM was added 1% of 1<sup>st</sup> generation Grubbs catalyst and left stirring at 60°C overnight. After complete consumption of the reagent (TLC chromatography) the reaction mixture was diluted and filtered to eliminate the catalyst, then concentrated under vacuum. Flash chromatography (Cyclohexane/AcOEt 100:0 to 70:30) gave intermediate **14** (1.31 g, 3.65 mmol, 91.0%) as a yellow oil.

$R_f=0.42$  (Cyclohexane/AcOEt 7:3)

<sup>1</sup>H NMR (500 MHz, [D<sub>6</sub>]DMSO)  $\delta=7.43 - 7.26$  (m, 5H), 7.18 (d,  $J = 7.2$  Hz, 1H), 5.66 (q,  $J = 10.8$  Hz, 2H), 5.00 (s, 2H), 4.11 (d,  $J = 18.6$  Hz, 1H), 3.98 (d,  $J = 18.6$  Hz, 1H), 3.55 (s, 3H), 3.45 - 3.34 (m, 1H), 2.74 (d,  $J = 13.2$  Hz, 1H), 2.59 (d,  $J = 13.2$  Hz, 1H), 2.15 (d,  $J = 17.4$  Hz, 1H), 1.91 (d,  $J = 17.4$  Hz, 1H), 1.81 (d,  $J = 11.6$  Hz, 1H), 1.56 (d,  $J = 13.3$  Hz, 1H), 1.39 (dd,  $J = 26.6, 13.3$  Hz, 1H), 1.21 (ddd,  $J = 25.1, 12.3, 4.1$  Hz, 1H), 1.06 (t,  $J = 12.4$  Hz, 1H), 0.99 (t,  $J = 12.4$  Hz, 1H).

## Scaffold A



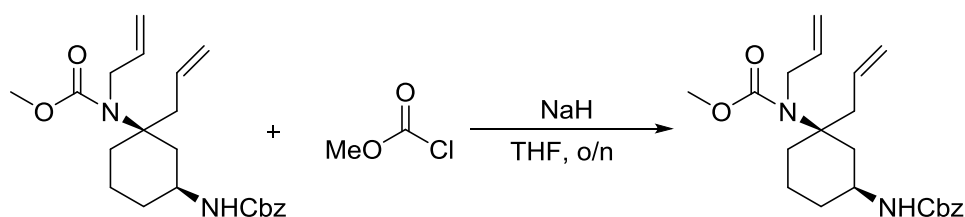
Pd/C (10 wt.%, 31.3 mg) was added to a solution of intermediate **14** (1.40 g, 3.91 mmol) in isopropanol (3.9 ml) with catalytic amount of TFA (25  $\mu$ l). After three cycles of vacuum/H<sub>2</sub>, the solution is kept under vigorous stirring in an atmosphere of H<sub>2</sub> until the complete disappearance of the starting material was observed in TLC (DCM/MeOH 9:1). The crude was then filtered to remove the catalyst and concentrated under vacuum. Flash chromatography (DCM/MeOH/NH<sub>3</sub> 99:1:0.1 to 90:10:0.1) gave scaffold **A** (873.6 mg, 3.86 mmol, 98.7%) as an highly hygroscopic solid.

$R_f=0.13$  (DCM/MeOH/NH<sub>3</sub> 9:1:0.1).

<sup>1</sup>H NMR (500 MHz, [D<sub>6</sub>]DMSO)  $\delta=7.87$  (bs, 2H), 3.62 – 3.53 (m, 4H), 3.38 – 3.29 (m, 1H), 3.16 – 3.05 (m, 1H), 3.01 (d,  $J = 13.1$  Hz, 1H), 2.72 (d,  $J = 12.7$  Hz, 1H), 1.98 – 1.88 (m,  $J = 12.1$  Hz, 1H), 1.76 – 1.65 (m, 1H), 1.65 – 1.56 (m, 2H), 1.47 (t,  $J = 6.1$  Hz, 2H), 1.44 – 1.38 (m, 1H), 1.38 – 1.23 (m, 3H), 1.13 (t,  $J = 12.5$  Hz, 1H), 0.93 (td,  $J = 13.7, 2.7$  Hz, 1H).

HRMS-ESI  $m/z$  [ $M+H$ ]<sup>+</sup> calcd for C<sub>12</sub>H<sub>23</sub>N<sub>2</sub>O<sub>2</sub>: 227,175585, found: 227,175404

## Intermediate 13

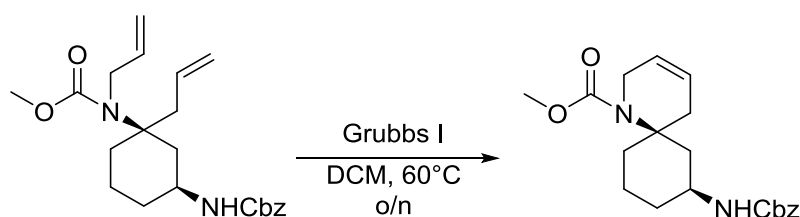


A solution of intermediate **11** (0.66 g, 2.01 mmol) in dry THF was cooled at  $-78^{\circ}\text{C}$  and treated with NaH (0.24 g, 10.05 mmol). After the solution had been stirred for 30 min at  $-78^{\circ}\text{C}$  the reaction was brought to room temperature and methylchloroformate was added dropwise (0.77 ml, 10.05 mmol) and left reacting overnight. At the end of the reaction (TLC chromatography) the crude was diluted with DCM and quenched with HCl 1M. The organic layer was separated and extracted three times with HCl 1M, once with brine and then collected, dried ( $\text{NaSO}_4$ ) and evaporated under vacuum. The residue was purified by flash chromatography (Cyclohexane/AcOEt 100:0 to 50:50) to give intermediate **13** (0.53 g, 1.36 mmol, 67.8%) as a yellow oil.

$R_f=0.57$  (Cyclohexane/AcOEt 7:3).

$^1\text{H NMR}$  (300 MHz,  $\text{CDCl}_3$ )  $\delta=7.40 - 7.31$  (m, 5H), 5.84 - 5.63 (m, 1H), 5.30 (s, 1H), 5.15 - 5.02 (m, 4H), 4.57 (d,  $J = 8.2$  Hz, 1H), 3.92 - 3.85 (m, 2H), 3.65 (s, 3H), 2.81 - 2.64 (m, 3H), 2.42 - 2.32 (m, 1H), 2.01 (d,  $J = 12.4$  Hz, 1H), 1.74 - 1.59 (m, 4H), 1.50 - 1.34 (m, 1H), 1.34 - 1.21 (m, 2H), 1.06 - 0.95 (m, 1H).

## Intermediate 15

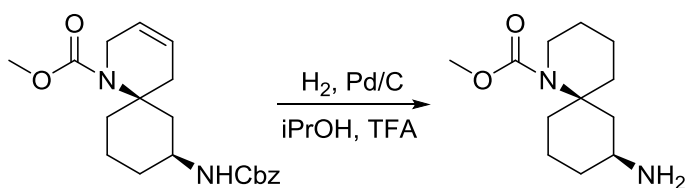


To a solution of intermediate **13** (1.26 g, 3.25 mmol) in DCM was added 1% of 1<sup>st</sup> generation Grubbs catalyst and left stirring at 60°C overnight. After complete consumption of the reagent (TLC chromatography) the reaction mixture was diluted and filtered to eliminate the catalyst, then concentrated under vacuum. Flash chromatography (Cyclohexane/AcOEt 100:0 to 50:50) gave intermediate **15** (0.99 g, 2.76 mmol, 84.9%) as a yellow oil.

$R_f=0.38$  (Cyclohexane/AcOEt 7:3).

<sup>1</sup>H NMR (300 MHz, CDCl<sub>3</sub>)  $\delta=7.39 - 7.28$  (m, 5H), 5.92 - 5.77 (m, 1H), 5.07 (s, 1H), 4.75 - 4.64 (m, 1H), 3.96 (s, 2H), 3.62 (s, 3H), 2.35 - 2.27 (m, 2H), 2.27 - 2.16 (m, 1H), 2.13 - 2.03 (m, 2H), 1.95 (d,  $J = 13.2$  Hz, 1H), 1.80 - 1.60 (m, 2H), 1.51 - 1.32 (m, 3H), 1.26 - 1.06 (m, 2H).

## Scaffold B



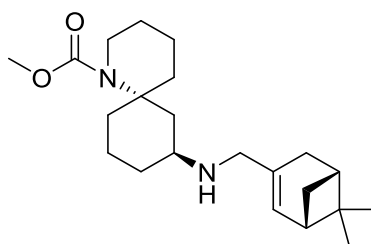
Pd/C (10 wt.%, 0.17 mg) was added to a solution of intermediate **15** (0.75 g, 2.11 mmol) in isopropanol (20 ml) with catalytic amount of TFA (25  $\mu$ l). After three cycles of vacuum/H<sub>2</sub>, the solution is kept under vigorous stirring in an atmosphere of H<sub>2</sub> until the complete disappearance of the starting material was observed in TLC (DCM/MeOH 9:1). The crude was then filtered to remove the catalyst and concentrated under vacuum. Flash chromatography (DCM/MeOH/NH<sub>3</sub> 99:1:0.1 to 90:10:0.1) gave scaffold **B** (0.33 g, 1.44 mmol, 68.3%) as an highly hygroscopic solid.

$R_f$ =0.13 (DCM/MeOH/NH<sub>3</sub> 9:1:0.1).

<sup>1</sup>H NMR (300 MHz, CDCl<sub>3</sub>)  $\delta$ =3.67 (d,  $J$  = 8.7 Hz, 2H), 3.61 (s, 3H), 3.43 (d,  $J$  = 13.8 Hz, 2H), 3.22 (s, 1H), 2.70 (t,  $J$  = 12.2 Hz, 1H), 2.32 (d,  $J$  = 9.8 Hz, 2H), 2.07 (d,  $J$  = 10.9 Hz, 2H), 1.66 (d,  $J$  = 23.4 Hz, 4H), 1.38 (s, 2H), 1.25 (s, 1H), 1.15 (d,  $J$  = 6.2 Hz, 2H).

HRMS-ESI  $m/z$  [ $M+H$ ]<sup>+</sup> calcd for C<sub>12</sub>H<sub>23</sub>N<sub>2</sub>O<sub>2</sub>: 227,175585, found: 227,175965.

## Compound 10

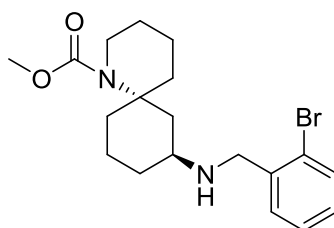


Compound **10** was prepared according to general procedure by reacting (-)-**myrtenal** (33.0 mg, 0.22 mmol) with **A** (50 mg, 0.22 mmol). Compound **10** was isolated as a light yellow oil (14 mg, 0.04 mmol, 18.2%).

$R_f=0.44$  (DCM/MeOH 9:1).

$^1\text{H NMR}$  (500 MHz,  $\text{CD}_3\text{OD}$ )  $\delta=5.79$  (s, 1H), 3.87 - 3.77 (m, 1H), 3.65 (s, 4H), 3.58 (s, 1H), 3.52 (d,  $J = 14.3$  Hz, 1H), 3.38 - 3.32 (m, 1H), 3.28 - 3.21 (m, 1H), 2.77 (d,  $J = 14.5$  Hz, 1H), 2.55 - 2.47 (m, 1H), 2.36 (d,  $J = 9.8$  Hz, 2H), 2.27 - 2.21 (m, 1H), 2.14 (s, 2H), 1.89 - 1.72 (m, 3H), 1.72 - 1.60 (m, 2H), 1.59 - 1.38 (m, 4H), 1.35 (s, 2H), 1.23 (dd,  $J = 8.9, 2.5$  Hz, 1H), 1.01 (t,  $J = 12.9$  Hz, 1H), 0.92 - 0.84 (m, 6H).

HRMS-ESI  $m/z$   $[M+H]^+$  calcd for  $\text{C}_{22}\text{H}_{37}\text{N}_2\text{O}_2$ : 361.284955, found: 361.283845.

**Compound 11**

Compound **11** was prepared according to general procedure by reacting 2-bromobenzaldehyde (40.7 mg, 0.22 mmol) with **A** (50 mg, 0.22 mmol). Compound **11** was isolated as a orange oil (83 mg, 0.21 mmol, 94.5%).

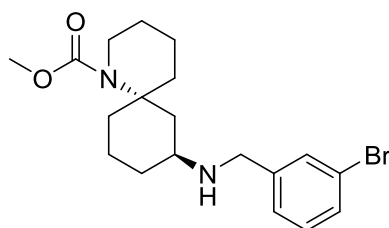
$R_f=0.50$  (DCM/MeOH 9:1).

$^1\text{H NMR}$  (600 MHz,  $\text{CD}_3\text{OD}$ )  $\delta=7.74$  (dd,  $J = 7.4, 4.1$  Hz, 1H), 7.62 (dd,  $J = 7.6, 1.4$  Hz, 1H), 7.48 (t,  $J = 7.5$  Hz, 1H), 7.38 (td,  $J = 7.9, 1.5$  Hz, 1H), 4.48 (t,  $J = 11.2$  Hz, 1H), 4.40 (t,  $J = 11.6$  Hz, 1H), 3.90 (t,  $J = 3.7$  Hz, 1H), 3.88 (t,  $J = 3.7$  Hz, 1H), 3.67 (s, 3H), 3.59 - 3.52 (m, 1H), 3.48 (dd,  $J = 12.6, 2.5$  Hz, 1H), 3.26 - 3.20 (m, 1H), 2.82 - 2.75 (m, 1H), 2.24 (d,  $J = 10.7$  Hz, 1H), 1.92 - 1.78 (m, 3H), 1.69 (m, 2H), 1.60 - 1.52 (m, 3H), 1.52 - 1.45 (m, 2H), 1.36 (t,  $J = 12.3$  Hz, 1H).

HRMS-ESI  $m/z$   $[M+H]^+$  calcd for  $\text{C}_{19}\text{H}_{28}\text{BrN}_2\text{O}_2$ : 395.132867, found: 395.134011.



## Compound 12

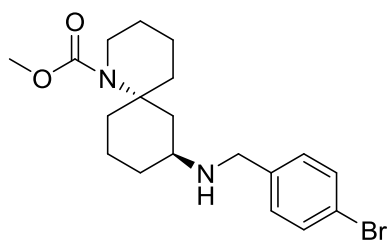


Compound **14** was prepared according to general procedure by reacting 3-bromobenzaldehyde (40.7 mg, 0.22 mmol) with **A** (50 mg, 0.22 mmol). Compound **14** was isolated as a orange oil (82 mg, 0.21 mmol, 94.5%).

$R_f=0.50$  (DCM/MeOH 9:1).

$^1\text{H NMR}$  (600 MHz,  $\text{CD}_3\text{OD}$ )  $\delta=7.74$  (s,  $J = 8.7$  Hz, 1H), 7.61 (d,  $J = 8.0$  Hz, 1H), 7.48 (d,  $J = 7.7$  Hz, 1H), 7.38 (t,  $J = 7.9$  Hz, 1H), 4.27 (t,  $J = 13.4$  Hz, 1H), 4.20 (d,  $J = 13.3$  Hz, 1H), 3.90 - 3.80 (m, 1H), 3.65 (s, 3H), 3.45 (tt,  $J = 13.8, 4.6, 3.0$  Hz, 1H), 3.40 (dd,  $J = 12.6, 2.5$  Hz, 1H), 3.22 (ddd,  $J = 14.5, 11.5, 2.9$  Hz, 1H), 3.00 (s, 1H), 2.77 (dd,  $J = 14.7, 2.3$  Hz, 1H), 2.16 (t,  $J = 16.7$  Hz, 1H), 1.91 - 1.81 (m, 1H), 1.81 - 1.75 (m, 1H), 1.71 - 1.62 (m, 2H), 1.60 - 1.51 (m, 2H), 1.50 - 1.37 (m, 3H), 1.30 (t,  $J = 12.3$  Hz, 1H), 1.08 - 0.99 (m, 1H).

HRMS-ESI  $m/z$   $[M+H]^+$  calcd for  $\text{C}_{19}\text{H}_{28}\text{BrN}_2\text{O}_2$ : 395.132867, found: 395.132189.

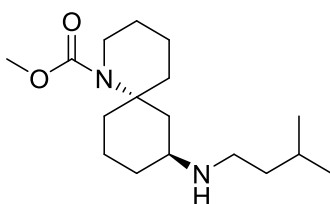
**Compound 13**

Compound **13** was prepared according to general procedure by reacting 4-bromobenzaldehyde (40.7 mg, 0.22 mmol) with **A** (50 mg, 0.22 mmol). Compound **13** was isolated as a orange oil (78 mg, 0.20 mmol, 90.9%).

$R_f=0.35$  (DCM/MeOH 9:1).

$^1\text{H NMR}$  (300 MHz,  $\text{CDCl}_3$ )  $\delta=7.58$  (d,  $J = 8.6$  Hz, 2H), 7.10 (d,  $J = 8.6$  Hz, 2H), 3.82 (s, 2H), 3.61 (s, 3H), 3.11 (d,  $J = 12.4$  Hz, 1H), 2.91 (d,  $J = 22.1$  Hz, 2H), 2.68 (d,  $J = 12.1$  Hz, 1H), 2.33 - 2.22 (m, 1H), 2.06 - 1.80 (m, 4H), 1.70 - 1.53 (m, 2H), 1.52 - 1.39 (m, 1H), 1.11 - 0.94 (m, 2H), 0.92 - 0.76 (m, 4H).

RMS-ESI  $m/z$   $[M+H]^+$  calcd for  $\text{C}_{19}\text{H}_{28}\text{BrN}_2\text{O}_2$ : 395.132867, found: 395.13285.

**Compound 14**

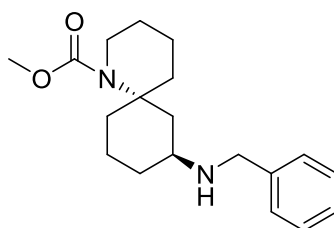
Compound **14** was prepared according to general procedure by reacting isovaleraldehyde (23.2 mg, 0.27 mmol) with **A** (60.0 mg, 0.27 mmol). Compound **14** was isolated as a light yellow oil (61.4 mg, 0.21 mmol, 77.8%).

$R_f=0.25$  (DCM/MeOH 9:1).

$^1\text{H NMR}$  (300 MHz,  $\text{CDCl}_3$ )  $\delta=3.26$  (s, 3H), 3.23 – 3.16 (m, 1H), 3.12 – 3.00 (m, 2H), 2.64 – 2.54 (m, 2H), 2.44 – 2.32 (m, 2H), 2.32 – 2.26 (m, 2H), 1.64 – 1.52 (m, 1H), 1.37 – 1.19 (m, 4H), 1.18 – 1.05 (m, 4H), 1.00 (dt,  $J = 8.2, 6.4$  Hz, 2H), 0.78 – 0.56 (m, 3H), 0.53 (s, 3H), 0.51 (s, 3H).

HRMS-ESI  $m/z$   $[M+H]^+$  calcd for  $\text{C}_{17}\text{H}_{33}\text{N}_2\text{O}_2$ : 297.253655, found: 297.253655.

## Compound 15

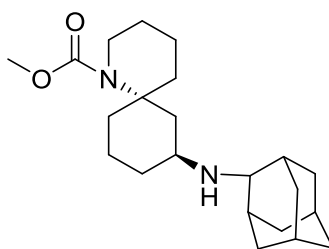


Compound **15** was prepared according to general procedure by reacting benzaldehyde (20 mg, 0.088 mmol) with **A** (9.35 mg, 0.088 mmol). Compound **15** was isolated as a yellow oil (20 mg, 0.063 mmol, 71.6%).

$R_f=0.43$  (DCM/MeOH 9:1).

$^1\text{H NMR}$  (600 MHz,  $[\text{D}_6]\text{DMSO}$ )  $\delta=7.49$  (d,  $J = 7.0$  Hz, 2H), 7.46 – 7.37 (m, 1H), 4.24 – 4.17 (m, 1H), 4.16 – 4.09 (m, 1H), 3.56 – 3.49 (m, 4H), 3.35 – 3.29 (m, 1H), 3.20 – 3.13 (m, 1H), 2.72 (d,  $J = 14.1$  Hz, 1H), 2.13 – 2.08 (m, 1H), 2.06 (s, 2H), 1.80 – 1.56 (m, 4H), 1.53 – 1.26 (m, 6H), 1.20 (t,  $J = 13.0$  Hz, 1H), 1.00 – 0.90 (m, 1H).

HRMS-ESI  $m/z$   $[\text{M}+\text{H}]^+$  calcd for  $\text{C}_{19}\text{H}_{29}\text{N}_2\text{O}_2$ : 317.222355, found: 317.222713.

**Compound 16**

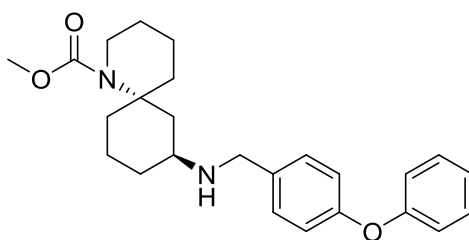
Compound **16** was prepared according to general procedure by reacting adamantan-2-one (81.1 mg, 0.27 mmol) with **A** (60.0 mg, 0.27 mmol). Compound **16** was isolated as a light yellow oil (60.0 mg, 0.17 mmol, 61.6%).

$R_f=0.40$  (DCM/MeOH 9:1).

$^1\text{H NMR}$  (300 MHz,  $\text{CDCl}_3$ )  $\delta=3.72$  (dt,  $J = 14.3, 4.5$  Hz, 1H), 3.55 (s, 3H), 3.47 (s, 1H), 3.45 - 3.26 (m, 2H), 3.23 - 3.13 (m, 2H), 2.62 (d,  $J = 14.2$  Hz, 1H), 2.40 - 2.22 (m, 3H), 2.28 - 2.07 (m, 2H), 1.94 - 1.81 (m, 3H), 1.81 - 1.60 (m, 6H), 1.60 - 1.46 (m, 5H), 1.47 - 1.33 (m, 3H), 1.21 - 1.15 (m, 2H), 1.09 - 0.97 (m, 2H).

LRMS-ESI  $m/z$   $[M+H]^+$  calcd for  $\text{C}_{22}\text{H}_{37}\text{N}_2\text{O}_2$ : 361.28, found: 361.43.

## Compound 17



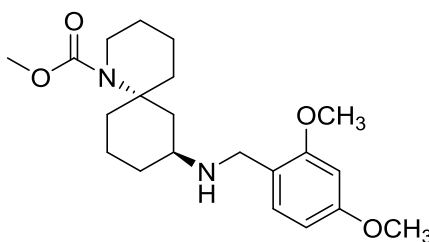
Compound **17** was prepared according to general procedure by reacting 4-phenoxybenzaldehyde (53.5 mg, 0.27 mmol) with **A** (60 mg, 0.27 mmol). Compound **17** was isolated as a yellow oil (81.3 mg, 0.20 mmol, 74.1%).

$R_f=0.38$  (DCM/MeOH 9:1).

$^1\text{H NMR}$  (600 MHz,  $[\text{D}_6]\text{DMSO}$ )  $\delta=8.71$  (s, 1H), 7.52 (d,  $J = 8.6$  Hz, 2H), 7.44 - 7.40 (m, 2H), 7.18 (t,  $J = 7.4$  Hz, 1H), 7.07 (d,  $J = 8.6$  Hz, 1H), 7.02 (dd,  $J = 8.6, 1.0$  Hz, 1H), 4.24 - 4.16 (m, 1H), 4.16 - 4.08 (m, 1H), 3.59 - 3.52 (m, 4H), 3.32 - 3.29 (m, 1H), 3.19 (d,  $J = 10.9$  Hz, 2H), 2.74 (d,  $J = 14.1$  Hz, 1H), 2.12 (s, 1H), 1.74 - 1.59 (m, 4H), 1.52 - 1.30 (m, 7H), 1.21 (t,  $J = 13.0$  Hz, 1H), 0.98 (dd,  $J = 18.7, 8.0$  Hz, 1H).

HRMS-ESI  $m/z$   $[M+H]^+$  calcd for  $\text{C}_{25}\text{H}_{33}\text{N}_2\text{O}_3$ : 409.248569, found: 409.249469.

## Compound 18

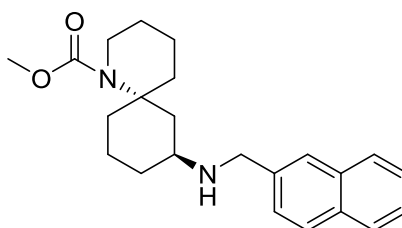


Compound **18** was prepared according to general procedure by reacting 2,4-dimethoxybenzaldehyde (44.9 mg, 0.27 mmol) with **A** (60 mg, 0.27 mmol). Compound **18** was isolated as a yellow oil (67 mg, 0.18 mmol, 66.7%).

$R_f=0.42$  (DCM/MeOH 9:1).

$^1\text{H NMR}$  (600 MHz,  $\text{CD}_3\text{OD}$ )  $\delta=7.29$  (d,  $J = 8.3$  Hz, 1H), 6.62 (d,  $J = 2.3$  Hz, 1H), 6.56 (dd,  $J = 8.3, 2.3$  Hz, 1H), 4.19 (t,  $J = 13.0$  Hz, 1H), 4.12 (t,  $J = 13.5$  Hz, 1H), 3.90 (s, 3H), 3.84 (t,  $J = 3.9$  Hz, 1H), 3.82 (s,  $J = 2.7$  Hz, 3H), 3.64 (s, 3H), 3.40 - 3.33 (m, 2H), 3.27 - 3.18 (m, 1H), 2.79 - 2.72 (m, 1H), 2.19 - 2.13 (m, 1H), 1.89 - 1.74 (m, 3H), 1.70 - 1.61 (m, 2H), 1.59 - 1.49 (m, 2H), 1.49 - 1.40 (m, 3H), 1.30 (t,  $J = 12.9$  Hz, 1H), 1.05 - 0.97 (m, 1H).

HRMS-ESI  $m/z$   $[M+H]^+$  calcd for  $\text{C}_{21}\text{H}_{33}\text{N}_2\text{O}_4$ : 377.243484, found: 377.243882.

**Compound 19**

Compound **19** was prepared according to general procedure by reacting 2-naphthaldehyde (42.2 mg, 0.27 mmol) with **A** (60 mg, 0.27 mmol). Compound **19** was isolated as a yellow oil (49 mg, 0.13 mmol, 49.5%).

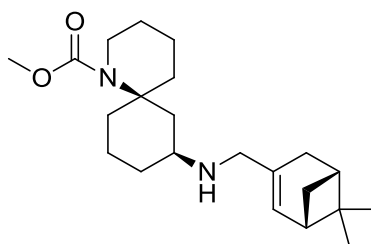
$R_f=0.37$  (DCM/MeOH 9:1).

$^1\text{H NMR}$  (300 MHz,  $\text{CDCl}_3$ )  $\delta=7.88 - 7.72$  (m, 4H), 7.54 - 7.36 (m, 3H), 4.01 (s, 2H), 3.70 - 3.49 (m, 4H), 3.45 - 3.30 (m, 2H), 3.10 (d,  $J = 15.9$  Hz, 1H), 2.91 - 2.64 (m, 2H), 2.01 (d,  $J = 13.9$  Hz, 1H), 1.86 - 1.30 (m, 7H), 1.28 - 1.07 (m, 1H), 1.05 - 0.89 (m, 2H).

HRMS-ESI  $m/z$   $[M+H]^+$  calcd for  $\text{C}_{23}\text{H}_{31}\text{N}_2\text{O}_2$ : 367.238005, found: 367.237119.



## Compound 20

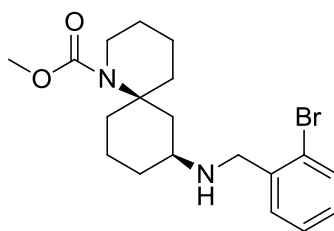


Compound **20** was prepared according to general procedure by reacting (-)-**myrtenal** (19.5 mg, 0.13 mmol) with **B** (30 mg, 0.13 mmol). Compound **20** was isolated as a light yellow oil (5 mg, 0.013 mmol, 10%).

$R_f=0.40$  (DCM/MeOH 9:1).

$^1\text{H NMR}$  (300 MHz,  $\text{CDCl}_3$ )  $\delta=5.34$  (t,  $J = 4.9$  Hz, 1H), 3.71 - 3.66 (m, 1H), 3.62 (s, 3H), 3.54 - 3.47 (m, 2H), 3.12 (s, 2H), 2.61 - 2.40 (m, 2H), 2.40 - 2.31 (m, 2H), 2.29 - 2.19 (m, 2H), 2.07 (d,  $J = 5.2$  Hz, 1H), 1.97 - 1.81 (m, 2H), 1.76 - 1.64 (m, 3H), 1.27 (s, 2H), 1.25 (s, 3H), 1.17 - 1.11 (m, 3H), 0.94 - 0.85 (m, 4H), 0.82 (s, 3H).

HRMS-ESI  $m/z$   $[M+H]^+$  calcd for  $\text{C}_{22}\text{H}_{37}\text{N}_2\text{O}_2$ : 361.284955, found: 361.285951.

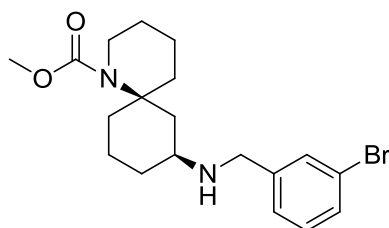
Compound **21**

Compound **21** was prepared according to general procedure by reacting 2-bromobenzaldehyde (24.0 mg, 0.13 mmol) with **B** (30 mg, 0.13 mmol). Compound **21** was isolated as a orange oil (4 mg, 0.010 mmol, 3.85%).

$R_f=0.50$  (DCM/MeOH 9:1).

$^1\text{H NMR}$  (300 MHz,  $\text{CDCl}_3$ )  $\delta=7.52$  (d,  $J = 7.9$  Hz, 1H), 7.42 (d,  $J = 7.6$  Hz, 1H), 7.31 - 7.27 (m, 1H), 7.15 - 7.07 (m, 1H), 3.88 (d,  $J = 3.7$  Hz, 2H), 3.70 (t,  $J = 4.1$  Hz, 1H), 3.63 (s, 3H), 3.52 (dd,  $J = 9.0, 2.9$  Hz, 2H), 2.70 - 2.54 (m, 2H), 2.49 (dd,  $J = 13.3, 4.5$  Hz, 1H), 2.35 (t,  $J = 12.1$  Hz, 1H), 2.06 - 1.91 (m, 1H), 1.73 - 1.51 (m, 5H), 1.41 - 1.04 (m, 4H), 0.92 - 0.79 (m, 1H).

HRMS-ESI  $m/z$   $[M+H]^+$  calcd for  $\text{C}_{19}\text{H}_{28}\text{BrN}_2\text{O}_2$ : 395.132867, found: 395.132867.

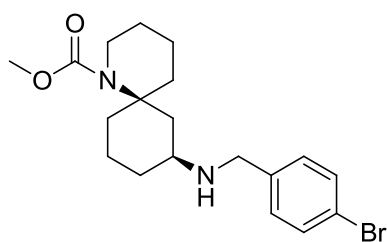
Compound **22**

Compound **22** was prepared according to general procedure by reacting 3-bromobenzaldehyde (24.0 mg, 0.13 mmol) with **B** (30 mg, 0.13 mmol). Compound **22** was isolated as a orange oil (20 mg, 0.05 mmol, 38.5%).

$R_f=0.50$  (DCM/MeOH 9:1).

$^1\text{H NMR}$  (300 MHz,  $\text{CDCl}_3$ )  $\delta=7.51$  (d,  $J = 14.3$  Hz, 1H), 7.36 (d,  $J = 7.6$  Hz, 1H), 7.23 - 7.12 (m, 2H), 3.79 (s, 2H), 3.72 - 3.68 (m, 1H), 3.63 (s, 2H), 3.55 - 3.48 (m, 2H), 2.66 - 2.41 (m, 2H), 2.38 - 2.25 (m, 1H), 2.06 - 1.86 (m, 3H), 1.74 - 1.49 (m, 4H), 1.38 - 1.17 (m, 4H), 0.86 (dd,  $J = 14.7, 7.5$  Hz, 2H).

HRMS-ESI  $m/z$   $[M+H]^+$  calcd for  $\text{C}_{19}\text{H}_{28}\text{BrN}_2\text{O}_2$ : 395.132867, found: 395.133935.

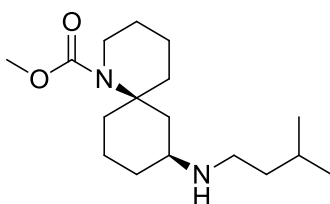
**Compound 23**

Compound **23** was prepared according to general procedure by reacting 4-bromobenzaldehyde (24.0 mg, 0.13 mmol) with **B** (30 mg, 0.13 mmol). Compound **23** was isolated as a orange oil (5.7 mg, 0.014 mmol, 10.8%).

$R_f=0.33$  (DCM/MeOH 9:1).

$^1\text{H NMR}$  (300 MHz,  $\text{CDCl}_3$ )  $\delta=7.45 - 7.39$  (m, 2H), 7.22 - 7.17 (m, 2H), 3.77 (s, 2H), 3.71 - 3.68 (m, 1H), 3.63 (s, 3H), 3.54 - 3.48 (m, 2H), 2.67 - 2.43 (m, 2H), 2.38 - 2.25 (m, 2H), 2.00 - 1.86 (m, 1H), 1.74 - 1.58 (m, 4H), 1.38 - 1.15 (m, 3H), 1.15 - 0.99 (m, 2H), 0.94 - 0.79 (m, 1H).

HRMS-ESI  $m/z$   $[M+H]^+$  calcd for  $\text{C}_{19}\text{H}_{28}\text{BrN}_2\text{O}_2$ : 395.132867, found: 395.132896.

**Compound 24**

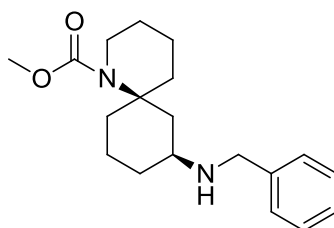
Compound **24** was prepared according to general procedure by reacting isovaleraldehyde (11.2 mg, 0.13 mmol) with **B** (30.0 mg, 0.13 mmol). Compound **24** was isolated as a light yellow oil (9.0 mg, 0.037 mmol, 23.1%).

$R_f=0.40$  (DCM/MeOH 9:1).

$^1\text{H NMR}$  (300 MHz,  $\text{CDCl}_3$ )  $\delta=3.69$  (t,  $J = 4.2$  Hz, 3H), 3.62 (s, 3H), 3.51 (d,  $J = 10.0$  Hz, 2H), 2.67 - 2.55 (m, 2H), 2.55 - 2.46 (m, 1H), 2.29 (dd,  $J = 26.0, 12.1$  Hz, 1H), 2.09 - 1.82 (m, 3H), 1.77 - 1.45 (m, 5H), 1.42 - 1.12 (m, 4H), 1.07 - 0.93 (m, 3H), 0.90 (s, 2H), 0.87 (s, 3H).

HRMS-ESI  $m/z$   $[M+H]^+$  calcd for  $\text{C}_{17}\text{H}_{33}\text{N}_2\text{O}_2$ : 297.253655, found: 297.253632.

## Compound 25

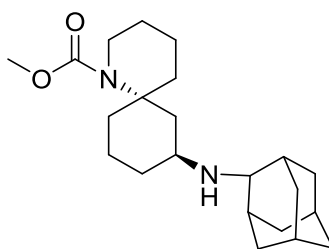


Compound **25** was prepared according to general procedure by reacting benzaldehyde (13.8 mg, 0.13 mmol) with **B** (30.0 mg, 0.13 mmol). Compound **25** was isolated as a yellow oil (2 mg, 0.006 mmol, 4.9%).

$R_f=0.25$  (DCM/MeOH 9:1).

$^1\text{H NMR}$  (300 MHz,  $\text{CDCl}_3$ )  $\delta=7.32$  (d,  $J = 5.9$  Hz, 3H), 7.26 (d,  $J = 18.2$  Hz, 2H), 3.84 (s, 2H), 3.63 (s, 3H), 3.54 - 3.49 (m, 1H), 2.73 - 2.58 (m, 1H), 2.57 - 2.43 (m, 1H), 2.37 (t,  $J = 12.0$  Hz, 1H), 1.99 (d,  $J = 8.5$  Hz, 1H), 1.90 - 1.71 (m, 2H), 1.72 - 1.46 (m, 4H), 1.44 - 1.20 (m, 3H), 1.18 - 1.04 (m, 2H), 0.94 - 0.79 (m, 2H).

HRMS-ESI  $m/z$   $[M+H]^+$  calcd for  $\text{C}_{19}\text{H}_{29}\text{N}_2\text{O}_2$ : 317.222355, found: 317.222198.

**Compound 26**

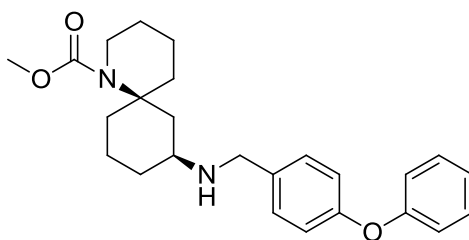
Compound **26** was prepared according to general procedure by reacting adamantan-2-one (20.0 mg, 0.13 mmol) with **B** (30.0 mg, 0.13 mmol). Compound **26** was isolated as a light yellow oil (5.5 mg, 0.015 mmol, 11.5%).

$R_f=0.40$  (DCM/MeOH 9:1).

$^1\text{H NMR}$  (300 MHz,  $\text{CDCl}_3$ )  $\delta$  3.85 (s, 1H), 3.69 (d,  $J = 8.1$  Hz, 1H), 3.63 (s,  $J = 10.9$  Hz, 3H), 3.52 (s, 2H), 3.09 – 2.78 (m, 2H), 2.64 (d,  $J = 11.8$  Hz, 1H), 2.61 – 2.35 (m, 3H), 2.17 – 1.91 (m, 4H), 1.89 – 1.76 (m,  $J = 22.8$  Hz, 5H), 1.78 – 1.46 (m, 6H), 1.39 – 1.10 (m, 6H), 0.92 – 0.78 (m, 2H).

HRMS-ESI  $m/z$   $[M+H]^+$  calcd for  $\text{C}_{22}\text{H}_{37}\text{N}_2\text{O}_2$ : 361.284955, found: 361.285308.

## Compound 27



Compound **27** was prepared according to general procedure by reacting 4-phenoxybenzaldehyde (13.9 mg, 0.07 mmol) with **B** (15 mg, 0.07 mmol). Compound **27** was isolated as a yellow oil (5.5 mg, 0.013 mmol, 18.6%).

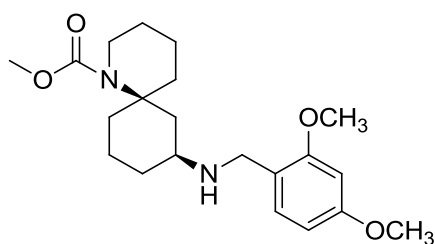
$R_f=0.50$  (DCM/MeOH 9:1).

$^1\text{H NMR}$  (600 MHz,  $[\text{D}_6]\text{DMSO}$ )  $\delta=8.71$  (s, 1H), 7.52 (d,  $J = 8.6$  Hz, 2H), 7.44 – 7.40 (m, 2H), 7.18 (t,  $J = 7.4$  Hz, 1H), 7.07 (d,  $J = 8.6$  Hz, 1H), 7.02 (dd,  $J = 8.6, 1.0$  Hz, 1H), 4.24 – 4.16 (m, 1H), 4.16 – 4.08 (m, 1H), 3.59 – 3.52 (m, 4H), 3.32 – 3.29 (m, 1H), 3.19 (d,  $J = 10.9$  Hz, 2H), 2.74 (d,  $J = 14.1$  Hz, 1H), 2.12 (s, 1H), 1.74 – 1.59 (m, 4H), 1.52 – 1.30 (m, 7H), 1.21 (t,  $J = 13.0$  Hz, 1H), 0.98 (dd,  $J = 18.7, 8.0$  Hz, 1H).

LRMS-ESI  $m/z$   $[M+H]^+$  calcd for  $\text{C}_{25}\text{H}_{33}\text{N}_2\text{O}_3$ : 409.25, found: 409.24.



## Compound 28

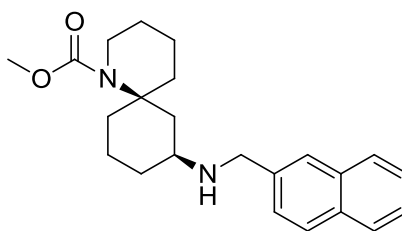


Compound **28** was prepared according to general procedure by reacting 2,4 dimethoxybenzaldehyde (22.0 mg, 0.13 mmol) with **B** (30 mg, 0.13 mmol). Compound **28** was isolated as a yellow oil (6.4 mg, 0.017 mmol, 13.1%).

$R_f=0.25$  (DCM/MeOH 9:1).

$^1\text{H NMR}$  (300 MHz,  $\text{CDCl}_3$ )  $\delta=7.17$  (d,  $J = 8.9$  Hz, 1H), 6.43 (d,  $J = 5.9$  Hz, 1H), 6.41 (d,  $J = 2.2$  Hz, 1H), 3.81 (s,  $J = 3.7$  Hz, 3H), 3.79 (s,  $J = 3.6$  Hz, 3H), 3.78 - 3.73 (m, 2H), 3.73 - 3.66 (m, 1H), 3.63 (s, 3H), 3.57 - 3.45 (m, 2H), 2.74 - 2.57 (m, 1H), 2.50 (td,  $J = 13.2, 4.5$  Hz, 1H), 2.41 - 2.26 (m, 1H), 2.13 - 1.77 (m, 3H), 1.74 - 1.47 (m, 4H), 1.46 - 1.02 (m, 3H), 0.95 - 0.76 (m, 2H).

HRMS-ESI  $m/z$   $[M+H]^+$  calcd for  $\text{C}_{21}\text{H}_{33}\text{N}_2\text{O}_4$ : 377.243484, found: 377.243739.

Compound **29**

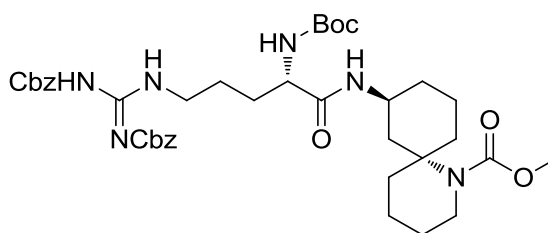
Compound **29** was prepared according to general procedure by reacting 2-naphthaldehyde (20.3 mg, 0.13 mmol) with **B** (30 mg, 0.13 mmol). Compound **29** was isolated as a yellow oil (2.6 mg, 0.007 mmol, 5.4%).

$R_f=0.38$  (DCM/MeOH 9:1).

$^1\text{H NMR}$  (300 MHz,  $\text{CDCl}_3$ )  $\delta=7.87 - 7.72$  (m, 4H),  $7.52 - 7.38$  (m, 3H),  $4.00$  (s, 2H),  $3.64$  (s, 3H),  $3.52$  (t,  $J = 5.8$  Hz, 2H),  $2.68$  (t,  $J = 11.2$  Hz, 1H),  $2.56 - 2.45$  (m, 1H),  $2.39$  (t,  $J = 12.0$  Hz, 1H),  $2.01$  (t,  $J = 10.5$  Hz, 2H),  $1.77 - 1.47$  (m, 4H),  $1.46 - 1.10$  (m, 4H),  $0.97 - 0.74$  (m,  $J = 7.4$  Hz, 3H).

HRMS-ESI  $m/z$   $[M+H]^+$  calcd for  $\text{C}_{23}\text{H}_{31}\text{N}_2\text{O}_2$ : 367.238005, found: 367.23829.

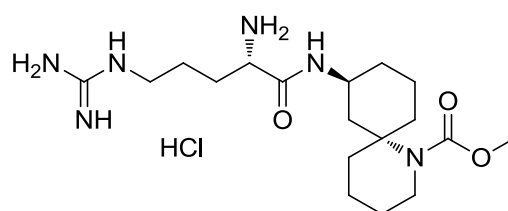
## Intermediate 16



Intermediate **16** was prepared according to general procedure by reacting scaffold **A** (63 mg, 0.28 mmol) with BocArg(Cbz)<sub>2</sub>OH (170 mg, 0.31 mmol). Intermediate **16** was isolated as a yellow solid (130 mg, 0.17 mmol, 60.7%).

$R_f=0.6$  (Cyclohexane/AcOEt 5:5).

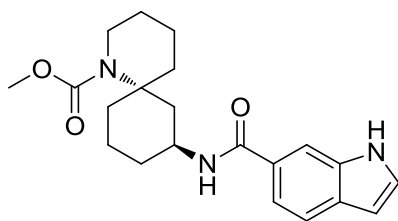
<sup>1</sup>H NMR (300 MHz, CDCl<sub>3</sub>)  $\delta=7.38-7.27$  (m, 10H), 5.49 (s, 2H), 5.38 (s, 2H), 4.77 (t,  $J = 6.99$  Hz, 1H), 4.06-3.86 (m, 3H), 3.72-3.64 (m, 1H), 3.62 (s, 3H), 3.31-3.23 (m, 1H), 2.71-2.74 (s, 1H), 1.91 - 1.80 (m, 2H), 1.71-1.14 (m, 13H), 1.39 (s, 10H).

**Compound 30**

Compound **30** was prepared according to general procedure by subjecting intermediate **16** (130 mg, 0.17 mmol) to Cbz- deprotection followed by Boc-deprotection. Compound **30** was isolated as a off-white solid (74 mg, 0.15 mmol, 88.2%).

$R_f=0.12$  (Cyclohexane/ AcOEt 5:5).

$^1\text{H NMR}$  (300 MHz,  $\text{CDCl}_3$ )  $\delta=8.19$  (s, 2H), 7.46 (m, 2H), 7.21 (m, 3H), 3.88 (m, 2H), 3.72-3.65 (m, 1H), 3.62 (s, 3H), 3.38-3.21 (m, 3H), 2.63-2.59 (m, 1H), 2.01 (dd,  $J = 13.0$  Hz, 7.0, 1H), 1.94-1.74 (m, 2H), 1.66-1.08 (m, 13H), 0.95 (m, 1H).

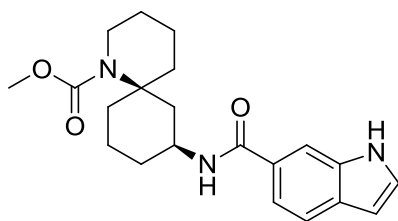
**Compound 31**

Compound **31** was prepared according to general procedure by reacting scaffold **A** (64 mg, 0.28 mmol) with 6-carboxyindole (36 mg, 0.31 mmol). Compound **31** was isolated as a gray solid (35 mg, 0.10 mmol, 34.6%).

$R_f=0.48$  (Cyclohexane/ AcOEt 5:5).

$^1\text{H NMR}$  (300 MHz,  $\text{CDCl}_3$ )  $\delta=8.09$  (d,  $J = 7.5$ , 1H), 7.01 (s, 1H), 7.64 (dd,  $J = 7.5$ , 1.5 Hz, 1H), 7.43 (d,  $J = 7.5$  Hz, 1H), 6.64 (d,  $J = 7.5$  Hz, 1H), 3.95-3.86 (m, 2H), 3.62 (s, 3H), 3.39-3.32 (m, 1H), 2.61 (m, 1H), 2.19-2.16 (m, 1H), 1.97-1.88 (m, 1H), 1.67-1.39 (m, 7H), 1.32-1.05 (m, 4H).

## Compound 32



Compound **32** was prepared according to general procedure by reacting scaffold **B** (131 mg, 0.58 mmol) with 6-carboxyindole (103 mg, 0.64 mmol). Compound **32** was isolated as a gray solid (40 mg, 0.11 mmol, 19%).

$R_f=0.48$  (Cyclohexane/ AcOEt 5:5).

$^1\text{H NMR}$  (300 MHz,  $\text{CDCl}_3$ )  $\delta=8.09$  (d,  $J = 7.5$ , 1H), 7.01 (s, 1H), 7.64 (dd,  $J = 7.5$ , 1.5 Hz, 1H), 7.43 (d,  $J = 7.5$  Hz, 1H), 6.64 (d,  $J = 7.5$  Hz, 1H), 3.95-3.86 (m, 2H), 3.62 (s, 3H), 3.39-3.32 (m, 1H), 2.61 (m, 1H), 2.19-2.16 (m, 1H), 1.97-1.88 (m, 1H), 1.67-1.39 (m, 7H), 1.32-1.05 (m, 4H).

## 7. Bibliography

- (1) In [www.malaria.org](http://www.malaria.org).
- (2) WHO 2010.
- (3) Porter-Kelley, J. M.; Cofie, J.; Jean, S.; Brooks, M. E.; Lassiter, M.; Mayer, D. C. G. *Infection and Drug Resistance* **2010**, *3*, 87.
- (4) [www.segretariatosociale.rai.it/codici/malaria/malaria.html](http://www.segretariatosociale.rai.it/codici/malaria/malaria.html).
- (5) Rug, M.; Prescott, S. W.; Fernandez, K. M.; Cooke, B. M.; Cowman, A. F. *Blood* **2006**, *108*, 370.
- (6) Haldar, K.; Murphy Sean, C.; Milner Dan, A.; Taylor Terrie, E. *Annual review of pathology* **2007**, *2*, 217.
- (7) Uyoga, S.; Skorokhod, O. A.; Opiyo, M.; Orori, E. N.; Williams, T. N.; Arese, P.; Schwarzer, E. *British Journal of Haematology* **2012**, *157*, 116.
- (8) Chang, K.-H.; Tam, M.; Stevenson, M. M. *Blood* **2004**, *103*, 3727.
- (9) Wickramasinghe, S. N.; Abdalla, S. H. *Bailliere's best practice & research. Clinical haematology* **2000**, *13*, 277.
- (10) Maier, A. G.; Cooke, B. M.; Cowman, A. F.; Tilley, L. *Nature Reviews Microbiology* **2009**, *7*, 341.
- (11) Kyes, S.; Horrocks, P.; Newbold, C. *Annual Review of Microbiology* **2001**, *55*, 673.
- (12) Rowe, J. A.; Kyes, S. A. *Molecular Microbiology* **2004**, *53*, 1011.
- (13) Deitsch, K. W.; Wellems, T. E. *Molecular & Biochemical Parasitology* **1996**, *76*, 1.
- (14) Marti, M.; Baum, J.; Rug, M.; Tilley, L.; Cowman, A. F. *Journal of Cell Biology* **2005**, *171*, 587.
- (15) Lanzer, M.; Wickert, H.; Krohne, G.; Vincensini, L.; Braun Breton, C. *International Journal for Parasitology* **2006**, *36*, 23.
- (16) Cooke, B. M.; Lingelbach, K.; Bannister, L. H.; Tilley, L. *Trends in Parasitology* **2004**, *20*, 581.
- (17) Przyborski, J. M.; Wickert, H.; Krohne, G.; Lanzer, M. *Molecular & Biochemical Parasitology* **2003**, *132*, 17.
- (18) Langreth, S. G.; Jensen, J. B.; Reese, R. T.; Trager, W. *The Journal of protozoology* **1978**, *25*, 443.
- (19) Wickert, H.; Krohne, G. *Trends Parasitol* **2007**, *23*, 502.
- (20) Hanssen, E.; Sougrat, R.; Frankland, S.; Deed, S.; Klonis, N.; Lippincott-Schwartz, J.; Tilley, L. *Molecular Microbiology* **2008**, *67*, 703.
- (21) Mohandas, N.; Chasis, J. A. *Seminars in Hematology* **1993**, *30*, 171.
- (22) Luna, E. J.; Hitt, A. L. *Science (Washington, D. C., 1883-)* **1992**, *258*, 955.
- (23) Shen, B. W.; Josephs, R.; Steck, T. L. *Journal of Cell Biology* **1986**, *102*, 997.
- (24) Derick, L. H.; Liu, S.-C.; Chishti, A. H.; Palek, J. *European Journal of Cell Biology* **1992**, *57*, 317.
- (25) An, X.; Guo, X.; Zhang, X.; Baines, A. J.; Debnath, G.; Moyo, D.; Salomao, M.; Bhasin, N.; Johnson, C.; Discher, D.; Gratzner, W. B.; Mohandas, N. *Journal of Biological Chemistry* **2006**, *281*, 10527.
- (26) Johnson Colin, P.; Tang, H.-Y.; Carag, C.; Speicher David, W.; Discher Dennis, E. *Science (New York, N.Y.)* **2007**, *317*, 663.
- (27) Delaunay, J. *Blood Reviews* **2007**, *21*, 1.
- (28) Dhermy, D.; Schrevel, J.; Lecomte, M.-C. *Current Opinion in Hematology* **2007**, *14*, 198.
- (29) An, X.; Mohandas, N. *British Journal of Haematology* **2008**, *141*, 367.
- (30) Baum, J.; Papenfuss, A. T.; Baum, B.; Speed, T. P.; Cowman, A. F. *Nature Reviews Microbiology* **2006**, *4*, 621.

- (31) Mikkelsen, R. B.; Kamber, M.; Wadwa, K. S.; Lin, P. S.; Schmidt-Ullrich, R. *Proceedings of the National Academy of Sciences of the United States of America* **1988**, *85*, 5956.
- (32) McPherson, R. A.; Donald, D. R.; Sawyer, W. H.; Tilley, L. *Molecular & Biochemical Parasitology* **1993**, *62*, 233.
- (33) Roggwiler, E.; Betoulle, M. E. M.; Blisnick, T.; Breton, C. B. *Molecular & Biochemical Parasitology* **1996**, *82*, 13.
- (34) Li, X.; Chen, H.; Oh, S. S.; Chishti, A. H. *Molecular & Biochemical Parasitology* **2008**, *158*, 22.
- (35) Dluzewski, A. R.; Mitchell, G. H.; Fryer, P. R.; Griffiths, S.; Wilson, R. J.; Gratzner, W. B. *Journal of cell science* **1992**, *102* ( Pt 3), 527.
- (36) Dluzewski, A. R.; Fryer, P. R.; Griffiths, S.; Wilson, R. J.; Gratzner, W. B. *Journal of cell science* **1989**, *92* ( Pt 4), 691.
- (37) Culvenor, J. G.; Day, K. P.; Anders, R. F. *Infection and Immunity* **1991**, *59*, 1183.
- (38) Vincensini, L.; Fall, G.; Berry, L.; Blisnick, T.; Braun Breton, C. *Molecular & Biochemical Parasitology* **2008**, *160*, 81.
- (39) Duffy, P. E.; Fried, M. *Current Opinion in Microbiology* **2003**, *6*, 371.
- (40) Haldar, K.; Mohandas, N. *Curr Opin Hematol* **2007**, *14*, 203.
- (41) Atkinson, C. T.; Aikawa, M. *Blood cells* **1990**, *16*, 351.
- (42) Albano, F. R.; Berman, A.; La Greca, N.; Hibbs, A. R.; Wickham, M.; Foley, M.; Tilley, L. *European Journal of Cell Biology* **1999**, *78*, 453.
- (43) Hayashi, M.; Taniguchi, S.; Ishizuka, Y.; Kim, H.-S.; Wataya, Y.; Yamamoto, A.; Moriyama, Y. *Journal of Biological Chemistry* **2001**, *276*, 15249.
- (44) Wickert, H.; Wissing, F.; Andrews, K. T.; Stich, A.; Krohne, G.; Lanzer, M. *European Journal of Cell Biology* **2003**, *82*, 271.
- (45) Hiller, N. L.; Bhattacharjee, S.; van Ooij, C.; Liolios, K.; Harrison, T.; Lopez-Estrano, C.; Haldar, K. *Science (Washington, DC, United States)* **2004**, *306*, 1934.
- (46) Marti, M.; Good, R. T.; Rug, M.; Knuepfer, E.; Cowman, A. F. *Science (Washington, DC, United States)* **2004**, *306*, 1930.
- (47) de Koning-Ward, T. F.; Gilson, P. R.; Boddey, J. A.; Rug, M.; Smith, B. J.; Papenfuss, A. T.; Sanders, P. R.; Lundie, R. J.; Maier, A. G.; Cowman, A. F.; Crabb, B. S. *Nature (London, United Kingdom)* **2009**, *459*, 945.
- (48) Chang, H. H.; Falick, A. M.; Carlton, P. M.; Sedat, J. W.; DeRisi, J. L.; Marletta, M. A. *Molecular & Biochemical Parasitology* **2008**, *160*, 107.
- (49) Richard, D.; Kats, L. M.; Langer, C.; Black, C. G.; Mitri, K.; Boddey, J. A.; Cowman, A. F.; Coppel, R. L. *PLoS Pathogens* **2009**, *5*, No pp given.
- (50) Danis, M.; Bricaire, F. *Fundamental & Clinical Pharmacology* **2003**, *17*, 155.
- (51) WHO *WHO Report* **2001**.
- (52) Greenwood, B. *American Journal of Tropical Medicine and Hygiene* **2004**, *70*, 1.
- (53) Karen, I. B. *Milestones in drug ther.* **2012**.
- (54) Trape, J. F. *The American journal of tropical medicine and hygiene* **2001**, *64*, 12.
- (55) Sanchez, C. P.; McLean, J. E.; Stein, W.; Lanzer, M. *Biochemistry* **2004**, *43*, 16365.
- (56) Sidhu, A. B. S.; Verdier-Pinard, D.; Fidock, D. A. *Science (Washington, DC, United States)* **2002**, *298*, 210.
- (57) Reed, M. B.; Saliba, K. J.; Caruana, S. R.; Kirk, K.; Cowman, A. F. *Nature (London)* **2000**, *403*, 906.
- (58) Vaidya, A. B.; Mather, M. W. *Drug Resistance Updates* **2000**, *3*, 283.
- (59) Vaidya, A. B.; Lashgari, M. S.; Pologe, L. G.; Morrissey, J. *Molecular and Biochemical Parasitology* **1993**, *58*, 33.
- (60) Suswam, E.; Kyle, D.; Lang-Unnasch, N. *Experimental Parasitology* **2001**, *98*, 180.
- (61) Srivastava, I. K.; Morrissey, J. M.; Darrouzet, E.; Daldal, F.; Vaidya, A. B. *Molecular Microbiology* **1999**, *33*, 704.



- (62) Mok, S.; Imwong, M.; MacKinnon, M. J.; Sim, J.; Ramadoss, R.; Yi, P.; Mayxay, M.; Chotivanich, K.; Liong, K.-Y.; Russel, B.; Socheat, D.; Newton, P. N.; Day, N. P. J.; White, N. J.; Preiser, P. R.; Nosten, F.; Dondorp, A. M.; Bozdech, Z. *BMC Genomics* **2011**, *12*, 391.
- (63) Newman, D. J.; Cragg, G. M. *Journal of natural products* **2004**, *67*, 1216.
- (64) Newman, D. J.; Cragg, G. M. *Journal of natural products* **2007**, *70*, 461.
- (65) Cragg, G. M.; Newman, D. J.; Snader, K. M. *Journal of natural products* **1997**, *60*, 52.
- (66) Lam, K. S. *Trends in microbiology* **2007**, *15*, 279.
- (67) Newman, D. J.; Cragg, G. M. *Journal of natural products* **2012**, *75*, 311.
- (68) Ganesan, A. *Current opinion in chemical biology* **2008**, *12*, 306.
- (69) Newman, D. J.; Cragg, G. M. *Future medicinal chemistry* **2009**, *1*, 1415.
- (70) Harvey, A. L. *Drug discovery today* **2008**, *13*, 894.
- (71) Williams, P. G. *Trends in biotechnology* **2009**, *27*, 45.
- (72) Hert, J.; Irwin, J. J.; Laggner, C.; Keiser, M. J.; Shoichet, B. K. *Nature chemical biology* **2009**, *5*, 479.
- (73) In [www.dpd.cdc.gov/DPDx/HTML/Malaria.HTM](http://www.dpd.cdc.gov/DPDx/HTML/Malaria.HTM).
- (74) Boddey, J. A.; Hodder, A. N.; Guenther, S.; Gilson, P. R.; Patsiouras, H.; Kapp, E. A.; Pearce, J. A.; de Koning-Ward, T. F.; Simpson, R. J.; Crabb, B. S.; Cowman, A. F. *Nature (London, United Kingdom)* **2010**, *463*, 627.
- (75) Russo, I.; Babbitt, S.; Muralidharan, V.; Butler, T.; Oksman, A.; Goldberg, D. E. *Nature (London, United Kingdom)* **2010**, *463*, 632.
- (76) Coombs, G. H.; Goldberg, D. E.; Klemba, M.; Berry, C.; Kay, J.; Mottram, J. C. *Trends Parasitol* **2001**, *17*, 532.
- (77) Berry, C.; Humphreys, M. J.; Matharu, P.; Granger, R.; Horrocks, P.; Moon, R. P.; Certa, U.; Ridley, R. G.; Bur, D.; Kay, J. *FEBS Letters* **1999**, *447*, 149.
- (78) Banerjee, R.; Liu, J.; Beatty, W.; Pelosof, L.; Klemba, M.; Goldberg, D. E. *Proceedings of the National Academy of Sciences of the United States of America* **2002**, *99*, 990.
- (79) Le Bonniec, S.; Deregnaucourt, C.; Redeker, V.; Banerjee, R.; Grellier, P.; Goldberg, D. E.; Schrevel, J. *Journal of Biological Chemistry* **1999**, *274*, 14218.
- (80) Wyatt, D. M.; Berry, C. *FEBS Letters* **2002**, *513*, 159.
- (81) Rosenthal, P. J.; McKerrow, J. H.; Aikawa, M.; Nagasawa, H.; Leech, J. H. *Journal of Clinical Investigation* **1988**, *82*, 1560.
- (82) Francis, S. E.; Gluzman, I. Y.; Oksman, A.; Knickerbocker, A.; Mueller, R.; Bryant, M. L.; Sherman, D. R.; Russell, D. G.; Goldberg, D. E. *EMBO Journal* **1994**, *13*, 306.
- (83) Klemba, M.; Goldberg, D. E. *Molecular & Biochemical Parasitology* **2005**, *143*, 183.
- (84) Athauda, S. B. P.; Matsumoto, K.; Rajapakshe, S.; Kuribayashi, M.; Kojima, M.; Kubomura-Yoshida, N.; Iwamatsu, A.; Shibata, C.; Inoue, H.; Takahashi, K. *Biochemical Journal* **2004**, *382*, 1039.
- (85) Dame, J. B.; Yowell, C. A.; Omara-Opyene, L.; Carlton, J. M.; Cooper, R. A.; Li, T. *Molecular & Biochemical Parasitology* **2003**, *130*, 1.
- (86) Khan, A. R., 1999.
- (87) Shi, X.-P.; Chen, E.; Yin, K.-C.; Na, S.; Garsky, V. M.; Lai, M.-T.; Li, Y.-M.; Platchek, M.; Register, R. B.; Sardana, M. K.; Tang, M.-J.; Thiebeau, J.; Wood, T.; Shafer, J. A.; Gardell, S. J. *Journal of Biological Chemistry* **2001**, *276*, 10366.
- (88) Nguyen, J.-T.; Hamada, Y.; Kimura, T.; Kiso, Y. *Archiv der Pharmazie (Weinheim, Germany)* **2008**, *341*, 523.
- (89) Foye *Principi di chimica farmaceutica*; IV ed.; PICCIN, 1998.
- (90) Gambini, L. **2010**.
- (91) Rizzi, L.; Vaiana, N.; Sagui, F.; Genesio, E.; Pilli, E.; Porcari, V.; Romeo, S. *Protein & Peptide Letters* **2009**, *16*, 86.
- (92) Alewood, P. F.; Brinkworth, R. I.; Dancer, R. J.; Garnham, B.; Jones, A.; Kent, S. B. H. *Tetrahedron Letters* **1992**, *33*, 977.
- (93) Albeck, A.; Persky, R. *Tetrahedron* **1994**, *50*, 6333.

- 
- (94) Flausino, O., Jr.; Santos Lde, A.; Verli, H.; Pereira, A. M.; Bolzani Vda, S.; Nunes-de-Souza, R. L. *Journal of natural products* **2007**, *70*, 48.
- (95) Saker, M. L.; Nogueira, I. C.; Vasconcelos, V. M.; Neilan, B. A.; Eaglesham, G. K.; Pereira, P. *Ecotoxicology and environmental safety* **2003**, *55*, 243.
- (96) Iranshahi, M.; Vu, H.; Pham, N.; Zencak, D.; Forster, P.; Quinn, R. J. *Planta medica* **2012**, *78*, 730.
- (97) Dutta, S.; Abe, H.; Aoyagi, S.; Kibayashi, C.; Gates, K. S. *Journal of the American Chemical Society* **2005**, *127*, 15004.
- (98) Maeng, J. H.; Funk, R. L. *Organic letters* **2002**, *4*, 331.
- (99) Faulkner, D. J. *Natural product reports* **1991**, *8*, 97.
- (100) Ghosh, A. K.; Dawson, Z. L.; Mitsuya, H. *Bioorgan Med Chem* **2007**, *15*, 7576.
- (101) Srivastava, N.; Banik, B. K. *J Org Chem* **2003**, *68*, 2109.
- (102) Wright, D. L.; Schulte, I. J.; Page, M. A. *Organic letters* **2000**, *2*, 1847.
- (103) In [www.rollbackmalaria.org](http://www.rollbackmalaria.org).